

UC Berkeley

UC Berkeley Electronic Theses and Dissertations

Title

Polymers for Drug Delivery: Extended Circulation and siRNA Transfection

Permalink

<https://escholarship.org/uc/item/6111q40t>

Author

KIERSTEAD, PAUL HENRY

Publication Date

2013

Peer reviewed|Thesis/dissertation

Polymers for Drug Delivery: Extended Circulation and siRNA Transfection

by

Paul Henry Kierstead

A dissertation submitted in partial satisfaction of the
requirements for the degree of

Doctor of Philosophy

in

Chemistry

in the

Graduate Division

of the

University of California, Berkeley

Committee in charge:

Professor Jean M. J. Fréchet, Chair

Professor Matthew Francis

Professor Francis Szoka

Fall 2013

Polymers for Drug Delivery: Extended Circulation and siRNA Transfection

Copyright 2013

by

Paul Henry Kierstead

Abstract

Polymers for Drug Delivery: Extended Circulation and siRNA Transfection

by

Paul Henry Kierstead

Doctor of Philosophy in Chemistry

University of California, Berkeley

Professor Jean M. J. Fréchet, Chair

Polymers are extensively used in the field of drug delivery for many applications. The ability to tailor the physical and *in vivo* properties of polymers allows them to fulfill many roles in drug delivery. Polymers have found value as both direct drug conjugates and coatings of various other delivery systems such as nanoparticles and liposomes. Here, we investigate both types of systems, polymers as liposome coatings and dendrimers directly bound to siRNA.

Chapter 1 presents a brief overview of polymers and macromolecules in the field of drug delivery. Polymeric drug delivery is a very broad and diverse topic, and this chapter mainly addresses areas within the field that relate directly to this dissertation. The history of polymers in drug delivery is presented, and both current capabilities and challenges are discussed.

Chapter 2 describes the synthesis of two distearyl poly(ethylene glycol) (PEG) conjugates for the incorporation into liposomes. PEG has the ability to stabilize lipid membranes, extend circulation half-life *in vivo*, and protect lipid membranes from other unfavorable interactions that may occur in biological settings. Commonly, PEG conjugated to a 1,2-distearoyl-*sn*-glycero-3-phosphoethanolamine (DSPE) lipid anchor is used to install PEG onto the surface of lipid monolayers and bilayers. However, PEG-DSPE can phase separate in the membrane surface leading to its possible expulsion from the membrane. Additionally, PEG causes a broadening of the phase transition temperature which makes its use in thermally responsive liposomes challenging. We present the synthesis of two distearyl PEG molecules and preliminary characterization of their behavior in lipid membranes.

Chapter 3 is an evaluation of polymers for extended circulation. We investigate the physical and *in vivo* properties of a panel of polymers for extended circulation on the surface of liposomes as a model platform, although the conclusions drawn are relevant to many types of drug delivery systems. In this chapter we have synthesized well-defined hydrophilic polymers under controlled polymerization techniques and found that all five polymers investigated have lower intrinsic viscosities to that of PEG under consistent experimental conditions. Furthermore, we show that each polymer extends the circulation half-life of liposomes in mice and rats in comparison to conventional liposomes. We also find an immune response and accelerated blood

clearance of poly(2-methyl-2-oxazoline) (PMOX) coated liposomes upon repeated administration and no such response to the other four polymers in the panel.

Chapter 4 describes the design, synthesis, and *in vitro* characterization of pH-responsive, biodegradable dendrimers for the delivery of siRNA. Polycationic materials have been extensively investigated for the delivery of RNAi, however, the inherent toxicity of such materials is a major drawback to their use. We envisioned that by installing multiple amines to a dendrimer core through pH-sensitive hydrazone linkages we would be able to circumvent this roadblock to RNAi delivery. Furthermore, by designing a biodegradable dendrimer with orthogonal sets of functional groups, we were able to install other delivery aids onto the dendrimer periphery. In an *in vitro* firefly luciferase knockdown assay, polymers displayed decreased toxicity in comparison to other cationic delivery strategies and modest knockdown capabilities.

Chapter 5 gives a brief overview of the findings presented in this dissertation followed by a short perspective on the future of polymers in the field of drug delivery.

Table of Contents

Dedication.....	ii
Acknowledgements.....	iii
Chapter 1: Introduction to Macromolecular Drug Delivery.....	1
Chapter 2: Disterol PEG Conjugates: Synthesis and Incorporation into Liposomes.....	23
Chapter 3: The Evaluation of Polymer for Extended Circulation.....	33
Chapter 4: Development and Analysis of pH-Sensitive Dendrimers for siRNA Delivery.....	54
Chapter 5: Conclusions and Future Perspectives.....	74

Dedication

To my parents, Hal and Chris, who have always given me unwavering love and support.

And to Kelly, for her patience, support, and love throughout and forever.

Acknowledgements

I acknowledge with great gratitude the contributions and guidance of Prof. Jean Fréchet and Prof. Frank Szoka to this research. I consider myself very fortunate to have been able to work with these two extremely gifted researchers during my graduate school career.

I also acknowledge the contributions of all members of the Fréchet and Szoka groups with whom I overlapped. These fellow students and post-docs were fantastic coworkers and many of them became close friends as well. I would like to single out Dr. Derek van der Poll, Dr. Vince Venditto, and Dr. Matt Kade whose assistance and friendship was invaluable to me. Additionally, Dr. Hideaki Okochi, Dr. Saul Kivimae, Dr. Peter Wich, and Tracy Chuong made considerable contributions to the work presented here.

Thank you all, this would not have been possible without you.

Chapter 1

Introduction to Macromolecular Drug Delivery

1.1 IMPORTANCE OF MACROMOLECULES FOR DRUG DELIVERY

The total global pharmaceutical market is steadily increasing, and in 2012, was just shy of \$1 trillion.¹ This growth is partially due to increasingly effective drugs; however, even the most successful drugs have potential for further improved efficacy. In general, drugs work by binding specific sites within the body (e.g. cell surface receptors, inter/intracellular proteins, bacterial enzymes, genetic material, etc.), which then initiates a biological pathway to bring about the intended results. For each drug, the receptor binding properties are critically important, and thus typically optimized. However, a major challenge in many treatment strategies is getting the therapeutic to the correct binding site *in vivo*.

There are many roadblocks that must be overcome between the administration of a drug and target-binding. Specifically for intravenous administration, these roadblocks can include low drug solubility, poor drug stability, undesirable biodistribution, off-target binding, short circulation times, inefficient cellular uptake, and the initiation of an immune response. While many of these factors are often intertwined, improving upon any one of them can lead to improved drug efficacy and reduced side effects. In recent years, macromolecular carriers have become a common route for addressing these issues.

By selecting, or designing, the appropriate macromolecular carrier, it is possible to overcome the delivery barriers that may exist for a given drug, and thus increase its efficacy. The solubility of a drug can be improved by conjugation to a hydrophilic polymer or formulation into the hydrophobic core of a micelle. The stability, circulation lifetime, cellular uptake, and immunogenicity of a drug can be improved by enclosing the drug in a protective layer such as a hydrophilic polymer or in a nanoparticle. Off-target binding and poor biodistribution can also be improved by masking problematic functional groups with a macromolecule until the drug has reached the desired destination. The introduction of a macromolecular carrier can address many of the challenges associated with getting a drug to its site of action, however, macromolecular carriers increase the complexity of the therapeutic.

Some of the complexities relate to the fact that the carrier must be able to efficiently load the drug before administration and release the drug once at the desired location. Furthermore, after delivery of the drug, the carrier must be eliminated from the body without any long term side effects. These requirements make the selection of the correct macromolecular carrier critically important, and with the right carrier, drug efficacy can be greatly improved.

1.2 HISTORY OF MACROMOLECULES FOR DRUG DELIVERY

By the mid 20th century it was becoming increasingly clear that both the temporal and spatial *in vivo* properties of a therapeutic are very important. Borrowing from the agriculture industry, the term “selective toxicity” began being applied to drug therapies in an effort to increase efficacy and decrease undesired side effects.² While this concept originally described on-target vs. off-target effects of a drug, it was soon realized that these effects were also dependent on the concentration of a drug at each specific site. Moreover, researchers began to understand that the relationship between administered dose and drug concentration at specific sites *in vivo* is both difficult to predict and imperative to the success of a drug.^{3,4} It was observed

that achieving a therapeutic effect is dependent on attaining the correct concentration of a drug, at a specific target site, over a suitable duration of time. In order to modify the pharmacokinetics and biodistribution of a drug, researchers began modifying current small molecule drugs, often taking advantage of reversible modifications that leave a drug in its original form once at its site of action. When these modifications to a drug are small, the new molecule is often referred to as a *prodrug*. However, when these modifications involve conjugation or encapsulation into a macromolecule, the macromolecule is typically referred to as a drug delivery vehicle or carrier. Today, drug delivery vehicles include many different varieties of macromolecular and supramolecular structures, and two of the most successful and prevalent classes of drug delivery vehicles are liposomes and synthetic polymers.

1.3 LIPOSOMES FOR DRUG DELIVERY

1.3.1 Introduction to Liposomes

Liposomes are self-assembled, spherical vesicles with a lipid bilayer membrane (Figure 1.1). These vesicles generally enclose an aqueous core, and can range in size from tens of nanometers to micrometers in diameter.⁵ Typically, the lipid bilayer is composed of natural or “nature inspired” synthetic lipid molecules with a hydrophilic head group and a hydrophobic tail. There are a very large number of both hydrophilic head groups and hydrophobic tails that can be used to formulate liposomes. Common lipid head group classes include phosphatidylcholines (PC), phosphatidylethanolamines (PE), phosphatidylglycerol (PG), and phosphatidylserine (PS). Lipid tails range from short (C4) to long (C28), saturated to polyunsaturated, and natural to synthetically functionalized. Additionally, other types of lipids, including sterols, are often formulated into liposomes. By selecting specific lipids in specific ratios, both the physical and *in vivo* properties of a liposome can be tailored to fit a desired application. Size, stability, polydispersity, number of bilayers, immunogenicity, circulation half-life, and cellular uptake are just a few factors dependent on the specific lipids incorporated into a liposome.⁵

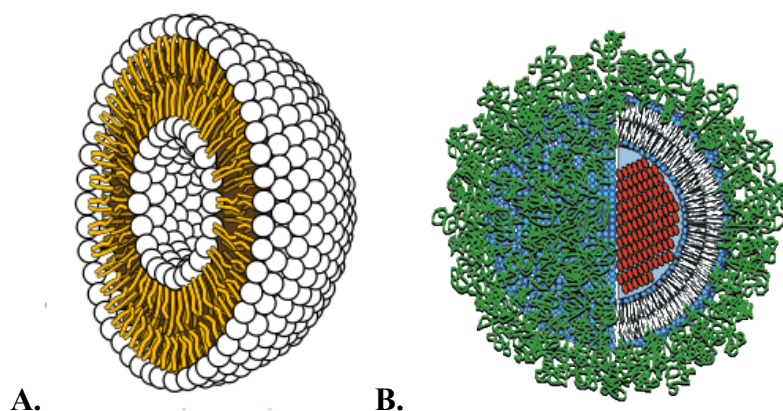


Figure 1.1 Liposomes are small, self-assembled vesicles composed of lipid bilayers with an aqueous core. A: Cartoon representation of a cross-section of a conventional liposome. B: Liposome with PEG (green) coating and drug (red) loaded in the aqueous core.

1.3.2 Liposomes for Drug Delivery

As is the case with most successful drug carriers, liposomes have multiple characteristics that can be tailored to make them ideal for specific drug delivery applications. First, the physical properties of liposomes, including both size and stability, are easily tailored through lipid composition and formulation techniques.⁵ Second, the lipid bilayer is able to protect a drug from degradation that would otherwise be unstable *in vivo*. This also means that a drug will remain biologically inactive until released from the liposomes and exposed to the body. Furthermore, once integrated into a liposome, pharmacokinetics and biodistribution are generally dictated by the carrier rather than the free drug. Lastly, the ability of liposomes to uptake and release a drug at desired times and locations make liposomes an attractive platform for drug delivery.⁶

1.3.3 Sterically Stabilized Liposomes

Conventional liposomes (CL), those without steric stabilization, have been used for most liposomal drug delivery applications. These liposomes are cleared from circulation by the phagocytic cells of the Mononuclear Phagocyte System (MPS) and accumulate mostly within the spleen and liver.⁷ Sterically stabilized liposomes (SL), however, prevent protein adsorption to the lipid membrane, conceal surface charge, reduce liposome adhesion to cell surfaces, and generally have longer circulation times. The first SLs incorporated glycolipids such as GM1 ganglioside, cerebroside sulfate, or phosphatidylinositol.^{8,9} Each of these glycolipids has a large carbohydrate domain that helps protect the liposome surface from interactions with proteins and macrophages, and decreases uptake by the liver and spleen. This causes dose-independent kinetics, which is not seen with CL.^{7,10} Today, the most common method of steric stabilization of liposomes is to incorporate a hydrophilic polymer, most commonly poly(ethylene glycol) (PEG), into the bilayer to shield the membrane surface. Polymers can sterically prevent the adsorption of opsonins in the blood and greatly extend circulation times, which in turn allows for either passive or active targeting.

1.4 POLYMERS FOR DRUG DELIVERY

1.4.1 History of Polymers for Drug Delivery

The emergence of polymer drug delivery closely coincided with that of liposomal drug delivery. In the 1940's, N-vinylpyrrolidone (PVP) gained traction as a blood plasma substitute,¹¹ and in 1955 Jatzkewitz conjugated glycyl-L-leucine-mescaline to PVP as one of the first ever polymer drug conjugates.¹² However, the field of polymer drug-delivery did not take off until the early 1970's with some of the earliest reports coming from Roseman's investigation of silicone polymers for steroid delivery,¹³ Rudel's investigation of polydimethylsiloxane also for steroid delivery,¹⁴ Bankers series on drug entrapment and release with polymeric materials,^{15,16,17} and Wise's lactic/glycolic acid copolymer delivery systems.^{18,19} By 1975, the potential of polymers as drug carriers had been clearly established.²⁰

In 1977, Abuchowski first observed the ability of PEG to alter immunological properties of bovine serum albumin.²¹ Abuchowski followed up this discovery by also demonstrating that when *E. Coli* L-asparaginase is conjugated to PEG it is no longer

immunogenic.²² This material was FDA approved in 1994, becoming the third clinically available polymer therapeutic, behind styrene maleic acid neocarcinostatin (SMANCS) in 1993 and PEG-adenosine deaminase in 1990.²³ Today, there are 11 polymer-drug direct conjugates on the market (not including other PEGylated materials such as Doxil®), and many more in clinical development.^{23,24,25,26,27,28}

1.4.2 Polymer Architectures for Drug Delivery

Polymers can be synthesized in many shapes and sizes, and both shape and size are critical factors when used for drug delivery.²⁹ The ideal size of a polymer for drug delivery very much depends on the system of delivery. For example, Micera®, an FDA approved drug, is composed of a 30 kDa PEG chain conjugated to a continuous erythropoietin receptor activator, where another FDA approved drug, Doxil®, incorporates much smaller 2 kDa PEG chains into the bilayer of liposomes.^{24,23} Low molecular weight polymers allow higher wt% drug loading, demonstrate lower long-term accumulation in the body, and when multiple low weight polymers are utilized on a single carrier to provide steric protection, they can outperform single, large polymer chains. However, high molecular weight polymers lead to increased circulation and better steric protection in systems where the number of polymer chains is limited.^{25,26} Additional properties are also size-dependant, including solubility, cellular uptake and trafficking, and biodistribution.

Similar to molecular weight, shape, also known as polymer architecture, plays a vital role in drug delivery.^{30,31} Thus far, the simplest architecture, linear homopolymers, have been most successful in the clinic.²⁶ Still, more complex polymer architectures for drug delivery can offer significant advantages. Block copolymers,^{32,33,34} branched and hyperbranched polymers,^{35,36} comb/brush polymers,^{37,38,39,40} star polymers,^{41,42,43} cyclic polymers,^{44,45} crosslinked polymer hydrogels,^{46,47,48} dendrimers,^{30,49,49,50,51} and other variations offer rewards such as increased drug loading sites, multifunctionality, multivalent binding, tailored drug loading and release rates, and steric protection for the specified system (Figure 1.2). Additionally, physical and in vivo properties are influenced by architecture, including solubility, viscosity, cellular uptake and trafficking, pharmacokinetics, and biodistribution.⁵²

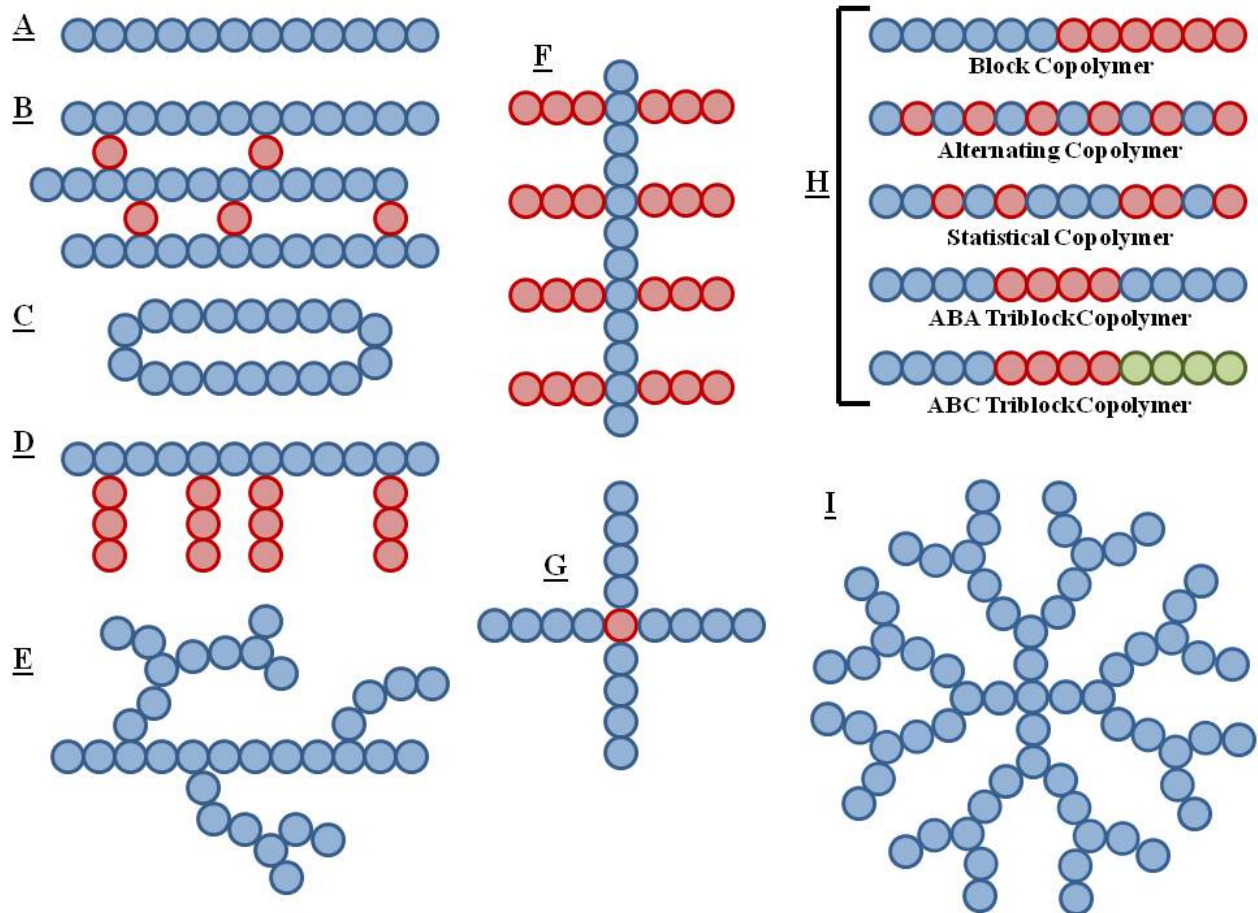


Figure 1.2: Polymer architectures for drug delivery: linear homopolymer (A), crosslinked polymer (B), cyclic polymer (C), comb polymer (D), branched/hyperbranched polymer (E), brush polymer (F), star polymer (G), block copolymers (H), dendrimer (I)

1.4.3 Polymer Synthesis

Even for the simplest architecture, linear homopolymers, there are a large variety of polymerization techniques available. The choice of polymerization technique for a specific polymer is dictated by the monomer. In a step-growth polymerization, bifunctional monomers react at both functional sites to first form dimers, then trimers, oligomers, and ultimately full length polymers.^{53,54} For this type of polymer, a high degree of polymerization is necessary to reach high molecular weights, which requires highly pure monomers. Additionally, due to lack of control during polymerization, these polymers often suffer from high polydispersity.^{4,55} Step growth polymers can be synthesized through addition polymerizations or condensation polymerizations. In addition polymerizations, each monomer is added to the polymer chain without releasing a small molecule byproduct.⁵⁶ Examples of polymers formed through addition polymerizations include poly- β -aminoesters⁵⁷ and polyurethanes,⁵⁸ In condensation polymerizations, each reaction with a new monomer releases a small molecule, commonly water.

Examples of polymers formed through condensation polymerizations include polyesters and polyamides.⁵³

Chain-growth polymerizations are those in which monomers are added to the end of a growing polymer chain one at a time.⁵⁹ Chain-growth polymerizations typically require an initiator to begin the polymerization, and can often lead to polymer with low polydispersity depending on the type of chain growth polymerization. Many chain-growth polymerizations are living, meaning that unless an irreversible termination step has taken place, polymer growth can be stopped and restarted by the removal or addition of monomer.⁶⁰ The two most common types of chain-growth polymerizations are ring-opening polymerizations and radical polymerizations. Ring-opening chain-growth polymers such as PEG or PMOX are those in which a growing polymer chain reacts with and opens a cyclic monomer.⁶¹ In radical polymerizations, a radical initiator is used to begin polymerization, and chain growth occurs through the reaction of a radical at the chain end with additional monomers.⁵⁹ Common polymers synthesized through radical polymerizations include polyethylene and polyacrylamides. Many techniques have been developed to gain strict control over the molecular weight and the polydispersity index (PDI) of polymers formed through radical polymerizations. Atom transfer radical polymerization (ATRP),⁶² reversible addition-fragmentation chain transfer (RAFT),⁶³ and nitroxide mediated polymerization (NMP)⁶⁴ are three common radical polymerization techniques for achieving well-defined polymers with low PDI's. These are also sometimes referred to as reversible-deactivation polymerizations because at any given time during the polymerization the majority of the polymer chain ends are reversibly capped by a chain transfer agent. This means that there are only a very few growing chains at once which helps prevent unwanted termination events. In these polymerizations, monomer selection is limited and it is critical to match the reactivity of monomers with the reactivity of the chain transfer agents.⁶⁶

1.4.4 Drug Loading and Release

Loading a drug into a polymeric carrier has been accomplished through numerous techniques. In general, these techniques can be classified as non-covalent and covalent. In either case, the drug must be efficiently taken up by the carrier, and released at the right time and location. Examples of non-covalent drug loading into polymer carriers include the encapsulation of hydrophobic drugs in the core of polymer micelles,³⁴ multivalent electrostatic binding to DNA or RNA,⁶⁵ loading of drugs into the interstitial space within dendrimers,⁶⁶ and physical entrapment in polymer hydrogels⁴⁶. Release from these systems can be passive,⁶⁷ occurring slowly over a long period of time, or triggered by an internal or external trigger. These triggers include changes in temperature,⁶⁸ pH,⁶⁹ and light,⁷⁰ and usually result in either a conformational change or degradation of the carrier in order to release the drug. When the payload is attached to the carrier through covalent bonds, release typically occurs by breaking a bond in the linkage between the payload and carrier. In these cases, the linkage can also degrade slowly under physiological conditions for a slow passive release or degrade rapidly as a result of any of the same triggers utilized for non-covalent release.^{71,72,73}

1.4.5 Polymers for Extended Circulation

The majority of the success that polymer drug delivery vehicles have seen is due to their ability to extend circulation in the blood. This allows enough time for a drug to have a slow, passive release, or accumulate at the desired location. A slow release combined with long circulation allows for a steady drug concentration in the blood over extended periods. This way, an effective drug concentration can be maintained in circulation for extended periods, where as a naked drug would have high spikes in concentration upon administration, followed by rapidly decreasing concentration until below its ineffective point (Figure 1.3). Examples of polymers that have been shown to extend the circulation times of therapeutics *in vivo* include PEG, HPMA (poly[N-(2-hydroxypropyl) methacrylamide]),⁷⁴ PVP (poly(vinylpyrrolidone)),²⁵ PMOX (poly(2-methyl-2-oxazoline)),^{75,76,77} PAcM (poly(N-acryloyl morpholine)),⁷⁸ and PG (polyglycerol)⁷⁹ (Figure 1.4).

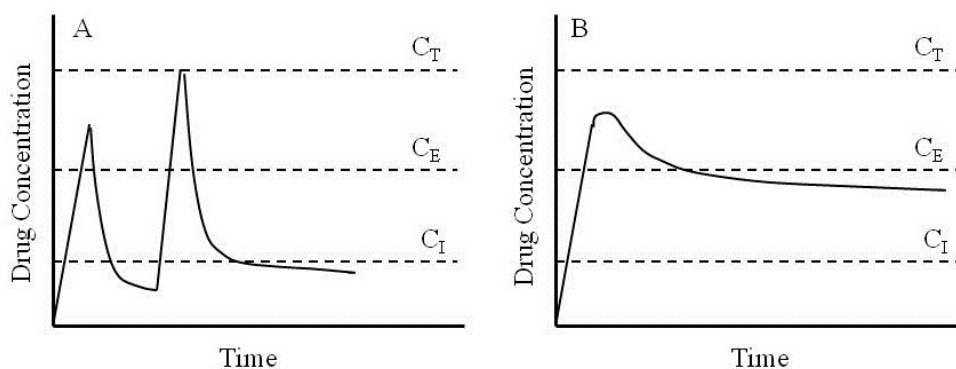


Figure 1.3: Free drug nearly reaches the concentration where it becomes toxic (C_T) upon administration, then the concentration quickly drops through the effective concentration (C_E) and approaches ineffective concentration (C_I) until another dose is administered (A). Slow release carriers regulate the concentration of the drug to keep it in the effective concentration range for as long as possible (B).

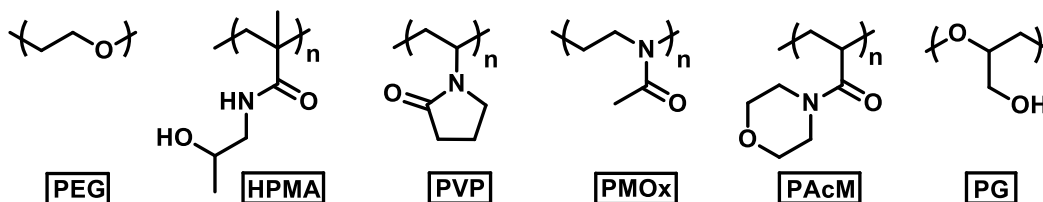


Figure 1.4: Selected polymers for extended circulation: PEG (poly(ethylene glycol)), HPMA (poly[N-(2-hydroxypropyl) methacrylamide]), PVP (poly(vinylpyrrolidone)), PMOX (poly(2-methyl-2-oxazoline)), PAcM (poly(N-acryloyl morpholine)), and PG (polyglycerol)

Without a specific strategy for increasing circulation time, small molecule drugs, liposomes, nanoparticles, and other drug carriers are usually quickly removed from circulation. This rapid clearance is due to both size based renal clearance and the action of the MPS. Materials under 10 nm, or about 5 kDa, are easily removed from circulation by renal clearance.⁸² Materials that are above the threshold for renal clearance are susceptible to opsonization followed by phagocytic uptake.

Phagocytes typically do not directly recognize foreign materials, but rather recognize opsonins that have associated with the foreign material.⁸⁰ Common opsonins include complement proteins such as C3, C4, and C5 immunoglobulins but, in general, can be any serum component that aids phagocytic uptake.⁸¹ These opsonins are preexisting serum factors and come into contact with nearly all other materials in circulation (including injected therapeutics) through simple Brownian motion. The binding of opsonins to foreign materials in the blood can occur through a number of attractive forces, including van der Waals forces, electrostatic, ionic, hydrophobic/hydrophilic, hydrogen bonding, and others.⁸² Once a material has been opsonized, it can be recognized by phagocytes. Specifically, cell surface receptors on phagocytes recognize bound opsonins and initiate phagocytic uptake. After endocytosis, phagocytes begin secreting enzymes and oxidating molecules to break down the phagocytosed material.⁸³ If the phagocytosed material cannot be broken down, it will be sequestered and start to accumulate in the organs of the mononuclear phagocytic system (MPS), such as the spleen or liver. Hydrophilic polymers can prevent this clearance pathway by preventing the initial binding of opsonins.⁸⁴

The most successful polymer for increasing circulation time is PEG. PEG accomplishes extended circulation by preventing the binding of opsonins to its payload. This is achieved by providing steric forces that either are greater than the opsonin's attractive forces, or prevent opsonins from getting within the range where attractive forces between the opsonins and the payload occur.⁸⁵ As opsonins approach a PEGylated therapeutic, they first interact with the surrounding PEG chains. Upon first interaction with the PEG chains, little repulsive force will be applied. However, as the flexible PEG chains are compressed, the conformation of the PEG enters a more condensed, higher energy state. This creates a repulsive force and can either prevent the opsonins from reaching potential binding areas on the therapeutic, or provide a strong enough repulsive force to overcome the attractive forces acting upon the opsonins.⁸² Materials that are charged or hydrophobic are normally recognized very quickly by opsonins that are attracted to those physical characteristics; however, the attachment of PEG can prevent interaction between those materials and their opsonins through steric repulsion.^{86,87,88,89} The ability of PEG to provide these repulsive steric forces is dependent on polymer size, graft density, and flexibility.

When conjugated to a surface such as liposomes or nanoparticles, polymer conformation plays a critical role in preventing opsonin interaction. For PEG, conformation is heavily dependent on chain length and graft density. Longer chains at lower graft density tend to take up mushroom conformations, while shorter chains at high graft density lead to semi-linear brush conformations.^{90,91} It is important for the graft density to be high enough that there are no gaps in PEG coverage, but too high of a graft density decreases PEG mobility and thus decreases the steric repulsive forces from the PEG.⁹² The ideal graft density is one that provides complete surface coverage while allowing for maximum chain mobility. It has been proposed that this compromise occurs when either the hydrodynamic thickness of the protective layer is 5% of the

total particle diameter or greater than twice the radius of the free polymer coil in dilute solution.^{92,93}

In some cases, polymers can extend circulation even when they fail to prevent the adsorption of opsonizing factors. For example, the PEG chains on Doxil ® are not able to completely suppress the opsonization process, and PEGylated liposomes can initiate the complement system through both classical and alternative pathways.⁹⁴ In these cases, it was found that complement activation was linked to negatively charged lipids on the liposome surface. Even with the protective PEG layer, the complement component iC3b was able to bind the surface of the liposome. However, this complement activation proved insignificant as the PEG was still able to sterically prevent the bound iC3b from interacting with the corresponding macrophage complement receptor.

In a similar fashion to the prevention of opsonization, steric forces from polymers can prevent other disadvantageous interactions while in circulation. For instance, polymers can prevent serum enzymes from degrading a therapeutic before it reaches its target site⁸⁵. Polymers imbedded into a lipid bilayer have also been shown to decrease interaction with hydrophilic small molecules, amphiphilic monomers and micelles, viral fusion peptides, pH sensitive polymers, and binding ligands/receptors.⁹⁵ Furthermore, Evans *et. al.* have demonstrated sterically stabilized liposomes have reduced adhesion to other membrane surfaces.⁹⁶ The repulsive steric forces produced by PEG in a lipid bilayer have been measured by Kenworthy *et. al.* through x-ray diffraction⁹⁰ and by Kuhl *et. al.* with a surface force apparatus.⁹⁷ Additionally, Peracchia *et. al.* have directly observed the ability of PEG chains to prevent protein adhesion through freeze-fracture transmission electron microscopy (TEM).⁹⁸

1.4.6 Polymer Immunogenicity

As previously mentioned, one way polymers are able to increase circulation in the blood stream is by minimizing immune response to their conjugate. This means that it is also necessary for the polymer itself to avoid initiating an immune response, though this is not always the case. Immunogenicity of a polymer can compromise animal studies when evaluating the safety and pharmacodynamic properties of drug conjugates, and possibly reduce the safety and efficacy of the final product in the clinic.

Most polymers do elicit some type of immune response under specific conditions, including both vinyl polymers⁹⁹ and PEG.¹⁰⁰ In 1984, Richter and Akerblom found preexisting anti-PEG antibodies in 0.2 % of healthy donors and 3.3 % of allergic patients.¹⁰¹ Furthermore, after a single treatment with PEGylated ragweed extract and honey bee venom, anti-PEG antibodies were found in 50% of the patients. However, that number dropped to 28.5% after two years of continuous treatment.

More recent reports from Garratty *et. al.* place the occurrence of anti-PEG antibodies in normal donors as high as 25%.^{102,103} This large difference in percent of patients with preexisting anti-PEG antibodies could be attributed to increasing exposure to products containing PEG in modern times.¹⁰⁴ However, there are other possible explanations as well, including greater sensitivity in the experimental assays or missing controls used in Garratty's assay.¹⁰⁰ The most recent report on the percentage of normal donors exhibiting anti-PEG antibodies seems to suggest the latter; in 2011 Liu *et. al.* found only 4% of 350 healthy blood donors exhibit

antibodies against PEG.¹⁰⁵ Other studies by Tillmann *et. al.* found preexisting anti-PEG antibodies in 44% of patients with hepatitis C but only in 6.9% of healthy blood donors.¹⁰⁶

1.4.7 Accelerated Blood Clearance Effect

The Accelerated Blood Clearance (ABC) effect is a very specific immune response to PEG, first observed by Dams *et. al.*¹⁰⁷ in 2000 and extensively further investigated by Ishida and colleagues. With the ABC effect, an initial dose of a PEGylated material (or free PEG) initiates anti-PEG IgM production, and subsequent doses of PEGylated materials are quickly recognized and removed from circulation (Figure 1.5). During this T-cell independent, humoral immune response, the first dose of a PEGylated material (or free PEG) binds preexisting, low affinity PEG receptors on the surface of splenic B-cells.^{108,109} This then initiates the production of anti-PEG IgM. The production of anti-PEG IgM takes 3-5 days and thus has minimal effect on the first dose of a PEGylated material. However, if a second dose of PEGylated material is administered 5-28 days after the first, the PEG will no longer be able to provide stealth and the presence of anti-PEG IgM leads to rapid clearance from circulation and accumulation in the liver and spleen. This effect has been observed in mice,¹¹⁰ rats,¹⁰⁷ rabbits,¹¹¹ beagles,¹¹⁰ monkeys,¹⁰⁷ and humans¹¹² with many types of PEGylated materials including liposomes,¹⁰⁷ micelles,¹¹³ nanoparticles,¹¹⁴ and proteins.¹¹⁵ A number of factors influence the degree of the immune response to a PEGylated material, including overall conjugate size,¹¹³ PEG molecular weight,¹¹⁶ PEG end groups,¹¹⁷ and payload.¹¹⁸

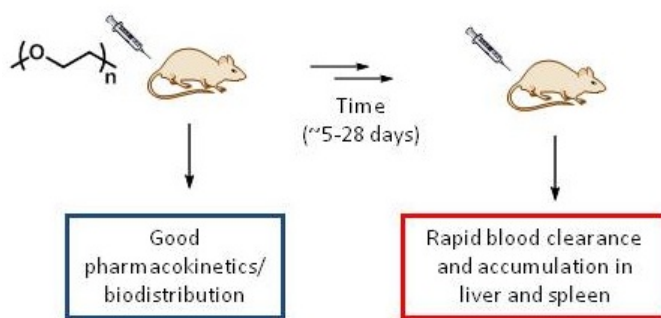


Figure 1.5. The ABC effect is caused by production of anti-PEG IgM following the first dose of a PEGylated material. In this case, first dose of the PEGylated material typically demonstrates long circulation times and good biodistribution. However, a second dose administered 5-28 days later will be rapidly cleared from circulation and accumulate heavily in the liver and spleen.

The ABC effect can lead to unexpected pharmacokinetics, decreased drug efficacy, and increased side effects; however, it is not observed in all treatment strategies involving PEGylated materials. When the payload is a cytotoxic drug (i.e. Doxil®), the production of anti-PEG IgM is inhibited, likely due to the toxic drug interfering with B-cell proliferation and IgM

production.¹¹⁸ High doses of PEGylated materials also induce minimal anti-PEG IgM production because of extensive over-crosslinking of the surface receptors of B-cells.¹⁰⁸ Although both PEG-conjugates with a toxic drug and high doses of PEGylated material do not effectively initiate an immune response, a patient that has recently been exposed to PEG from some other source may already have anti-PEG antibodies in their blood. These preexisting antibodies can cause rapid clearance regardless of toxicity of the payload or the size of the dose.¹¹⁸

Other methods for avoiding the ABC effect include macrophage depletion either before the induction dose or the subsequent doses, administering the second dose outside the 5-28 day window where the ABC effect is the greatest, or the extreme approach of removing the spleen to prevent IgM production.^{109,118} Directly related to the topic, recent reports suggest that two other polymers, PG⁷⁹ and PVP¹¹⁹ do not exhibit an ABC effect and therefore could potentially be used in place of PEG to extend the circulation of therapeutics that require multiple doses. I am interested in confirming and extending these findings to other polymer types.

1.4.8 Additional Potential Benefits of Polymer Drug Delivery

Polymers are able to load, traffic, and deliver a huge range of drugs because of their versatility. Polymers can efficiently load and release drugs, both passively and through triggered release mechanisms, protect a drug from degradation *in vivo*, and greatly extend the circulation times of drugs. Furthermore, polymers can increase solubility of a drug, increase cellular uptake,^{120,121,122} and aid in endosomal escape.^{123,124} Polymers also allow for targeting, either passive targeting through the EPR effect¹²⁵ or active targeting.¹²⁶

1.5 CONCLUSION

Polymers are important tools in increasing the efficacy of many drugs. These macromolecules alter the physical and physiological properties of the drug and can provide a number of services to improve upon the naked drug. These services include protection from degradation, extended circulation, increased solubility, increased cellular uptake, aid in endosomal escape, decreased side-effects, and passive or active targeting. However, it is rare that a single drug delivery vehicle can offer all of these advantages, and the selection of the appropriate carrier is highly dependent on the specific drug to be delivered. Each drug delivery system has its limitations, which are vital to some applications and irrelevant to others. Two examples of these limitations include an immune response to PEG upon multiple doses under specific conditions¹⁰⁷ and the phase separation and ejection of PEG chains from certain stealth liposomes.¹²⁷ Moreover, general challenges across each platform exist for specific drugs.

The success polymers have experienced in the clinic as aids in drug delivery has been, for the most part, limited to the delivery of macromolecules. Both polymer-coated liposomes and protein-polymer conjugates have found success, however, small molecule polymer conjugates have not been able to replicate that success. A major reason for this is that the most successful synthetic polymer in the clinic, PEG, lacks available drug loading sites on its backbone, resulting in low weight percent drug loading. Furthermore, systems such as liposomes offer many of the same advantages gained with polymer drug delivery, and often offer improved characteristics such as higher drug loading and biodegradability.

While extremely versatile platforms for many drugs, there are systems in which delivery with a polymeric carrier is very challenging. Polymer drug loading and/or release at the proper time and location can be problematic depending on both the drug and the ailment. An example of this is RNAi delivery, where a clinically relevant carrier able to achieve steric protection, efficient loading, and release at the proper location has remained elusive.⁶⁵ It is clear that polymers are valuable tools for drug delivery, however, each system needs to be specifically tailored to the explicit application and general shortcomings of polymers for drug delivery can still be improved upon.

1.6 REFERENCES

1. *IMS Health Market Prognosis*.
http://www.imshealth.com/deployedfiles/imshealth/Global/Content/Corporate/Press%20Room/Total_World_Pharma_Market_Topline_metrics_2012-17_regions.pdf (2013).
2. Albert, A. Selective toxicity. *Nature* **165**, 12–6 (1950).
3. Kristensen, M. *et al.* Drug elimination and renal function. *J. Clin. Pharmacol.* **14**, 307–308 (1974).
4. Gibaldi, M. & Perrier, D. Route of administration and drug disposition. *Drug Metab. Rev.* **3**, 185–99 (1974).
5. Torchilin, V., Weissig, V. *Liposomes: A Practical Approach*. 396 (Oxford University Press, 2003).
6. Janoff, Andrew S., ed. *Liposomes: rational design*. Informa Healthcare, 1999.
7. Allen, T. M. & Hansen, C. Pharmacokinetics of stealth versus conventional liposomes: effect of dose. *Biochim. Biophys. Acta - Biomembr.* **1068**, 133–141 (1991).
8. Gabizon, A. & Papahadjopoulos, D. Liposome formulations with prolonged circulation time in blood and enhanced uptake by tumors. *Proc. Natl. Acad. Sci.* **85**, 6949–6953 (1988).
9. Gabizon, A. & Papahadjopoulos, D. The role of surface charge and hydrophilic groups on liposome clearance in vivo. *Biochim. Biophys. Acta - Biomembr.* **1103**, 94–100 (1992).
10. Papahadjopoulos, D. *et al.* Sterically stabilized liposomes: improvements in pharmacokinetics and antitumor therapeutic efficacy. *Proc. Natl. Acad. Sci.* **88**, 11460–11464 (1991).
11. Hecht, G., H. W. Periston, ein neuer Blutflüssigkeitsersatz. *Münch Med Wochenschr* **90**, 11–15 (1943).

12. Jatzkewitz, H. Peptamin (glycyl-L-leucyl-mescaline) bound to blood plasma expander (polyvinylpyrrolidone) as a new depot form of a biologically active primary amine (mescaline). *Z. Naturforsch* **10**, 27–31 (1955).
13. Roseman, T. J. & Higuchi, W. I. Release of medroxyprogesterone acetate from a silicone polymer. *J. Pharm. Sci.* **59**, 353–357 (1970).
14. Kind, F. A. & Rudel, H. W. Sustained release hormonal preparations. *Eur. J. Endocrinol.* **65**, S5–S30 (1970).
15. Goodman, H. & Banker, G. S. Molecular-scale drug entrapment as a precise method of controlled drug release I: Entrapment of cationic drugs by polymeric flocculation. *J. Pharm. Sci.* **59**, 1131–1137 (1970).
16. Rhodes, C. T., Wai, K. & Banker, G. S. Molecular scale drug entrapment as a precise method of controlled drug release III: In vitro and In vivo studies of drug release. *J. Pharm. Sci.* **59**, 1581–1584 (1970).
17. Boylan, J. C. & Banker, G. S. Molecular-scale drug entrapment as a precise method of controlled drug release IV: Entrapment of anionic drugs by polymeric gelation. *J. Pharm. Sci.* **62**, 1177–1184 (1973).
18. Wise, D. L. *et al.* Sustained release of an antimalarial drug using a copolymer of glycolic/lactic acid. *Life Sci.* **19**, 4–10 (1976).
19. Schwope, A. D., Wise, D. L. & Howes, J. F. Lactic/glycolic acid polymers as narcotic antagonist delivery systems. *Life Sci.* **17**, 1877–1885 (1975).
20. Ringsdorf, H. Structure and properties of pharmacologically active polymers. *J. Polym. Sci. Polym. Symp.* **51**, 135–153 (2007).
21. Abuchowski, A., van Es, T., Palczuk, N. C. & Davis, F. F. Alteration of immunological properties of bovine serum albumin by covalent attachment of polyethylene glycol. *J. Biol. Chem.* **252**, 3578–3581 (1977).
22. Abuchowski, A. *et al.* Cancer therapy with chemically modified enzymes. I. Antitumor properties of polyethylene glycol-asparaginase conjugates. *Cancer Biochem. Biophys.* **7**, 175–86 (1984).
23. Duncan, R. The dawning era of polymer therapeutics. *Nat. Rev. Drug Discov.* **2**, 347–60 (2003).
24. Zhang, Y., Chan, H. F. & Leong, K. W. Advanced materials and processing for drug delivery: the past and the future. *Adv. Drug Deliv. Rev.* **65**, 104–20 (2013).

25. Knop, K., Hoogenboom, R., Fischer, D. & Schubert, U. S. Poly(ethylene glycol) in drug delivery: pros and cons as well as potential alternatives. *Angew. Chem. Int. Ed. Engl.* **49**, 6288–308 (2010).
26. Alconcel, S. N. S., Baas, A. S. & Maynard, H. D. FDA-approved poly(ethylene glycol)–protein conjugate drugs. *Polym. Chem.* **2**, 1442 (2011).
27. Pasut, G. & Veronese, F. M. PEG conjugates in clinical development or use as anticancer agents: an overview. *Adv. Drug Deliv. Rev.* **61**, 1177–88 (2009).
28. Canal, F., Sanchis, J. & Vicent, M. J. Polymer--drug conjugates as nano-sized medicines. *Curr. Opin. Biotechnol.* **22**, 894–900 (2011).
29. Bahadur, D. *et al.* The effects of polymeric nanostructure shape on drug delivery. *Adv. Drug Deliv. Rev.* **63**, 1228–1246 (2011).
30. Lee, C. C., MacKay, J. A., Fréchet, J. M. J. & Szoka, F. C. Designing dendrimers for biological applications. *Nat. Biotechnol.* **23**, 1517–26 (2005).
31. Fox, M. E., Szoka, F. C. & Fréchet, J. M. J. Soluble polymer carriers for the treatment of cancer: the importance of molecular architecture. *Acc. Chem. Res.* **42**, 1141–51 (2009).
32. Zhang, Q., Ko, N. R. & Oh, J. K. Recent advances in stimuli-responsive degradable block copolymer micelles: synthesis and controlled drug delivery applications. *Chem. Commun. (Camb)*. **48**, 7542–52 (2012).
33. Adams, M. L., Lavasanifar, A. & Kwon, G. S. Amphiphilic block copolymers for drug delivery. *J. Pharm. Sci.* **92**, 1343–55 (2003).
34. Peppas, N. A., Rösler, A., Vandermeulen, G. W. M. & Klok, H.-A. Advanced drug delivery devices via self-assembly of amphiphilic block copolymers. *Adv. Drug Deliv. Rev.* **64**, 270–279 (2012).
35. Perumal, O. *et al.* Effects of branching architecture and linker on the activity of hyperbranched polymer-drug conjugates. *Bioconjug. Chem.* **20**, 842–6 (2009).
36. Shuai, X., Merdan, T., Unger, F., Wittmar, M. & Kissel, T. Novel Biodegradable Ternary Copolymers hy -PEI- g -PCL- b -PEG: Synthesis, Characterization, and Potential as Efficient Nonviral Gene Delivery Vectors. *Macromolecules* **36**, 5751–5759 (2003).
37. Graft copolymers as drug delivery systems. US WO 2009034053 A1 (2013). at <<http://www.google.com/patents/US8518444>>
38. Chen, B. *et al.* Synthesis and properties of star-comb polymers and their doxorubicin conjugates. *Bioconjug. Chem.* **22**, 617–24 (2011).

39. Yu, Y. *et al.* Well-defined degradable brush polymer-drug conjugates for sustained delivery of Paclitaxel. *Mol. Pharm.* **10**, 867–74 (2013).
40. Du, J.-Z., Tang, L.-Y., Song, W.-J., Shi, Y. & Wang, J. Evaluation of polymeric micelles from brush polymer with poly(epsilon-caprolactone)-b-poly(ethylene glycol) side chains as drug carrier. *Biomacromolecules* **10**, 2169–74 (2009).
41. Liu, J., Duong, H., Whittaker, M. R., Davis, T. P. & Boyer, C. Synthesis of functional core, star polymers via RAFT polymerization for drug delivery applications. *Macromol. Rapid Commun.* **33**, 760–6 (2012).
42. Etrych, T. *et al.* Biodegradable star HPMA polymer–drug conjugates: Biodegradability, distribution and anti-tumor efficacy. *J. Control. Release* **154**, 241–248 (2011).
43. Li, X. *et al.* Amphiphilic multiarm star block copolymer-based multifunctional unimolecular micelles for cancer targeted drug delivery and MR imaging. *Biomaterials* **32**, 6595–6605 (2011).
44. Nasongkla, N. *et al.* Dependence of pharmacokinetics and biodistribution on polymer architecture: effect of cyclic versus linear polymers. *J. Am. Chem. Soc.* **131**, 3842–3 (2009).
45. Hennink, W. E., Chen, B., Jerger, K., Fréchet, J. M. J. & Szoka, F. C. The influence of polymer topology on pharmacokinetics: Differences between cyclic and linear PEGylated poly(acrylic acid) comb polymers. *J. Control. Release* **140**, 203–209 (2009).
46. Hoare, T. R. & Kohane, D. S. Hydrogels in drug delivery: Progress and challenges. *Polymer (Guildf)*. **49**, 1993–2007 (2008).
47. Peppas, N. A., Qiu, Y. & Park, K. Environment-sensitive hydrogels for drug delivery. *Adv. Drug Deliv. Rev.* **64**, 49–60 (2012).
48. Gupta, P., Vermani, K. & Garg, S. Hydrogels: from controlled release to pH-responsive drug delivery. *Drug Discov. Today* **7**, 569–79 (2002).
49. Gillies, E. R. & Fréchet, J. M. J. Dendrimers and dendritic polymers in drug delivery. *Drug Discov. Today* **10**, 35–43 (2005).
50. Cheng, Y. *Dendrimer-Based Drug Delivery Systems: From Theory to Practice* (Wiley Online Library, 2012) at <<http://onlinelibrary.wiley.com/book/10.1002/9781118275238>>
51. Nanjwade, B. K., Bechra, H. M., Derkar, G. K., Manvi, F. V. & Nanjwade, V. K. Dendrimers: Emerging polymers for drug-delivery systems. *Eur. J. Pharm. Sci.* **38**, 185–196 (2009).

52. Qiu, L. Y. & Bae, Y. H. Polymer architecture and drug delivery. *Pharm. Res.* **23**, 1–30 (2006).
53. Flory, P. J. *Principles of Polymer Chemistry*. 672 (Cornell University Press, 1953). at <<http://books.google.com/books?hl=en&lr=&id=CQ0EbEkT5R0C&pgis=1>>
54. Weil, E. D., Mark, H., Bikales, N., Overberger, C. C., & Menges, G. *Encyclopedia of polymer science and engineering*. (Wiley-Interscience, 1990).
55. *Synthetic Methods in Step-Growth Polymers*. (John Wiley & Sons, Inc., 2003). doi:10.1002/0471220523
56. Ravve, A. *Principles of Polymer Chemistry (Google eBook)*. 816 (Springer, 2012). at <<http://books.google.com/books?hl=en&lr=&id=MJl3Fl3sHawC&pgis=1>>
57. Putnam, D. Polymers for gene delivery across length scales. *Nat. Mater.* **5**, 439–51 (2006).
58. Gogolewski, S. Selected topics in biomedical polyurethanes. A review. *Colloid Polym. Sci.* **267**, 757–785 (1989).
59. Odian, G. G. *Principles of polymerization*. (Wiley, 2007).
60. Webster, O. W. Living polymerization methods. *Science* **251**, 887–93 (1991).
61. Slugovc, C., Demel, S., Riegler, S., Hobisch, J. & Stelzer, F. Influence of functional groups on ring opening metathesis polymerisation and polymer properties. *J. Mol. Catal. A Chem.* **213**, 107–113 (2004).
62. Matyjaszewski, K. Atom Transfer Radical Polymerization (ATRP): Current Status and Future Perspectives. *Macromolecules* **45**, 4015–4039 (2012).
63. Moad, G. *et al.* Living free radical polymerization with reversible addition – fragmentation chain transfer (the life of RAFT). **1001**, 993–1001 (2000).
64. Grubbs, R. B. Nitroxide-Mediated Radical Polymerization: Limitations and Versatility. *Polym. Rev.* **51**, 104–137 (2011).
65. Whitehead, K. a, Langer, R. & Anderson, D. G. Knocking down barriers: advances in siRNA delivery. *Nat. Rev. Drug Discov.* **8**, 129–38 (2009).
66. Crampton, H. L. & Simanek, E. E. Dendrimers as drug delivery vehicles: non-covalent interactions of bioactive compounds with dendrimers. *Polym. Int.* **56**, 489–496 (2007).
67. Florence, A. T., Patri, A. K., Kukowska-Latallo, J. F. & Baker, J. R. Targeted drug delivery with dendrimers: Comparison of the release kinetics of covalently conjugated

- drug and non-covalent drug inclusion complex. *Adv. Drug Deliv. Rev.* **57**, 2203–2214 (2005).
68. Hoffman, A. S., Afrassiabi, L. C. D. Thermally reversible hydrogels. II. Delivery and selective removal of substances from aqueous solutions. *J Control Rel* **2**, 213 (1986).
 69. Pistolis, G., Malliaris, A., Tsiourvas, D. & Paleos, C. M. Poly(propyleneimine) Dendrimers as pH-Sensitive Controlled-Release Systems. *Chem. - A Eur. J.* **5**, 1440–1444 (1999).
 70. Mathiowitz, E., Raziel, A., Cohen, M. D. & Fischer, E. Photochemical rupture of microcapsules: A model system. *J. Appl. Polym. Sci.* **26**, 809–822 (1981).
 71. Gumbleton, M. & Schmaljohann, D. Thermo- and pH-responsive polymers in drug delivery. *Adv. Drug Deliv. Rev.* **58**, 1655–1670 (2006).
 72. Peppas, N. A., Kost, J. & Langer, R. Responsive polymeric delivery systems. *Adv. Drug Deliv. Rev.* **64**, 327–341 (2012).
 73. Farokhzad, O. C. & Langer, R. Impact of nanotechnology on drug delivery. *ACS Nano* **3**, 16–20 (2009).
 74. Lammers, T., Ulbrich, K., Duncan, R. & Vicent, M. J. Do HPMA copolymer conjugates have a future as clinically useful nanomedicines? A critical overview of current status and future opportunities. *Adv. Drug Deliv. Rev.* **62**, 272–282 (2010).
 75. Woodle, M. C., Engbers, C. M. & Zalipsky, S. New amphipatic polymer-lipid conjugates forming long-circulating reticuloendothelial system-evading liposomes. *Bioconjug. Chem.* **5**, 493–6 (1994).
 76. Zalipsky, S., Hansen, C. B., Oaks, J. M. & Allen, T. M. Evaluation of blood clearance rates and biodistribution of poly(2-oxazoline)-grafted liposomes. *J. Pharm. Sci.* **85**, 133–7 (1996).
 77. Gaertner, F. C., Luxenhofer, R., Blechert, B., Jordan, R. & Essler, M. Synthesis, biodistribution and excretion of radiolabeled poly(2-alkyl-2-oxazoline)s. *J. Control. Release* **119**, 291–300 (2007).
 78. Ranucci, E. *et al.* Synthesis and molecular weight characterization of low molecular weight end-functionalized poly(4-acryloylmorpholine). *Macromol. Chem. Phys.* **195**, 3469–3479 (1994).
 79. Abu Lila, A. S., Nawata, K., Shimizu, T., Ishida, T. & Kiwada, H. Use of polyglycerol (PG), instead of polyethylene glycol (PEG), prevents induction of the accelerated blood clearance phenomenon against long-circulating liposomes upon repeated administration. *Int. J. Pharm.* **456**, 235–242 (2013).

80. Frank, M. M. & Fries, L. F. The role of complement in inflammation and phagocytosis. *Immunol. Today* **12**, 322–326 (1991).
81. Moghimi, S. M. & Hamad, I. *Nanotechnology in Drug Delivery*. (Springer, 2009).
82. Owens, D. E. & Peppas, N. A. Opsonization, biodistribution, and pharmacokinetics of polymeric nanoparticles. *Int. J. Pharm.* **307**, 93–102 (2006).
83. Ratner, B. D., Hoffman, A. S., Schoen, F. J. & Lemons, J. E. *Biomaterials Science: An Introduction to Materials in Medicine* (Academic Press, 2004). at http://books.google.com/books/about/Biomaterials_Science.html?id=9PMU1iYGe34C&pgis=1
84. Needham, D. *et al.* Polymer-Grafted Liposomes: Physical Basis for the “Stealth” Property. *J. Liposome Res.* **2**, 411–430 (1992).
85. Jeon, S., Lee, J., Andrade, J. & De Gennes, P. Protein—surface interactions in the presence of polyethylene oxide. *J. Colloid Interface Sci.* **142**, 149–158 (1991).
86. Müller, B. W., R. H. Müller, H. C. Particle size, surface hydrophobicity and interaction with serum parenteral fat emulsions and model drug as parameters related to RES uptake. *Clin. Nut* **11**, 289–297 (1992).
87. Müller, R. H., Wallis, K. H., Tröster, S. D. & Kreuter, J. In vitro characterization of poly(methyl-methacrylate) nanoparticles and correlation to their in vivo fate. *J. Control. Release* **20**, 237–246 (1992).
88. Norman, M. E., Williams, P. & Illum, L. Human serum albumin as a probe for surface conditioning (opsonization) of block copolymer-coated microspheres. *Biomaterials* **13**, 841–849 (1992).
89. Roser, M., Fischer, D. & Kissel, T. Surface-modified biodegradable albumin nano- and microspheres. II: effect of surface charges on in vitro phagocytosis and biodistribution in rats. *Eur. J. Pharm. Biopharm.* **46**, 255–263 (1998).
90. Kenworthy, A. K., Hristova, K., Needham, D. & McIntosh, T. J. Range and magnitude of the steric pressure between bilayers containing phospholipids with covalently attached poly(ethylene glycol). *Biophys. J.* **68**, 1921–1936 (1995).
91. De Gennes, P. G. Polymers at an interface; a simplified view. *Adv. Colloid Interface Sci.* **27**, 189–209 (1987).
92. Storm, G., Belliot, S. O., Daemen, T. & Lasic, D. D. Surface modification of nanoparticles to oppose uptake by the mononuclear phagocyte system. *Adv. Drug Deliv. Rev.* **17**, 31–48 (1995).

93. Stolnik, S., Illum, L. & Davis, S. S. Long circulating microparticulate drug carriers. *Adv. Drug Deliv. Rev.* **16**, 195–214 (1995).
94. Moghimi, S. M., Hamad, I., Andresen, T. L., Jørgensen, K. & Szebeni, J. Methylation of the phosphate oxygen moiety of phospholipid-methoxy(polyethylene glycol) conjugate prevents PEGylated liposome-mediated complement activation and anaphylatoxin production. *FASEB J.* **20**, 2591–3 (2006).
95. Needham, D., D. V. Zhelev, T. J. M. in *Liposomes Ration. Des.* 13–62 (Marcel Dekker Inc, 1999).
96. Evans, E., Klingenberg, D. J., Rawicz, W. & Szoka, F. Interactions between Polymer-Grafted Membranes in Concentrated Solutions of Free Polymer. *Langmuir* **12**, 3031–3037 (1996).
97. Kuhl, T. L., Leckband, D. E., Lasic, D. D. & Israelachvili, J. N. Modulation of interaction forces between bilayers exposing short-chained ethylene oxide headgroups. *Biophys. J.* **66**, 1479–88 (1994).
98. Peracchia, M. T. *et al.* Visualization of in vitro protein-rejecting properties of PEGylated stealth® polycyanoacrylate nanoparticles. *Biomaterials* **20**, 1269–1275 (1999).
99. Gill, T. J. & Kunz, H. W. The immunogenicity of vinyl polymers. *Proc. Natl. Acad. Sci.* **61**, 490–496 (1968).
100. Schellekens, H., Hennink, W. E. & Brinks, V. The immunogenicity of polyethylene glycol: facts and fiction. *Pharm. Res.* **30**, 1729–34 (2013).
101. Richter, A. W. & Åkerblom, E. Polyethylene Glycol Reactive Antibodies in Man: Titer Distribution in Allergic Patients Treated with Monomethoxy Polyethylene Glycol Modified Allergens or Placebo, and in Healthy Blood Donors. *Int. Arch. Allergy Immunol.* **74**, 36–39 (1984).
102. Garratty, G. Modulating the red cell membrane to produce universal/stealth donor red cells suitable for transfusion. *Vox Sang.* **94**, 87–95 (2008).
103. Garratty, G. Progress in modulating the RBC membrane to produce transfusable universal/stealth donor RBCs. *Transfus. Med. Rev.* **18**, 245–256 (2004).
104. Armstrong, J. K. The occurrence , induction , specificity and potential effect of antibodies against poly (ethylene glycol). 147–168 (2009).
105. Gill, J. H. *et al.* A double antigen bridging immunogenicity ELISA for the detection of antibodies to polyethylene glycol polymers. *J. Pharmacol. Toxicol. Methods* **64**, 238–245 (2011).

106. Tillmann, H., N. J. Ganson, K. Patel, A. J. Thompson, M. Abdelmalek, T. Moody, J. G. McHutchison, M. S. H. High prevalence of preexisting antibodies against polyethylene glycol (PEG) in hepatitis C (HCV) patients which is not impaired response to PEG-interferon. *J. Hepatol.* **52**, S129 (2010).
107. Dams, E. T. *et al.* Accelerated blood clearance and altered biodistribution of repeated injections of sterically stabilized liposomes. *J. Pharmacol. Exp. Ther.* **292**, 1071–9 (2000).
108. Koide, H. *et al.* T cell-independent B cell response is responsible for ABC phenomenon induced by repeated injection of PEGylated liposomes. *Int. J. Pharm.* **392**, 218–23 (2010).
109. Ishida, T., Ichihara, M., Wang, X. & Kiwada, H. Spleen plays an important role in the induction of accelerated blood clearance of PEGylated liposomes. *J. Control. Release* **115**, 243–50 (2006).
110. Zhao, Y. *et al.* Repeated injection of PEGylated solid lipid nanoparticles induces accelerated blood clearance in mice and beagles. *Int. J. Nanomedicine* **7**, 2891–900 (2012).
111. Sroda, K. *et al.* Repeated injections of PEG-PE liposomes generate anti-PEG antibodies. *Cell. Mol. Biol. Lett.* **10**, 37–47 (2005).
112. Garay, R. P., El-Gewely, R., Armstrong, J. K., Garratty, G. & Richette, P. Antibodies against polyethylene glycol in healthy subjects and in patients treated with PEG-conjugated agents. *Expert Opin. Drug Deliv.* **9**, 1319–23 (2012).
113. Koide, H. *et al.* Particle size-dependent triggering of accelerated blood clearance phenomenon. *Int. J. Pharm.* **362**, 197–200 (2008).
114. Saadati, R., Dadashzadeh, S., Abbasian, Z. & Soleimanjahi, H. Accelerated blood clearance of PEGylated PLGA nanoparticles following repeated injections: effects of polymer dose, PEG coating, and encapsulated anticancer drug. *Pharm. Res.* **30**, 985–95 (2013).
115. Zhang, C., Fan, K., Ma, X. & Wei, D. Impact of large aggregated uricases and PEG diol on accelerated blood clearance of PEGylated canine uricase. *PLoS One* **7**, e39659 (2012).
116. Ishida, T. *et al.* Accelerated blood clearance of PEGylated liposomes following preceding liposome injection: effects of lipid dose and PEG surface-density and chain length of the first-dose liposomes. *J. Control. Release* **105**, 305–17 (2005).
117. Sherman, M. R., Williams, L. D., Sobczyk, M. a, Michaels, S. J. & Saifer, M. G. P. Role of the methoxy group in immune responses to mPEG-protein conjugates. *Bioconjug. Chem.* **23**, 485–99 (2012).

118. Laverman, P. *et al.* Factors affecting the accelerated blood clearance of polyethylene glycol-liposomes upon repeated injection. *J. Pharmacol. Exp. Ther.* **298**, 607–12 (2001).
119. Ishihara, T. *et al.* Evasion of the accelerated blood clearance phenomenon by coating of nanoparticles with various hydrophilic polymers. *Biomacromolecules* **11**, 2700–6 (2010).
120. He, C., Hu, Y., Yin, L., Tang, C. & Yin, C. Effects of particle size and surface charge on cellular uptake and biodistribution of polymeric nanoparticles. *Biomaterials* **31**, 3657–3666 (2010).
121. Yin Win, K. & Feng, S.-S. Effects of particle size and surface coating on cellular uptake of polymeric nanoparticles for oral delivery of anticancer drugs. *Biomaterials* **26**, 2713–2722 (2005).
122. Xia, T. *et al.* Polyethyleneimine coating enhances the cellular uptake of mesoporous silica nanoparticles and allows safe delivery of siRNA and DNA constructs. *ACS Nano* **3**, 3273–86 (2009).
123. Pittella, F. *et al.* Enhanced endosomal escape of siRNA-incorporating hybrid nanoparticles from calcium phosphate and PEG-block charge-conversional polymer for efficient gene knockdown with negligible cytotoxicity. *Biomaterials* **32**, 3106–3114 (2011).
124. Yessine, M.-A. & Leroux, J.-C. Membrane-destabilizing polyanions: interaction with lipid bilayers and endosomal escape of biomacromolecules. *Adv. Drug Deliv. Rev.* **56**, 999–1021 (2004).
125. Matsumura, Y. & Maeda, H. A New Concept for Macromolecular Therapeutics in Cancer Chemotherapy: Mechanism of Tumorotropic Accumulation of Proteins and the Antitumor Agent Smancs. *Cancer Res.* **46**, 6387–6392 (1986).
126. Stayton, P. S. *et al.* Molecular engineering of proteins and polymers for targeting and intracellular delivery of therapeutics. *J. Control. Release* **65**, 203–220 (2000).
127. Lozano, M. M. & Longo, M. L. Complex formation and other phase transformations mapped in saturated phosphatidylcholine/DSPE-PEG2000 monolayers. *Soft Matter* **5**, 1822 (2009).

Chapter 2

Disterol PEG Conjugates: Synthesis and Incorporation into Liposomes

2.1 INTRODUCTION

Self-assembling lipid nanostructures are widely used in biomedical applications. Liposomes and lipid-based microbubbles have found application in both drug delivery and imaging strategies.^{1,2} Achieving ideal physical properties of these lipid monolayer and bilayer systems is often critical for success as such attributes as stability, permeability, size, and biocompatibility play a significant role in most biomedical applications.^{3,4} A common method for increasing the stability and the *in vivo* stealth character of these materials is to attach poly(ethylene glycol) (PEG) to the membrane surface.⁵ This can be accomplished by conjugating PEG to lipid anchors which will then insert into the lipid monolayer or bilayer. Though this technique has become commonplace in the laboratory and is utilized by FDA approved materials, the exact behavior of PEGylated lipids in the bilayer is not fully understood. Recently, Longo *et. al.* have investigated the phase behavior and miscibility of PEG₂₀₀₀-DSPE in lipid monolayers and found that, depending on the system, PEG-DSPE can phase separate within the monolayer.⁶ This can lead to the ejection of PEG-DSPE from the monolayer, resulting in PEG-DSPE micelles and monolayers with altered physical properties.

The phase separation of lipids in a monolayer or bilayer can increase permeability of a membrane. When this occurs in drug-loaded liposomes, leakage of the encapsulated drug across the membrane can occur. As the fluidity of the membrane varies by temperature, leakage is also a temperature-dependent property. At the phase transition temperature of a membrane, the bilayer becomes fluid and permeable.⁷ This characteristic has been investigated as a possible method for triggered release of a drug from a liposome through external heating. This approach is challenging because an ideal system would be completely stable at physiological temperature (37 °C), and leak rapidly at 42 °C (at higher temperatures hyperthermia begins to cause tissue necrosis), however, phase transitions of lipid mixtures often occur over a broader range and a material that is permeable at 42 °C is likely to be leaky at 37 °C as well. 1,2-dipalmitoyl-*sn*-glycero-3-phosphocholine (DPPC), is a common phospholipid that has a sharp phase transition at 41 °C, however, the addition of PEG-DSPE causes a broadening of this phase transition.⁸ For temperature-triggered liposomal release, it would be valuable to find a PEG-lipid conjugate that causes minimal broadening of the membrane transition temperature.

PEG-DSPE conjugates are one of the most widespread materials used for the incorporation of PEG into lipid monolayers and bilayers. However, PEG conjugated to other lipid entities can also be incorporated into these systems. For instance, PEG-cholesterol may offer advantages over PEG-DSPE, but the rapid transfer of cholesterol from the liposome to biological membranes makes this approach less than ideal.⁹ Szoka *et.al.* have demonstrated that disterolphospholipids do not suffer from the same rapid exchange, and remain in the liposome bilayer for much longer durations.¹⁰ These observations lead us to the hypothesis that disterol-PEG derivatives may provide attractive membrane properties as a method for anchoring PEG to a lipid membrane surface. Herein, we describe the synthesis of two disterol-modified PEG molecules and preliminary evaluation of their effect when incorporated into liposomes.

2.2 EXPERIMENTAL

General: All reagents were purchased from commercial sources and used without further purification unless otherwise noted. 1,2-distearoyl-sn-glycero-3-phosphoethanolamine-N-[amino(polyethylene glycol)-2000] (ammonium salt) (PEG-DSPE) and DPPC were purchased from Avanti Polar Lipids (Alabaster, AL). Cholesterol and cholesteryl hemisuccinate were purchased from Sigma Aldrich and recrystallized from acetone/hexanes before use. Water was purified to a resistance of 18 M Ω using a Barnstead NANOpure[®] Diamond[™] purification system. All glassware was flame dried under vacuum or nitrogen purge prior to use and reactions were conducted under a nitrogen atmosphere. Unless otherwise noted, liquid reagents were introduced to the reaction flask via syringe or cannula. Volatile solvents were removed using a rotary evaporator under reduced pressure. All dialyses were performed in H₂O using Spectra/POR[®] regenerated cellulose (RC) dialysis bags.

Characterization: All NMR spectra were measured in CDCl₃, MeOD (d-4), or D₂O with TMS or solvent signals as the standards. ¹H spectra were recorded with a Bruker AVQ-300 and analyzed with Topspin software. MALDI-TOF data was collected on a Microflex Lt instrument (Bruker, Billerica, MA) in positive ion mode. MALDI samples were prepared using a matrix of a saturated solution of 2,5-hydroxybenzoic acid in MeOH unless otherwise specified. The spectra were analyzed with FlexAnalysis and PolyTools 1.0 software. Fluorescence was measured (Ex/Em = 490/520 nm) using a Spex Fluorolog Fluorimeter (Horiba Scientific, Edison, NJ). Liposome size measurements were carried out using a Nano-ZS Dynamic Light Scattering Instrument from Malvern (Westborough, MA). Differential Scanning Calorimetry (DSC) measurements were obtained using a high temperature MC-DSC 4100 calorimeter from Calorimetry Sciences Corp. (Lindonk, UT).

PEG-Diol (1): A solution of 2-amino-2-methyl-1,3-propanediol (210 mg, 2 mmol) and N,N-Diisopropylethylamine (DiPEA) (100 μ L) in DMF (1 mL) was charged with a stir bar and sparged with Ar for 10 min. To that solution, a solution of mPEG_{2kDa}-NPC (2 g, 1 mmol) in DMF (3 mL) was added dropwise. The reaction was stirred for 6 h and then precipitated into cold diethyl ether. The resulting yellow-white solid was dialyzed in a 2 kDa molecular weight cut off (MWCO) RC bag in H₂O for 12 h with three solvent changes and then lyophilized to yield a colorless solid (Yield: 83 %). ¹H NMR (CDCl₃), δ 1.19 (s, 3H); 3.37 (s, 3H); 3.45-3.79 (m, 202 H). M_{n,MALDI}: 2100 Da, PDI_{MALDI}: 1.01.

PEG-DiCHEMS (2): To a solution of PEG-Diol 1 (1 g, 0.5 mmol) in DCM (3 mL) was added cholesteryl hemisuccinate (608 mg, 1.25 mmol). The solution was sparged with Ar for 10 min and then 1-Ethyl-3-(3-dimethylaminopropyl)carbodiimide (EDC) (479 mg, 2.5 mmol), 4-Dimethylaminopyridine (DMAP) (6 mg, 0.05 mmol), and DiPEA (100 μ L) were added. The reaction was stirred for 12 h and then precipitated into cold diethyl ether four times followed by aqueous dialysis in a 50 kDa MWCO regenerated cellulose bag to yield a colorless solid (Yield: 73 %). Complete functionalization was confirmed by MALDI-TOF and H¹ NMR. ¹H NMR (CDCl₃), δ 0.68 (s, 6H); 0.84-1.67 (m, 69H); 1.76-2.07 (m, 10H); 2.27-2.32 (m, 4H); 2.56-2.69 (m, 8H); 3.37 (s, 3H); 3.45-3.79 (m, 182H); δ 4.14-4.21 (m, 2H); 4.21-4.32 (m, 2H); 4.54-4.65 (m, 2H); 5.37 (d, J = 4.4, 2H). M_{n,MALDI}: 3100 Da, PDI_{MALDI}: 1.01.

PEG-DiAcid (3): PEG-DiAcid was synthesized via methods previously reported for a similar molecule.¹¹ To a solution of β -glutamic acid (441 mg, 3 mmol) in 2 mL 0.1 M borate

buffer/acetonitrile (ACN) (3:2) at pH 8.0 was added mPEG_{2kDa}-NPC (2 g, 1 mmol). The reaction was stirred for 12 h and then the pH was adjusted to 4.5 with 0.2 N HCl. PEG-DiAcid was extracted into chloroform and the organic layer was washed four times with pH 4.5 buffer. The organic layer was isolated and dried over magnesium sulfate. After removing the magnesium sulfate by filtration, the product was precipitated into cold diethyl ether three times and isolated as a white solid (yield 68%). ¹H NMR (D₂O), δ 2.18-2.31 (m, 4H); 3.37 (s, 3H); 3.45-3.79 (m, 170 H). M_{n,MALDI}: 2200 Da, PDI_{MALDI}: 1.01.

PEG-DiChol (4): To a solution of PEG-DiAcid **3** (1 g, 0.5 mmol) in DCM (3 mL) was added cholesterol (483 mg, 1.25 mmol). The solution was sparged with Ar for 10 min and then 1-Ethyl-3-(3-dimethylaminopropyl)carbodiimide (EDC) (479 mg, 2.5 mmol), 4-Dimethylaminopyridine (DMAP) (6 mg, 0.05 mmol), and DiPEA (100 μL) were added. The reaction was stirred for 12 h and then precipitated into cold diethyl ether four times. Aqueous dialysis in a 50 kDa MWCO RC bag yielded **4** as a colorless solid (Yield: 73 %). Complete functionalization was confirmed by MALDI-TOF and H¹ NMR. ¹H NMR (CDCl₃), δ 0.68 (s, 6H); 0.84-1.67 (m, 66H); 1.76-2.07 (m, 10H); 2.19-2.34 (m, 4H); 2.59-2.71 (m, 6H); 3.37 (s, 3H); 3.45-3.79 (m, 194H); δ 4.41-4.52 (m, 1H); 5.37 (d, J = 4.4, 2H). M_{n,MALDI}: 3100 Da, PDI_{MALDI}: 1.01.

Differential scanning calorimetry: DSC experiments were run in accordance with a previously established protocol.⁹ Lipid solutions of 2.5 μmol total lipid in CHCl₃ at varying mole percentages were dried via rotary evaporation to yield a thin film which was subjected to high vacuum overnight. The lipid film was hydrated in 0.5 mL HEPES buffer (10 mM HEPES, 140 mM NaCl, pH 7.4) and sonicated at 65 °C for 10 min. 250 μL of the resulting solution was used for DSC measurements. DSC measurements were performed with a high-temperature MC-DSC 4100 calorimeter (Calorimetry Sciences Corp., Lindon, UT) with reusable Hastelloy sample ampoules and a reference ampoule with HEPES buffer. The data was collected over a range of 20 °C to 80 °C at 1 °C/min. The data was analyzed with CpCalc 2.1 software.

Liposome formulation: Lipid solutions of 2.5 μmol total lipid in CHCl₃ at varying mole percentages were dried via rotary evaporation to yield a thin film which was subjected to high vacuum overnight. The lipid film was hydrated in 0.5 mL HEPES (20 mM) MES (20 mM) buffer with carboxyfluorescein (CF) a (120 mM) at 65 °C and sonicated for 10 min. The resulting solution was extruded through 100 nm (x3), and then 80 nm (x3) polycarbonate membranes at 65 °C. Liposomes were purified from free CF by PD-10 chromatography in HEPES buffer (10 mM HEPES, 140 mM NaCl, pH 7.4). PEG-DiCHEMS and PEG-DiChol incorporation into liposomes was confirmed by size exclusion chromatography with sepharose CL 6B gel. PEG was detected only in fractions containing liposomes by thin layer chromatography (TLC) and staining with iodine.

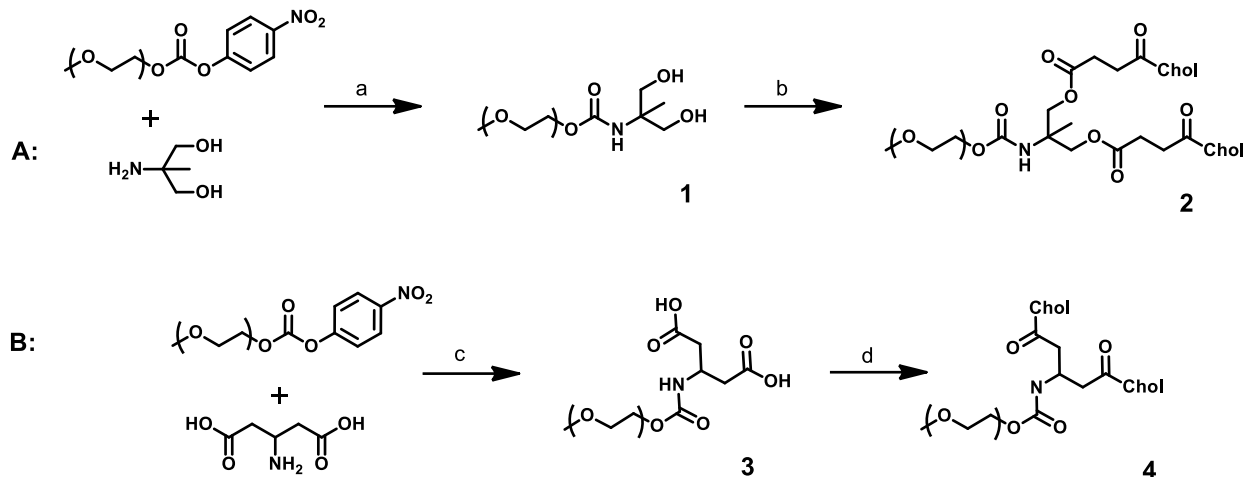
Carboxyfluorescein leakage assay: Liposome solutions from the PD-10 columns were diluted 100 fold in HEPES buffer (10 mM HEPES, 140 mM NaCl, pH 7.4). Cuvettes with 1.99 mL of the same HEPES buffer were stirred and heated in the instrument. After 15 minutes of equilibration time, 10 μL of the diluted liposome solution was added to the stirring, preheated cuvette in the instrument and measurements were taken every second for 20 minutes. After 20 minutes, 20 μL of Triton X-100 solution was added to the cuvette. Data was plotted as percent leakage over time, with 0% corresponding to the baseline after addition of the liposome solution

to the cuvette at 25 °C and 100% corresponding to the value of each sample after addition of Triton.

2.3 RESULTS

Synthesis: In order to investigate the effect of the lipid anchor for PEG incorporation into liposomes, we designed two diester-PEG molecules. As the spacer molecule between the PEG and the lipid anchor can affect the physical properties of the liposome¹², we targeted two diester-PEGs with different linkers. PEG-DiCHEMS and PEG-DiChol were each synthesized in two steps from commercial starting materials (Scheme 2.1). For PEG-DiCHEMS, PEG-NPC was reacted with an excess of 2-amino-2-methyl-1,3-propanediol in DMF. After purification by precipitation into cold diethyl ether and dialysis in a 2 kDa MWCO RC bag, the resulting PEG-Diol (**1**) was conjugated to CHEMS via carbodiimide coupling. Again, purification was accomplished by precipitation into cold diethyl ether. Next, aqueous dialysis in a 50 kDa MWCO RC bag was run to remove any unfuntionalized PEG.

PEG-DiChol was synthesized in a similar manner. First, PEG-NPC was reacted with β -glutamic acid in aqueous buffer to yield PEG-DiAcid **3** after purification by extraction and precipitation into cold diethyl ether. Next, cholesterol was conjugated to the PEG-DiAcid via carbodiimide coupling. The product, PEG-DiChol was purified by precipitation into cold diethyl ether followed by aqueous dialysis in 50 kDa MWCO RC bags to remove any remaining unfuntionalized PEG.



Scheme 2.1: A: Synthesis of PEG-DiCHEMS (a) DMF, TEA (b) CHEMS, EDC, DMAP, DiPEA, DCM B: Synthesis of PEG-DiChol (c) Borate buffer/ACN, pH 8 (d) Cholesterol, EDC, DMAP, DiPEA, DCM

Liposome preparation: Liposomes composed of DPPC and PEG with varying lipid anchors were prepared by hydrating lipid thin films with CF containing buffer. In order to control for the effect of cholesterol in the lipid bilayer, PEG-DSPE liposomes were also prepared with

comparable mole percent cholesterol. Sonication and multiple extrusions through a 100 nm membrane and an 80 nm membrane at 65 °C yielded liposomes encapsulating CF between 100-150 nm in diameter and with narrow polydispersities (Table 2.1). Liposomes were purified from free CF by PD-10 chromatography. To confirm incorporation of disterol PEGs into liposomes, size exclusion chromatography was performed and PEG was detected only in fractions containing liposomes.

Prep	DPPC	Chol	PEG-DiCHEMS	PEG-DiChol	PEG-DSPE	Diameter (nm)	PDI
1	95	0	5	0	0	119	0.056
2	95	0	10	0	0	119	0.065
3	80	0	20	0	0	123	0.17
4	90	10	0	5	0	116	0.178
5	80	20	0	10	0	115	0.086
6	60	40	0	20	0	133	0.072
7	95	0	0	0	5	109	0.061
8	85	10	0	0	5	111	0.057
9	75	20	0	0	5	110	0.07

Table 2.1: Liposome formulations and size.

T_m measurements: The transition temperature of the lipid bilayers incorporating PEG-DiCHEMS and PEG-DiChol at varying mole percent were measured by DSC (Figure 2.1). It is difficult to draw direct conclusions from the data, however, there are apparent trends. Increased cholesterol content decreases the extent of the phase transition, and increased PEG-DiCHEMS content appears to shift the phase transition to slightly lower temperatures. Further evaluation of the phase transition of these formulations is required.

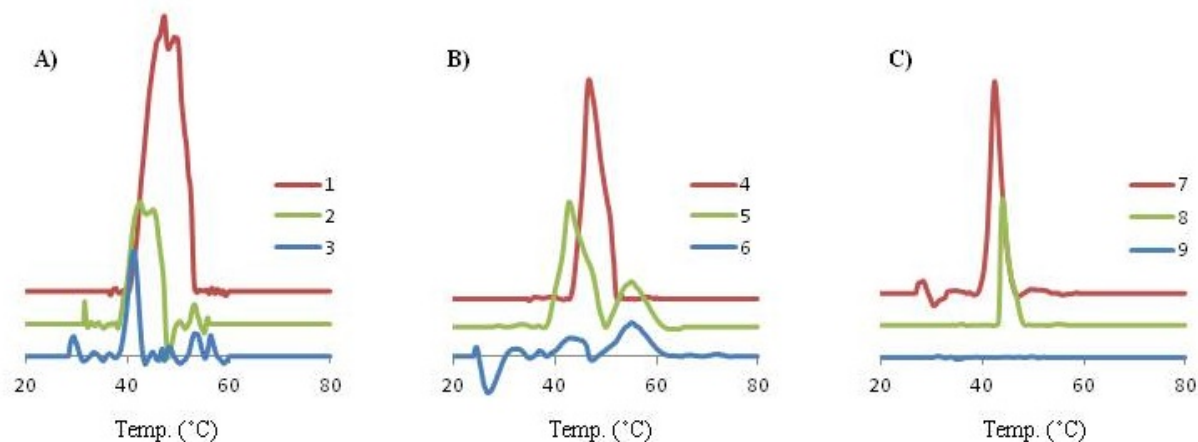


Figure 2.1: DSC data for formulations 1-9; DPPC/PEG-DiCHEMS (A), DPPC/PEG-DiChol (B), and DPPC/PEG-DSPE/Cholesterol.

Temperature dependent leakage of carboxyfluorescein: Leakage rates of liposomes encapsulating CF were measured by fluorimetry. CF is self-quenched when encapsulated within a liposome at high enough concentration, however, free CF can be readily detected by fluorimetry.¹³ In these experiments, liposomes were injected into a cuvette containing preheated buffer at a constant temperature, and fluorescence was measured over time. Leakage is reported as percent leaked from the liposomes over time (Figure 2.2). Leakage was measured at 25 °C, 37 °C, and 41 °C. All formulations leaked fastest at 41 °C, although all had significant leakage at 37 °C as well.

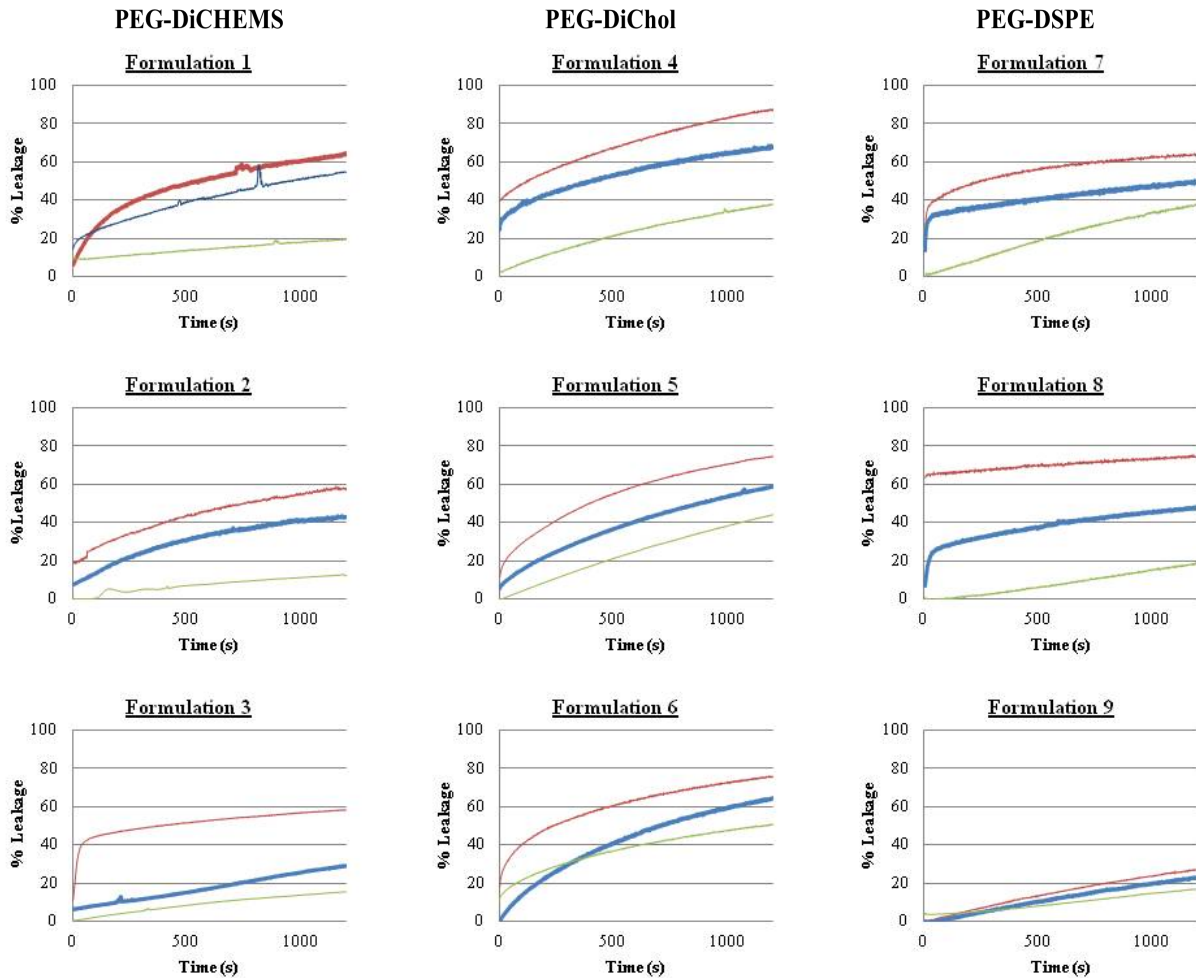


Figure 2.2: Percent of CF leakage from liposomes over 20 min at 41 °C (red), 37 °C (blue), and 25 °C (green).

2.4 DISCUSSION

PEG-DSPE is often incorporated into self-assembled lipid nanostructures in order to increase stability or *in vivo* stealth character. This incorporation leads to two potential disadvantages: the phase separation and liposome ejection of PEG-DSPE in some systems and the broadening of membrane T_m due to incorporation of PEG-DSPE into the bilayer. To overcome these issues, we hypothesized that sterol-modified PEGs may offer improved membrane properties. As liposome-incorporated cholesterol can rapidly exchange with biomembranes, we targeted disterol modified PEGs. Because the linkage between the PEG and the lipid anchor can affect the physical properties of the membrane, we designed, synthesized, and characterized two disterol PEGs with different linkages.

The T_m of the disterol PEGs incorporated into DPPC membranes was measured by DSC. Initial results are consistent with literature reports in that increasing cholesterol content decreases the magnitude of the phase transition. Also, it seems that increasing PEG-DiCHEMS may shift the T_m to slightly lower values, though this will need to be confirmed by further evaluation.

We also investigated the temperature dependent leakage of CF encapsulating liposomes composed of DPPC and disterol PEGs at 5, 10, and 20 mole percent. In preliminary results, all three formulations of PEG-DiChol had consistent leakage, even at lower temperatures. All three formulations of liposomes incorporating PEG-DiCHEMS also leaked extensively at 41 °C, although at 20 mole percent leakage at 37 °C was decreased, leading to a two-fold difference in percent leaked between 37 °C and 41 °C. Corresponding control liposomes formed with DPPC/PEG-DSPE/cholesterol at equivalent mole percent of cholesterol also demonstrated decreased leakage, although for this formulation the difference between 37 °C and 41 °C was minimal. The decrease in leakage is likely due to a loss of phase transition in liposomes at higher mole percent of cholesterol (>33%).¹⁴

In conclusion, we have presented the synthesis of two disterol-modified PEG molecules. We have incorporated these molecules into DPPC liposomes and characterized the phase transition temperature of those membranes. Additionally, initial leakage results suggest that PEG-DiCHEMS may offer favorable leakage rates when formulated in DPPC liposomes at 20 mole percent.

2.5 ACKNOWLEDGEMENTS

I gratefully acknowledge Dr. Vincent Venditto for his insightful scientific input and assistance in experimental design.

2.6 REFERENCES

1. Immordino, M. L., Dosio, F. & Cattel, L. Stealth liposomes: review of the basic science, rationale, and clinical applications, existing and potential. *Int. J. Nanomedicine* **1**, 297–315 (2006).

2. Ferrara, K., Pollard, R. & Borden, M. Ultrasound microbubble contrast agents: fundamentals and application to gene and drug delivery. *Annu. Rev. Biomed. Eng.* **9**, 415–47 (2007).
3. Verma, A. & Stellacci, F. Effect of surface properties on nanoparticle-cell interactions. *Small* **6**, 12–21 (2010).
4. Malam, Y., Loizidou, M. & Seifalian, A. M. Liposomes and nanoparticles: nanosized vehicles for drug delivery in cancer. *Trends Pharmacol. Sci.* **30**, 592–9 (2009).
5. Torchilin, V. P. *et al.* Poly(ethylene glycol) on the liposome surface: on the mechanism of polymer-coated liposome longevity. *Biochim. Biophys. Acta - Biomembr.* **1195**, 11–20 (1994).
6. Lozano, M. M. & Longo, M. L. Complex formation and other phase transformations mapped in saturated phosphatidylcholine/DSPE-PEG2000 monolayers. *Soft Matter* **5**, 1822 (2009).
7. Ta, T. & Porter, T. M. Thermosensitive liposomes for localized delivery and triggered release of chemotherapy. *J. Control. Release* **169**, 112–125 (2013).
8. Chen, J. *et al.* Influence of lipid composition on the phase transition temperature of liposomes composed of both DPPC and HSPC. *Drug Dev. Ind. Pharm.* **39**, 197–204 (2013).
9. Huang, Z. & Szoka, F. C. Sterol-modified phospholipids: cholesterol and phospholipid chimeras with improved biomembrane properties. *J. Am. Chem. Soc.* **130**, 15702–12 (2008).
10. Huang, Z., Jaafari, M. R. & Szoka, F. C. Disterylphospholipids: Nonexchangeable Lipids and Their Application to Liposomal Drug Delivery. *Angew. Chemie* **121**, 4210–4213 (2009).
11. Clementi, C., Miller, K., Mero, A., Satchi-Fainaro, R. & Pasut, G. Dendritic poly(ethylene glycol) bearing paclitaxel and alendronate for targeting bone neoplasms. *Mol. Pharm.* **8**, 1063–72 (2011).
12. Carrion, C., Domingo, J. & de Madariaga, M. Preparation of long-circulating immunoliposomes using PEG–cholesterol conjugates: effect of the spacer arm between PEG and cholesterol on liposomal characteristics. *Chem. Phys. Lipids* **113**, 97–110 (2001).
13. Gregoriadis, G. & Davis, C. Stability of liposomes *in vivo* and *in vitro* is promoted by their cholesterol content and the presence of blood cells. *Biochem. Biophys. Res. Commun.* **89**, 1287–1293 (1979).

14. Mabrey, S., Mateo, P. L. & Sturtevant, J. M. High-sensitivity scanning calorimetric study of mixtures of cholesterol with dimyristoyl- and dipalmitoylphosphatidylcholines. *Biochemistry* **17**, 2464–2468 (1978).

Chapter 3

The Evaluation of Polymers for Extended Circulation

3.1 INTRODUCTION

In the field of drug delivery, poly(ethylene glycol) (PEG) has seen great success.^{1,2} PEG has many qualities which make it an appropriate candidate for drug delivery including: high aqueous solubility, inexpensive manufacture, and FDA approval in many products.³ However, the single quality that makes PEG an almost ideal polymer for parenteral drug delivery systems is its ability to extend the circulation lifetimes of therapeutics.^{4,5} In addition to decreasing renal clearance through increased molecular weight, PEG also acts as a steric shield to prevent the adsorption of serum opsonins, which greatly reduces uptake by the mononuclear phagocyte system (MPS).⁶ Numerous clinical therapeutics employ PEG explicitly for its ability to extend the length of time in circulation.^{1,2} When conjugated to a therapeutic directly or to a drug carrier, PEG's stealth character increases circulation which in turn improves the material's pharmacokinetics (PK) and biodistribution (BD). These enhanced properties allow for prolonged therapeutic activity, increased efficacy, and decreased off-target effects.^{4,7} There are also drawbacks to using PEG in drug delivery systems, including the high intrinsic viscosity of PEG in aqueous solutions and a strong, anti-PEG immune response upon multiple dosings.^{8,9}

When compared to other hydrophilic polymers, PEG has a very high intrinsic viscosity.^{8,10} This high viscosity can impose limits on drug concentration and dose size during intravenous administration due to reduced syringability.¹¹ A direct comparison of the aqueous viscosity of PEG to the aqueous viscosity of other hydrophilic polymers is difficult to make as published viscosity values have been obtained using diverse experimental conditions including: polymer concentration, polymer molecular weight, temperature, and salt concentration.

In addition to its high intrinsic viscosity, PEG also can initiate an immune response to generate IgM antibodies. Between 0.6-25% of healthy blood donors exhibit preexisting anti-PEG IgM due to exposure to PEG at some point.^{12,13,14} This IgM can result in an accelerated blood clearance (ABC) phenomenon and was first reported by Dams *et. al.* in 2000. In this phenomenon, a first dose of a PEGylated material initiates the production of anti-PEG IgM, and subsequent doses are rapidly cleared from circulation due to the IgM binding to the PEG and accumulate extensively in the liver and spleen.⁹ The production of anti-PEG IgM takes 3-5 days, and thus no accelerated blood clearance is observed for the first dose of a PEGylated material.¹⁵ However, many treatment strategies require multiple doses within the time window of the accelerated blood clearance effect (3-28 days post first dose).^{15,16} In these cases, a therapeutic can completely lose its long circulating properties, and increased toxicity is possible due to altered biodistribution.^{9,17} Many factors can alter or inhibit the ABC effect, including dose size,¹⁷ therapeutic payload,¹⁸ administration regimen,¹⁵ and even PEG end-groups.¹⁹ Still, many materials can initiate the ABC effect, and patients who have been previously exposed to PEG may exhibit anti-PEG IgM. Another possible method for avoiding the ABC effect is to use a polymer similar to PEG that does not result in an immune response and reduced circulation lifetimes.

		Ref
Observed in:	Mice, rats, rabbits, beagles, monkeys, humans	9,20,21,22
PEGylated materials:	Liposomes, micelles, nanoparticles, proteins	9,23,24,25
Influential factors:	Conjugate size, PEG M_w , PEG end groups, payload, dose size, time between doses	23,15,26,19
To induce:	Pretreat with PEGylated material Pretreat with free PEG Blood/serum transfusion from a pre-treated animal Preexisting anti-PEG IgM (presumably due to prior exposure to PEG)	9,12,15
To suppress:	High dose Toxic Payload Splenectomy 2nd dose outside of 5-30 day time frame	9,15, 16,27

Table 3.1: Factors affecting the ABC phenomenon.

A number of other hydrophilic polymers have been reported to extend circulation times of drugs or liposomes. HPMA (poly[N-(2-hydroxypropyl) methacrylamide]),^{28,29,30} PVP (poly(vinylpyrrolidone)),^{31,32} PMOX (poly(2-methyl-2-oxazoline)),^{33,34,33} PAcM (poly(N-acryloyl morpholine)),^{35,36} and PDMA (poly(N,N-dimethylacrylamide))³⁷ have all demonstrated the ability to increase the circulation half-life of various materials. PVP, PMOX, PAcM, and HPMA have been investigated as polymer coatings on liposomes, however, inconsistent experiment procedures makes it difficult to compare their abilities to extend the circulation half lives of liposomes (Table 3.1). Though materials conjugated to these polymers do not exhibit as long of circulation half-lives as PEG, other favorable properties could make them a better choice for certain drug delivery applications. Advantages of other polymers can include improved physical properties, increased functional handles for drug loading, and more versatile post-polymerization functionalization.³ A handful of these polymers are currently undergoing clinical trials, however, the question remains whether or not the advantages of these polymers will be enough to make up for their shorter circulation times.^{1,38,39}

Polymer	Liposome Characteristics	Animal	Circulation half-life	M _w	Notes	Ref.
PVP	3 and 7 mol % polymer 155-180 nm	Mice	40-130 min	6 kDa	PE lipid anchor ¹¹¹ In	40
PVP	2.5 and 6.5 mol % polymer 165-190 nm	Mice	45-120 min	6-15 kDa	Palmityl lipid anchor ¹¹¹ In label	41
PMOX	5 mol % polymer 99-112 nm	Mice	17.8 h	2-4.3 kDa	DSPE lipid anchor ¹²⁵ I-Tl label	34
PMOX	5 mol % Polymer ~ 90 nm	Rats	>15 h	5 kDa	DSPE lipid anchor ⁶⁷ Ga label	42
PAcM	3 and 7 mol % polymer 155-180 nm	Mice	90-170 min	6 kDa	PE lipid anchor ¹¹¹ In	40
HPMA	0.3 and 3 mol % polymer 150-200 nm	Mice	45-150 min	2.9-4.3 kDa	Oleic acid lipid anchor ¹¹¹ In label	43

Table 3.2: Summary of previously published circulation half-lives of polymer liposomes.

Here, we have synthesized a panel of polymers with low polydispersity and evaluated their physical and pharmacological properties. The polymers evaluated are PEG, PMOX, HPMA, PVP, PDMA, and PAcM. We have measured the aqueous viscosities of polymers with similar molecular weights under consistent experimental conditions to allow for an accurate comparison among them. We have also compared the circulation times of liposomes modified with these polymers again with similar molecular weights in mice and rats under consistent experimental conditions. Most interestingly, we have investigated which of these polymers initiate an accelerated blood clearance phenomenon.

3.2 EXPERIMENTAL

General: All reagents were purchased from commercial sources and used without further purification unless otherwise noted. 1,2-distearoyl-*sn*-glycero-3-phosphoethanolamine-N-[amino(polyethylene glycol)-2000] (ammonium salt) (PEG-DSPE), hydrogenated L- α -phosphatidylcholine from soy (HSPC), cholesterol, 1-palmitoyl-2-oleoyl-*sn*-glycero-3-phospho-(1'-*rac*-glycerol) (POPG), and 1,2-dipalmitoyl-*sn*-glycero-3-phosphoethanolamine-N-[4-(*p*-maleimidomethyl)cyclohexane-carboxamide] (sodium salt) (MCC PE) were purchased from Avanti Polar Lipids (Alabaster, AL). Cholesterol was recrystallized from acetone/hexanes before use. AIBN was recrystallized from methanol before use. N-(2-Hydroxypropyl)methacrylamide was recrystallized from acetone and all other monomers were distilled prior to polymerization. Water was purified to a resistance of 18 M Ω using a Barnstead NANOpure® Diamond™ purification system. *N,N*-dimethylformamide (DMF), triethylamine (TEA), chloroform (CHCl₃) and methylene chloride (DCM) were purified by passing the solvents under nitrogen pressure through two packed columns of neutral alumina within a commercial solvent purification apparatus (Glass Contour, Laguna Beach, CA). All glassware was flame dried under vacuum or nitrogen purge prior to use and reactions were conducted under a nitrogen atmosphere. Unless

otherwise noted, liquid reagents were introduced to the reaction flask via syringe or cannula. Volatile solvents were removed using a rotary evaporator under reduced pressure. All dialyses were performed in MeOH or H₂O using Spectra/POR[®] regenerated cellulose dialysis bags.

Female CD-1 mice (6 - to 8-week old, 25 to 30 g in weight) were obtained from Harlan Laboratories, Inc. (Indianapolis, IN). All animals were handled in accordance with guidelines established by the National Institutes of Health Guidelines for the Care and Use of Laboratory Animals, and with the approval of the Committee of Animal Research at the University of California, San Francisco.

Male Wistar rats (250-275 g) with jugular vein cannulas were obtained from Charles River Laboratories, Inc. (Wilmington, MA) and housed in the University of California San Francisco animal care facility with a 12-h light/dark cycle and allowed free access to water and food. The studies described here were approved by the Committee on Animal Research, University of California, San Francisco.

Characterization: All NMR spectra were measured in CDCl₃, CD₂Cl₂, MeOD (d-4), or D₂O with TMS or solvent signals as the standards. ¹H NMR spectra were recorded with a Bruker AVQ-300, an AVQ-400, a DRX-500, or an AV-600 and analyzed with Topspin software. MALDI-TOF data was collected on a Microflex Lt instrument (Bruker, Billerica, MA) in positive ion mode. MALDI samples were prepared using a matrix of a saturated solution of 2,5-hydroxybenzoic acid in MeOH unless otherwise specified. The spectra were analyzed with FlexAnalysis and PolyTools 1.0 software. Size exclusion was performed on two different systems, both calibrated with PEG standards. Polymer samples were dissolved in the solvent of the mobile phase at a concentration of 2 mg/ml and filtered through a 0.2 μm PVDF filter before injection. The first system consisted of two PSS columns (7.5 x 300 mm) with particle size of 5 μm with DMF as the mobile phase. The system consisted of a Waters 510 pump, a Waters U6K injector, a Waters 486 UV-Vis detector, and a Waters 410 differential refractive index detector. The columns were maintained at 70 °C. The second system was run at 30° C in aqueous buffer (0.10 M NaNO₃, 0.02 wt% NaN₃) as eluent on three Waters Ultrahydrogel columns (exclusion limit = 3 x 10⁶; pore size = 5000Å; flow rate = 1 mL min⁻¹) equipped with a Wyatt T-rEX RI detector, a Water 2998 PDA detector, and a Wyatt MiniDAWN Treos multi-angle static light scattering detector using a *dn/dc* values measured using the Wyatt T-rEX RI. Fluorescence spectroscopy was measured on a FluoroLog-3 spectrofluorimeter equipped with a temperature-controlled stage (LFI-3751) with FluorEssence software (Horiba Scientific, Edison, NJ). Zeta potential and size measurements were carried out using a Nano-ZS Dynamic Light Scattering Instrument from Malvern (Westborough, MA). UV-vis measurements were performed with a Lambda 35 UV-vis spectrometer (PerkinElmer, Wellesley, MA). Measurements were performed in sealed, standard 1 cm quartz cells in the reaction solvent at room temperature.

General RAFT polymerization: All RAFT polymers were synthesized by adding monomer, RAFT chain transfer agent, solvent, and AIBN, in that order, to a flame dried flask. The solvent, RAFT agent, and molar equivalences varied by polymer, and are reported in the experimental details for each specific polymer. After 5 freeze-pump-thaw cycles the flask was backfilled with argon and stirred at 65 °C. The polymerizations were monitored by MALDI by removing a small aliquot from the reaction flask. To quench RAFT polymerizations, the solution was exposed to air and cooled in an ice bath. All polymers were purified by dialysis.

General post-polymerization modification of RAFT polymers: Aminolysis of all RAFT polymers yielded thiol terminated polymers which were then conjugated to MCC PE *in situ*. The general procedure for post-polymerization functionalization was as follows. Polymer was added to a flame dry flask charged with a stir bar and dissolved in either THF or DMF at 100 mg/mL. The solution was subjected to 5 freeze-pump-thaw cycles and back filled with Ar. Propylamine was added to the solution dropwise (10 mol eq). The reaction was stirred at room temperature for 3 hours at which point complete aminolysis was confirmed by UV-vis spectrometry. Without exposure to oxygen, propylamine and solvent were removed under reduced pressure. After all liquids were removed, the flask was then backfilled with Ar. For polymers for viscosity measurements, an Ar-sparged solution of additional monomer (20 mol eq) in THF (1:1 vol/vol) was added to the reaction flask. For polymers for liposome incorporation, an Ar-sparged solution of MCC PE (2.2 mol eq) in THF or DMF was added to the remaining solids. The reaction was stirred overnight at room temperature. The final polymer-lipid conjugate was purified by dialysis in MeOH in 2 kDa MWCO regenerated cellulose bags, dialysis in water in 50 kDa MWCO regenerated cellulose bags, and reverse phase column chromatography with PrepSep™ SPE tubes (Fisher Scientific International Inc., Hampton, NH). Polymer lipid conjugates are labeled based on the molecular weight of the polymer.

PDMA (2.1 kDa): Solvent: DMF. RAFT agent: 2-Cyano-2-propyl dodecyl trithiocarbonate Molar eq: vinyl-pyrrolidone/RAFT agent/AIBN = 25/1/0.2. ¹H NMR (300 MHz, CDCl₃): δ 0.82-0.95 (t, 3H), 1.11-1.95 (br m, 70H), 2.40-2.83 (br m, 21H), 2.83-3.31 (br m, 132H). M_{n,MALDI}: 2.1 kDa, PDI_{MALDI}: 1.04.

PDMA-MCC PE (2.1 kDa): ¹H NMR (300 MHz, CDCl₃): δ 0.85-0.93 (t, 6H), 1.15-1.96 (br m, 96H), 2.41-2.81 (br m, 21H), 2.81-3.41 (br m, 128H). M_{n,MALDI}: 3.0 kDa, PDI_{MALDI}: 1.06.

PAcM (2.4 kDa): Solvent: DMF. RAFT agent: 2-Cyano-2-propyl dodecyl trithiocarbonate Molar eq: vinyl-pyrrolidone/RAFT agent/AIBN = 25/1/0.3. ¹H NMR (300 MHz, CDCl₃): δ 0.82-0.96 (t, 3H), 1.15-1.95 (br m, 58H), 2.34-2.60 (br m, 18H), 3.20-3.91 (br m, 146H). M_{n,MALDI}: 2.4 kDa, PDI_{MALDI}: 1.04.

PAcM-MCC PE (2.4 kDa): ¹H NMR (300 MHz, CDCl₃): δ 0.82-0.94 (t, 6H), 0.94-1.1 (br m, 4H), 1.15-2.06 (br m, 82H), 2.34-2.86 (br m, 18H), 3.16-4.19 (br m, 152H). M_{n,MALDI}: 3.3 kDa, PDI_{MALDI}: 1.03.

PVP (2.2 kDa): Solvent: toluene. RAFT agent: Cyanomethyl *N*-methyl-*N*-phenyl dithiocarbamate Molar eq: vinyl-pyrrolidone/RAFT agent/AIBN = 25/1/0.3. δ 1.59-2.61 (br m, 120H), 2.98-3.48 (br m, 43H), 3.48-4.22 (br m, 21H), 7.21-7.70 (br m, 5H). M_{n,MALDI}: 2.1 kDa, PDI_{MALDI}: 1.07.

PVP-MCC PE (2.2 kDa): ¹H NMR (300 MHz, CD₂Cl₂): δ 0.79-0.96 (t, 6H), 1.03-2.58 (br m, 172H), 3.03-3.46 (br m, 44H), 3.46-4.32 (br m, 29H). M_{n,MALDI}: 3.1 kDa, PDI_{MALDI}: 1.07.

HPMA (2.4 kDa): Solvent: t-Butanol. RAFT agent: 2-Cyano-2-propyl benzodithioate Molar eq: vinyl-pyrrolidone/RAFT agent/AIBN = 25/1/0.3. ¹H NMR (300 MHz, MeOD): δ 0.89-1.41 (br m, 108H), 1.41-2.11 (br m, 34H), 2.91-2.31 (br m, 34H), 3.86-3.99 (br m, 17H), 7.33-7.90 (br m, 5H). M_{n,MALDI}: 2.5 kDa, PDI_{MALDI}: 1.06.

HPMA-MCC PE (2.4 kDa): ^1H NMR (300 MHz, MeOD): δ 0.82-0.91 (t, 6H), 0.91-1.42 (br m, 148H), 1.51-2.11 (br m, 30H), 2.91-2.29 (br m, 30H), 3.80-4.06 (br m, 15H). $M_{n,\text{MALDI}}$: 3.4 kDa, $\text{PDI}_{\text{MALDI}}$: 1.06.

General PMOX Polymerization: A flame dried, high-pressure reaction vial was charged with a stir bar, methyl oxazoline, and acetonitrile to yield a 5 M methyl oxazoline solution. The solution was sparged with Ar for 15 min and cooled to 0 °C. An Ar-sparged solution of methyltosylate in ACN was added to the reaction vial and the solution was heated at 90 °C. The polymerization was monitored by MALDI by removing a small aliquot from the reaction flask and adding it to 0.01 M NaOH solution in water. At the target molecular weight, the polymerization was quenched with one of two possible methods. Polymers for viscosity measurements were quenched with 0.01 M NaOH solution in water. Polymers for liposome incorporation were quenched with a solution of dioctyldecylamine (5 mol eq to methyltosylate) in ACN (0.5 M) at 90 °C. All polymers were purified by dialysis in MeOH.

PMOX-Dioctadecylamine (2.0 kDa): ^1H NMR (300 MHz, CDCl_3): δ 0.82-0.86 (t, 6H), 1.18-1.3 (br m, 62H), 2.01-2.16 (br m, 69H), 3.20-3.6 (br m, 95H). $M_{n,\text{MALDI}}$: 2.6 kDa, $\text{PDI}_{\text{MALDI}}$: 1.09.

Liposome formulation: Liposomes for *in vivo* experiments were prepared by an ethanol injection method followed by high pressure extrusion. A lipid solution in CHCl_3 consisting of HSPC, cholesterol, polymer-lipid conjugate, and DiD at a molar ratio of 54.5:40:5:0.5 (80 μmol total) was prepared. For conventional liposomes, polymer-lipid was replaced with POPG. The chloroform was removed via rotary evaporation to yield a thin film which was subjected to high vacuum overnight. The lipid film was dissolved in ethanol (300 μL) at 65 °C and added to 2.7 mL HEPES buffer (10 mM HEPES, 140 mM NaCl, pH 7.4) at 65 °C in one portion. The resulting solution was extruded through 200 nm (x3), 100 nm (x3), and then 80 nm (x3) polycarbonate membranes. Liposomes were purified by dialysis in HEPES buffer, diluted to desired concentrations for animal experiments, and then filtered through a 0.2 μm polyethersulfone sterile membrane.

PK and biodistribution in mice: Female CD-1 mice were administered DiD-labeled liposomes at 10 μmol phospholipid/kg via tail vein injection in 175-225 μL HEPES buffer. At selected time points (10 min, 30 min, 90 min, 4.5 h, 24 h, and 48 h), blood was collected into centrifuge tubes with 5 μL of heparin sulfate solution in PBS (5 mg/mL) by submandibular cheek bleeding. The blood samples were centrifuged for 5 min at 15,000 RPM at 4 °C. The supernatant was collected and analyzed by fluorimetry. Each group consisted of $n = 3$ mice.

24 h or 48 h after administration, animals were anesthetized with isoflurane. The liver, spleen, lung, and liver, of each mouse were excised and transferred into separate tubes with 1 mL of 0.075 M HCl in 90% isopropanol/10% water and 1 g zirconium beads. The tissues were then homogenized in a Mini-Beadbeater (Biospec Products, Inc., Bartlesville, OK) for 20 s. The homogenate was stored for 12 h at 4 °C and then clarified by centrifugation in a microcentrifuge at 12,000 RPM at 4 °C for 5 min. The supernatant was collected and analyzed by fluorimetry.

PK and biodistribution in rats: Male Wistar rats were administered DiD-labeled liposomes at 10 μmol phospholipid/kg via jugular cannula in 200-300 μL HEPES buffer. At selected time points (10 min, 30 min, 90 min, 4.5 h, 24 h, and 48 h), blood was collected from the jugular vein cannula into BD Microtainer® tubes coated with lithium heparin. The blood samples were

centrifuged for 5 min at 15,000 RPM at 4 °C. The supernatant was collected and analyzed by fluorimetry. Each group consisted of n = 3 rats.

48 h after administration, animals were anesthetized with an overdose of pentobarbital. The liver, spleen, lung, and liver, of each rat were excised and transferred into separate tubes with 0.075 M HCl in 90% isopropanol/10% water at a concentration of 1 g tissue/2.5 ml isopropanol solution. The tissues were then homogenized with an Omni THQ digital tissue homogenizer (Omni Int., Kennesaw, GA) for 120 s. The homogenate was stored for 12 h at 4 °C and then clarified by centrifugation at 5,000 RPM at 4 °C for 5 min. The supernatant was collected and analyzed by fluorimetry.

ABC effect in rats: Male Wistar rats were administered non-labeled liposomes at 0.1 μmol phospholipid/kg via jugular cannula in 200-300 μL HEPES buffer. Seven days later, rats were administered DiD-labeled liposomes at 10 μmol phospholipid/kg via jugular cannula in 200-300 μL HEPES buffer. At selected time points (10 min, 30 min, 90 min, 4.5 h, 24 h, and 48 h), blood was collected from the jugular vein cannula into BD Microtainer® tubes coated with lithium heparin. The blood samples were centrifuged for 5 min at 15,000 RPM at 4 °C. The supernatant was collected and analyzed by fluorimetry. Each group consisted of n = 4 rats. At 48 h, animals were anesthetized with an overdose of pentobarbital and biodistribution was determined following the same methods reported for the rat PK studies.

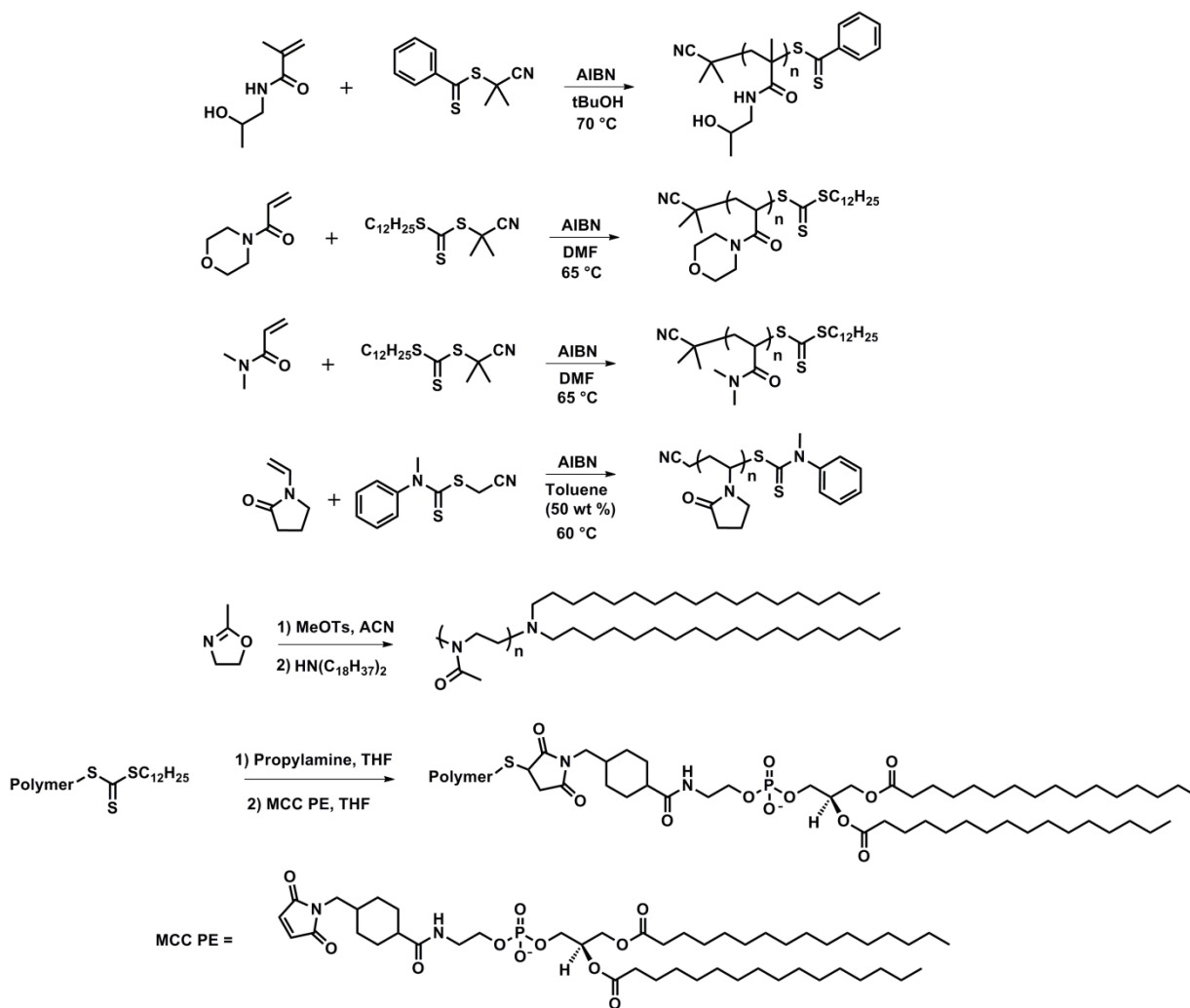
Sample and data analysis: Standard curves for each polymer-liposome were made by titrating DiD-labeled liposomes into the serum and tissues from an untreated animal. DiD (excitation 644 nm, emission 664 nm) was measured from each serum and tissue sample. The data for each group as a whole was fit to a two-compartment model using GraphPad Prism. The standard deviation for half-lives was calculated by fitting each individual animal to the two-compartment model and determining the standard deviation within each group. Once circulation half-life and accumulation in organs were found, *P* values were determined using the Student's *t*-test. A *P* value ≤ 0.05 was considered significant.

3.3 RESULTS

Synthesis: RAFT polymerizations were chosen for the vinyl polymers in order to achieve low polydispersity and a terminal functional handle for lipid conjugation. The selection of RAFT chain transfer agent and solvent for each polymerization were based upon previous literature reports, and proved critical for attaining low polydispersity polymers.⁴⁴ Following polymerization, RAFT endgroups were converted to thiols by aminolysis with propylamine under inert atmosphere. The free thiol end group was then either reacted with additional monomer for viscosity measurements, or MCC PE for liposome incorporation.

Unlike the RAFT polymers, PMOX was synthesized through a cationic ring-opening polymerization according to previous literature procedures.⁴⁵ The polymerization of oxazolines is commonly initiated by a variety of alkylating agents and can be terminated with a wide variety of nucleophiles. For viscosity measurements, PMOX polymerizations were terminated with basic water to yield a terminal hydroxyl on the polymer. For incorporation into liposomes, PMOX

polymerizations were terminated with dioctyldecylamine, yielding a lipid anchor on the polymer chain end.



Scheme 3.1: Synthetic schemes for HPMA polymerization, PAcM polymerization, PDMA polymerization, PVP polymerization, PMOX polymerization with lipid termination, and general polymer conjugation to MCC PE lipid (top to bottom).

Viscosity measurements: The viscosities of each polymer were measured under identical experimental conditions and are reported in Table 3.3. Solution viscosities are dependent on molecular weight, solvent (including salt concentration), and temperature and thus consistent experimental conditions are necessary in order to make an accurate comparison between polymer viscosities. We found that each of the five polymers tested have lower solution viscosities than PEG of corresponding molecular weight.

Polymer	M_w (kDa)	PDI	Viscosity (η)
HPMA	12	1.07	0.147
	68	1.16	0.306
PMOX	11	1.2	0.201
	26	1.5	0.289
PDMA	10	1.04	0.086
	53	1.2	0.45
PVP	10	1.2	0.131
	53	1.6	0.207
PAcM	14	1.03	0.08
	64	1.2	0.328
PEG	10	1.05	0.234
	22	1.05	0.371
	67	1.06	0.839

Table 3.3: Polymer viscosities in aqueous solution compared to PEG of similar molecular weight.

Liposome formulation: To investigate the ability of the selected polymers to extend circulation and avoid an ABC effect, polymers were conjugated to fluorescently labeled liposomes. Liposomes are a versatile platform that can be tailored to yield desired *in vivo* properties, and have been extensively investigated for drug delivery applications.⁴⁶ When liposomes are formulated with stealth character, circulation half-life is greatly increased and uptake by the Mononuclear Phagocyte System (MPS) is greatly decreased.⁴⁷ Stealth character is most commonly introduced by PEGylating the surface of liposomes, although other polymers have also been shown to extend circulation when conjugated to the surface of liposomes.³¹

Stable liposomes composed of HSPC, cholesterol, polymer-lipid conjugate, and DiD were formed through an ethanol injection method followed by high pressure extrusion. Following formation, liposomes were purified by dialysis in regenerated cellulose dialysis bags in HEPES buffer. All liposome solutions were passed through a sterile filter and measured by DLS prior to *in vivo* studies. The final size of the liposomes was ~100 nm with low polydispersity (Table 3.4).

Polymer	Diameter (nm)	PDI
PEG	107.7	0.126
PMOX	106.7	0.138
PVP	91.42	0.025
HPMA	110	0.067
PAcM	100.2	0.052
PDMA	99.8	0.13
No Polymer	98.7	0.057

Table 3.4: Liposome sizes with polymer coatings for *in vivo* studies.

PK in mice: To investigate the ability of the panel of polymers to extend the circulation of a therapeutic, DiD-labeled polymer-coated liposomes were injected into mice. The concentration of the liposomes in the blood was monitored for 48 hours (Figure 3.1). All six polymers (PEG, HPMA, PVP, PDMA, PMOX, and PAcM) increased circulation half-life when compared to liposomes without polymer (Table 3.5). The concentration of liposomes in the liver, spleen, lung, and kidneys was measured at 24 hours and 48 hours. Incorporation of polymers into the liposomes led to reduced accumulation in the liver and spleen (Figure 3.2).

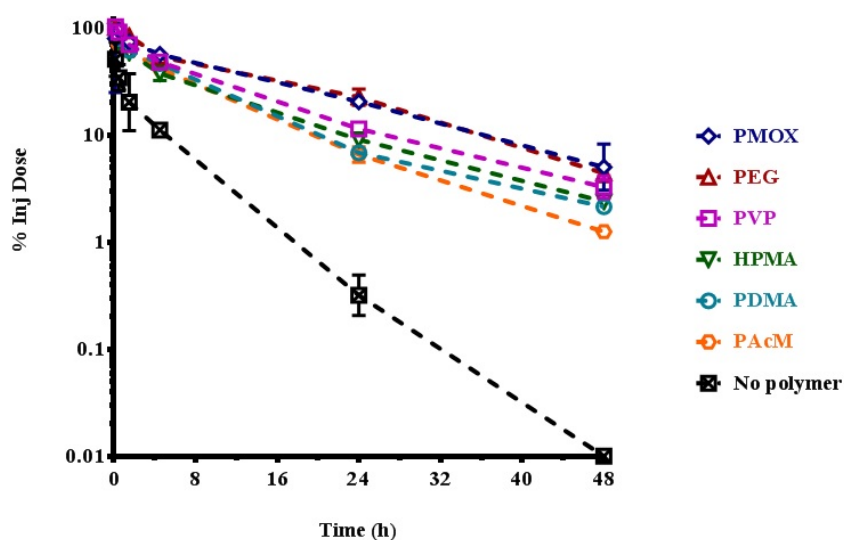


Figure 3.1: Pharmacokinetics of polymer coated liposomes in mice over 48 h.

	PEG	PMOX	PVP	PDMA	HPMA	PAcM	No Polymer
Half-life (h)	16.3 ± 0.7	14.8 ± 0.8	9.8 ± 1.5	7.5 ± 0.5	8.2 ± 1.1	6.3 ± 0.9	3.7 ± 1.2
AUC	1402	1371	1049	892	833.	815	183

Table 3.5: Circulation half-lives of liposomes in mice.

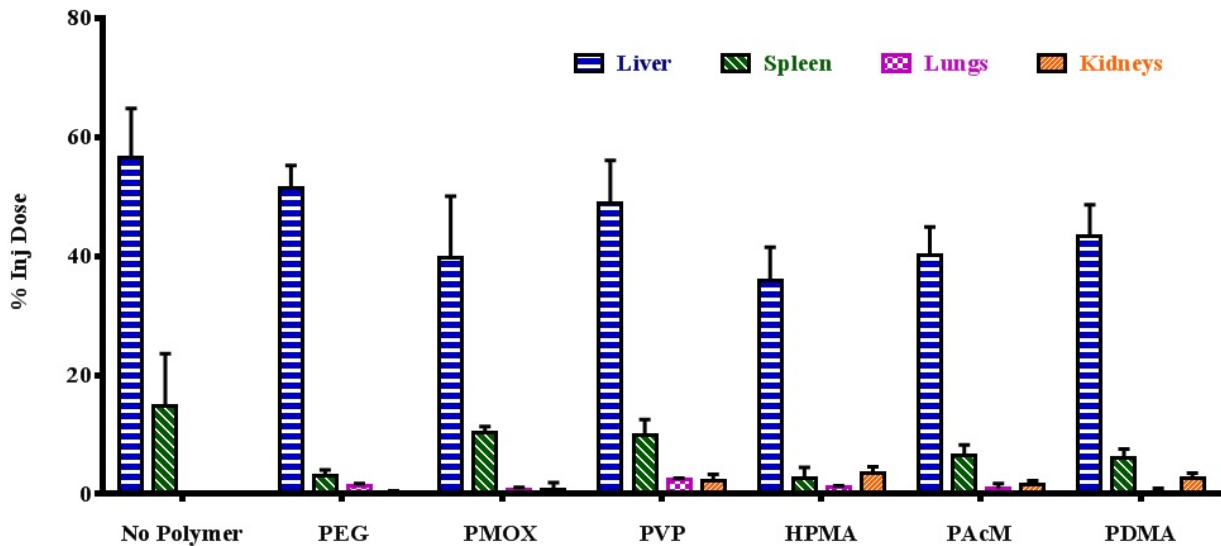


Figure 3.2: Biodistribution of liposomes in mice after 48 h.

PK and BD in rats: Once the ability of these polymers to extend liposome circulation in mice was established, the pharmacokinetics and biodistribution of each polymer-liposome at a 10 μmol phospholipid/kg dose were evaluated in rats. These experiments were run similarly to those in mice, and the data confirmed the results found in mice. All six polymers extended circulation in comparison to liposomes without polymer (Figure 3.3). PEG and PMOX were the two longest circulating materials with circulation half-lives >30 h. Additionally, accumulation in the liver and spleen was reduced when any of the six polymers were incorporated into the liposomes (Figure 3.5). Once again, PEG and PMOX were the top performers, with less than 20% of the injected dose in the liver after 48 h. All liposomes incorporating polymers had $<10\%$ of the injected dose in the spleen. Liposomes without polymer accumulated predominantly in the liver (31%) and spleen (11%). The fraction of the injected dose recovered in the plasma, liver, spleen, kidneys, and lungs was around 50 % for each polymer liposome.

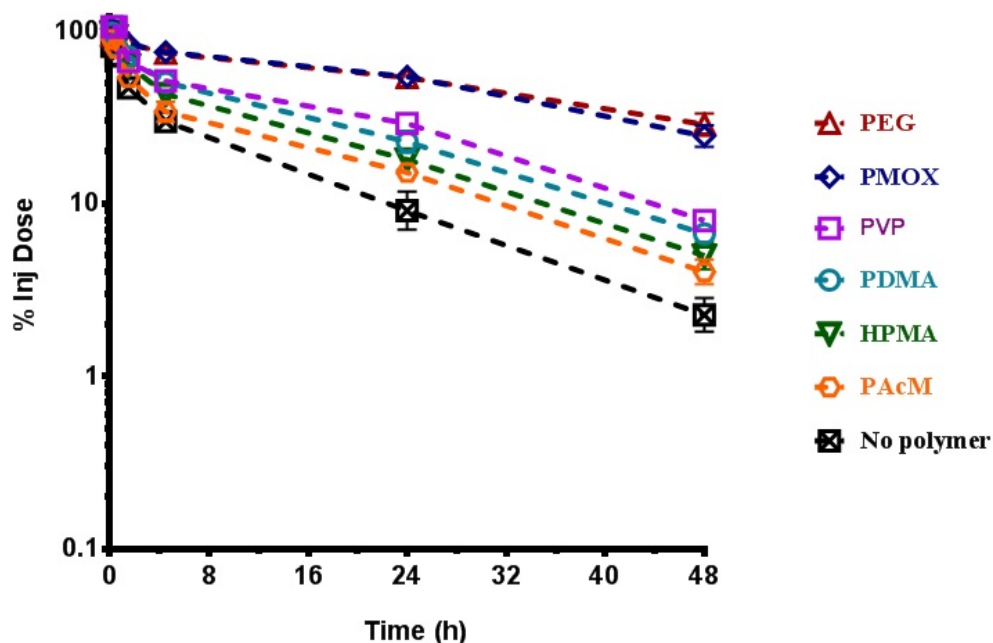


Figure 3.3: Pharmacokinetics of a single dose of liposomes in rats over 48 h.

ABC in rats: The ability of the selected polymers to evade the ABC effect was investigated in Wistar rats. The ABC effect is most prominent when a small (≤ 0.1 mol phospholipid/kg) first dose is followed 6-8 days later by a second dose.¹⁵ When the ABC effect is elicited, the second dose is rapidly cleared from circulation and increased accumulation in the liver and spleen is observed. If no ABC effect is observed, the second dose of a material should have similar pharmacokinetics and biodistribution to the first dose.

In these experiments, the pharmacokinetics and biodistribution of a second dose of a polymer-coated liposome is measured and compared to the previous results obtained for a single dose. To initiate the ABC effect, non-labeled polymer-coated liposomes were administered to rats at a concentration of $0.1 \mu\text{mol}$ phospholipid/kg. Seven days later, DiD-labeled polymer-coated liposomes were administered at $10 \mu\text{mol}$ phospholipid/kg. The concentration of liposomes in circulation was recorded over 48 hours, at which point the animals were sacrificed and the concentration of liposomes in the liver, spleen, lung, and kidneys was measured. Liposomes without polymer and liposomes with HPMA, PVP, PDMA, and PAcM did not exhibit an ABC effect (Table 3.6). The pharmacokinetics and biodistribution of the second dose of each of these materials were very similar to those observed for a single dose (Figure 3.4). PMOX, however, exhibited a strong ABC effect. The second dose completely lost its long circulating character (half-life < 2 hr), and had increased accumulation in the liver and spleen (Figure 3.5).

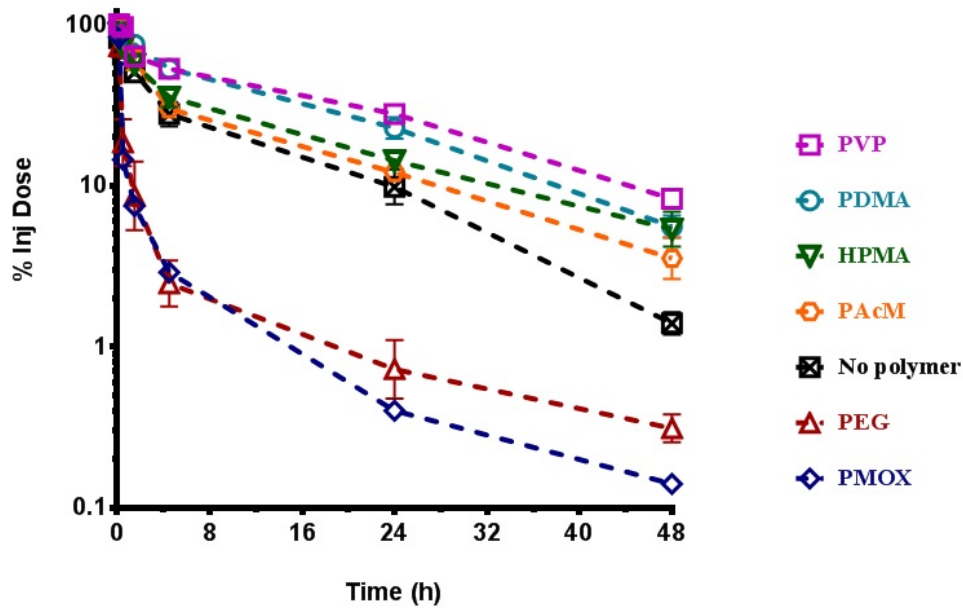


Figure 3.4: Pharmacokinetics of the second dose of liposomes in rats over 48 h.

	PEG	PMOX	PVP	PDMA	HPMA	PAcM	No Polymer	
Half-life(h)	33.6 ± 1.3	30.5 ± 2.5	20.7 ± 1.3	16.0 ± 1.2	16.0 ± 1.2	16.4 ± 1.8	12.0 ± 0.2	} Single dose
AUC	2590	2570	1524	1352	1138	933.3	716.6	
Half-life(h)	1.7 ± 0.8	2.1 ± 0.5	19.6 ± 2.6	15.0 ± 2.8	15.5 ± 2.8	16.3 ± 2.7	12.3 ± 1.8	} 2 nd dose
AUC	89	82	1512	1387	951	832	701	

Table 3.6: Circulation half-lives of liposomes incorporating polymers for a single dose vs. the second dose.

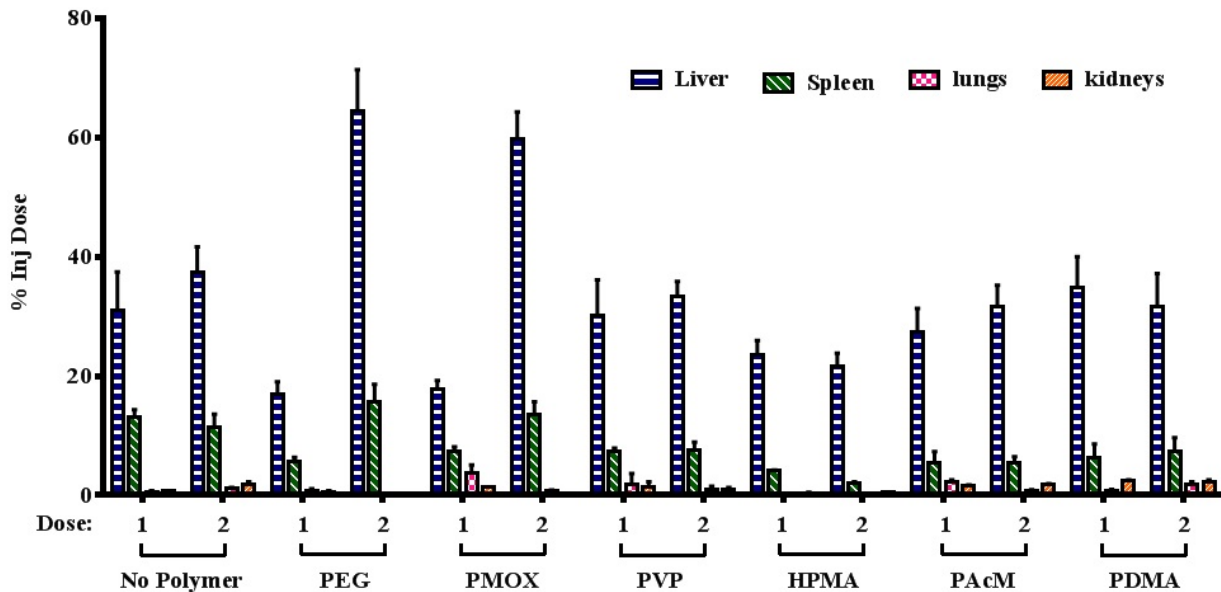


Figure 3.5: Biodistribution of the first and second dose liposomes in rats after 48 h.

3.4 DISCUSSION:

We have evaluated and compared a small library of sterically stabilizing polymers to learn which may provide an extended circulation time yet avoid the ABC effect. All of the polymers studied extend circulation times. Longer circulation allows for either extended drug release in the blood leading to constant available therapeutic concentrations over longer periods, or increased time/opportunity to reach a target site via passive or active targeting. Polymer modified liposomes were evaluated using consistent experimental conditions to allow a direct comparison of the effect on circulation half-life. The results are in accord with the previous literature that PEG and PMOX greatly extend the circulation half-life compared to the other polymers. However, when compared to unmodified, conventional liposomes, each polymer tested increased circulation half life.

The increased circulation in comparison to conventional liposomes is likely due to the ability of polymers to act as a steric shield. This ability to sterically shield the liposome surface can lead to decreased interaction with other membrane surfaces⁴⁸ and serum opsonizing factors.^{49,50} Additionally, if opsonizing factors do adsorb onto the surface of the liposome, it has been shown that sterically shielding polymers can still prevent those factors from interacting with the corresponding macrophage complement receptor.⁵¹ The differences observed in circulation times of polymer modified liposomes may be due to differences in the abilities of these polymers to sterically shield the liposome surface. When opsonins and other materials approach the surface of a polymer coated liposome, extended polymer chains are compressed into a higher energy conformation, which creates an opposing repulsive force.⁶ Thus, differences in polymer molecular weight, flexibility, and conformation affect the ability of a polymer to repel approaching materials.⁵² To provide optimal surface protection, polymer molecular weight

and graft density must be optimized to account for differences in polymer flexibility and conformation.

We compared pharmacokinetics and biodistribution of liposomes incorporating 5 mole percent of 2 kDa polymers. These values were chosen based on previous reports of the ideal mole percent and molecular weight of PEG for extending liposome circulation^{53,54} However, these may not be the optimal conditions for the other polymers investigated. The ideal graft density and molecular weight of polymers for the steric protection of liposomes *in vivo* is one that strikes a balance between providing complete surface coverage and allowing for maximum chain mobility.⁵⁴ Because the polymers we have investigated have different chain flexibilities and degrees of polymerization, 5 mole percent and 2 kDa molecular weight may not be ideal parameters for each polymer. Polymers of optimal molecular weight and liposomal graft density may further improve the circulation half-lives, strengthening the case for their use rather than PEG in certain applications.

Although PEG is excellent at preventing interactions between the surface of a liposome and serum opsonizing factors, specific anti-PEG IgM can efficiently bind PEG. When anti-PEG IgM is present in circulation as either preexisting antibodies or as a response to a first dose of PEGylated material, PEG is rapidly removed from circulation and accumulates extensively in the liver and spleen. This can compromise treatments in which repeated administration is necessary and may increase toxicity towards organs where the PEGylated materials accumulate. We have indentified four circulation-extending polymers (HPMA, PAcM, PDMA, and PVP) that do not induce the ABC effect upon repeated administration. Additionally, we found that PMOX, a polymer with similar pharmacokinetics and biodistribution to PEG, also illicit an ABC effect.

It remains unclear why some polymers induce an ABC effect and others do not. However, it is clear that the production of IgM plays an important role in the mechanism of the ABC effect. In a critical step during the PEG ABC mechanism, PEGylated materials crosslink surface receptors on B-cells which triggers the production of anti-PEG IgM. The quantity of anti-PEG IgM produced has been shown to correlate with the extent of the ABC phenomenon.⁵⁵ Furthermore, Ishihara *et. al.* found that PVP nanoparticles that did not exhibit an ABC effect also did not initiate the production of anti-PVP IgM.⁵⁶ These results may imply that polymers that avoid the ABC effect do so by avoiding specific IgM production. Whether this means the polymers are not able to efficiently bind B-cell receptors or somehow interfere with IgM production through an alternative mechanism is still uncertain.

In evaluating polymers for extended circulation, none achieved half-lives as long as PEG or PMOX liposomes. However, the circulation half-life of a second dose of PEG or PMOX liposomes was much shorter than both the first and second dose of all other polymer coated liposomes. This suggests that for applications that require multiple administrations within the parameters for initiation of the ABC effect, the four polymers that do not initiate an ABC effect may be better candidates. Additionally, for patients with preexisting anti-PEG antibodies, these four polymers or PMOX could offer improved pharmacokinetics and biodistribution.^{12,14}

In addition to *in vivo properties*, the intrinsic viscosity of a polymer in solution is an important physical property when considering a polymer for drug delivery. Highly viscous polymer solutions can limit dose concentration due to syringability of the polymer drug solution.¹¹ PEG, in particular, has a high intrinsic viscosity in aqueous solutions.⁸ Other

hydrophilic polymers have been reported to have much lower aqueous intrinsic viscosities, though the inconsistent experimental parameters prohibit an accurate comparison in viscosity values.^{37,58,59} In this work, polymer viscosities were measured under consistent conditions, including temperature, molecular weight, polymer concentration, salt concentration, and pH. Our results show that the five other polymers investigated have lower intrinsic viscosities than that of PEG.

In this study we have evaluated the physical and *in vivo* properties of a panel of hydrophilic polymers for extended circulation. We have identified 5 polymers with lower aqueous viscosities than PEG. We have also identified four polymers that are able to extend the circulation half-lives of liposomes without eliciting the ABC effect upon repeated administration. Our results suggest that in specific cases where PEG's high intrinsic viscosity or ABC effect is detrimental to a delivery system, other polymers can play the role of sterically stabilizing materials *in vivo*. Furthermore, we have found that PMOX, a polymer with very similar *in vivo* properties to PEG, does initiate the ABC effect. These observations may prove valuable for future design and application of polymers for drug delivery and extended circulation.

3.5 ACKNOWLEDGEMENTS

I gratefully acknowledge Dr. Hideaki Okochi for assistance with the rat experiments, Dr. Saul Kivimae for assistance with the mice experiments, Dr. Matthew Kade for assistance with viscosity measurements, and Tracy Chuong for assistance in synthesis. I would also like to acknowledge Dr. Vincent Venditto, Aditya Kohli, and Jonathan Sockolosky for their insightful scientific input.

3.6 REFERENCES

1. Duncan, R. The dawning era of polymer therapeutics. *Nat. Rev. Drug Discov.* **2**, 347–60 (2003).
2. Zhang, Y., Chan, H. F. & Leong, K. W. Advanced materials and processing for drug delivery: the past and the future. *Adv. Drug Deliv. Rev.* **65**, 104–20 (2013).
3. Knop, K., Hoogenboom, R., Fischer, D. & Schubert, U. S. Poly(ethylene glycol) in drug delivery: pros and cons as well as potential alternatives. *Angew. Chem. Int. Ed. Engl.* **49**, 6288–308 (2010).
4. Veronese, F. M. Peptide and protein PEGylation: a review of problems and solutions. *Biomaterials* **22**, 405–17 (2001).
5. Hamidi, M., Azadi, A. & Rafiei, P. Pharmacokinetic consequences of pegylation. *Drug Deliv.* **13**, 399–409 (2006).
6. Owens, D. E. & Peppas, N. A. Opsonization, biodistribution, and pharmacokinetics of polymeric nanoparticles. *Int. J. Pharm.* **307**, 93–102 (2006).
7. *PEGylated Protein Drugs: Basic Science and Clinical Applications*. (Birkhäuser Basel, 2009). doi:10.1007/978-3-7643-8679-5

8. Kirinčič, S. & Klofutar, C. Viscosity of aqueous solutions of poly(ethylene glycol)s at 298.15 K. *Fluid Phase Equilib.* **155**, 311–325 (1999).
9. Dams, E. T. *et al.* Accelerated blood clearance and altered biodistribution of repeated injections of sterically stabilized liposomes. *J. Pharmacol. Exp. Ther.* **292**, 1071–9 (2000).
10. Lee, J. & Tripathi, A. Intrinsic viscosity of polymers and biopolymers measured by microchip. *Anal. Chem.* **77**, 7137–47 (2005).
11. Liu, J., Nguyen, M. D. H., Andya, J. D. & Shire, S. J. Reversible self-association increases the viscosity of a concentrated monoclonal antibody in aqueous solution. *J. Pharm. Sci.* **94**, 1928–40 (2005).
12. Richter, A. W. & Åkerblom, E. Polyethylene Glycol Reactive Antibodies in Man: Titer Distribution in Allergic Patients Treated with Monomethoxy Polyethylene Glycol Modified Allergens or Placebo, and in Healthy Blood Donors. *Int. Arch. Allergy Immunol.* **74**, 36–39 (1984).
13. Garratty, G. Progress in modulating the RBC membrane to produce transfusable universal/stealth donor RBCs. *Transfus. Med. Rev.* **18**, 245–256 (2004).
14. Garratty, G. Modulating the red cell membrane to produce universal/stealth donor red cells suitable for transfusion. *Vox Sang.* **94**, 87–95 (2008).
15. Laverman, P. *et al.* Factors affecting the accelerated blood clearance of polyethylene glycol-liposomes upon repeated injection. *J. Pharmacol. Exp. Ther.* **298**, 607–12 (2001).
16. Suzuki, T. *et al.* Accelerated blood clearance of PEGylated liposomes containing doxorubicin upon repeated administration to dogs. *Int. J. Pharm.* **436**, 636–43 (2012).
17. Ishida, T. *et al.* Accelerated blood clearance of PEGylated liposomes following preceding liposome injection: effects of lipid dose and PEG surface-density and chain length of the first-dose liposomes. *J. Control. Release* **105**, 305–17 (2005).
18. Ishida, T., Atobe, K., Wang, X. & Kiwada, H. Accelerated blood clearance of PEGylated liposomes upon repeated injections: effect of doxorubicin-encapsulation and high-dose first injection. *J. Control. Release* **115**, 251–8 (2006).
19. Sherman, M. R., Williams, L. D., Sobczyk, M. a, Michaels, S. J. & Saifer, M. G. P. Role of the methoxy group in immune responses to mPEG-protein conjugates. *Bioconjug. Chem.* **23**, 485–99 (2012).
20. Zhao, Y. *et al.* Repeated injection of PEGylated solid lipid nanoparticles induces accelerated blood clearance in mice and beagles. *Int. J. Nanomedicine* **7**, 2891–900 (2012).
21. Sroda, K. *et al.* Repeated injections of PEG-PE liposomes generate anti-PEG antibodies. *Cell. Mol. Biol. Lett.* **10**, 37–47 (2005).

22. Garay, R. P., El-Gewely, R., Armstrong, J. K., Garratty, G. & Richette, P. Antibodies against polyethylene glycol in healthy subjects and in patients treated with PEG-conjugated agents. *Expert Opin. Drug Deliv.* **9**, 1319–23 (2012).
23. Koide, H. *et al.* Particle size-dependent triggering of accelerated blood clearance phenomenon. *Int. J. Pharm.* **362**, 197–200 (2008).
24. Saadati, R., Dadashzadeh, S., Abbasian, Z. & Soleimanjahi, H. Accelerated blood clearance of PEGylated PLGA nanoparticles following repeated injections: effects of polymer dose, PEG coating, and encapsulated anticancer drug. *Pharm. Res.* **30**, 985–95 (2013).
25. Zhang, C., Fan, K., Ma, X. & Wei, D. Impact of large aggregated uricases and PEG diol on accelerated blood clearance of PEGylated canine uricase. *PLoS One* **7**, e39659 (2012).
26. Ishida, T. *et al.* Accelerated blood clearance of PEGylated liposomes following preceding liposome injection: Effects of lipid dose and PEG surface-density and chain length of the first-dose liposomes. *J. Control. Release* **105**, 305–317 (2005).
27. Ishida, T., Ichihara, M., Wang, X. & Kiwada, H. Spleen plays an important role in the induction of accelerated blood clearance of PEGylated liposomes. *J. Control. Release* **115**, 243–50 (2006).
28. Lammers, T., Ulbrich, K., Duncan, R. & Vicent, M. J. Do HPMa copolymer conjugates have a future as clinically useful nanomedicines? A critical overview of current status and future opportunities. *Adv. Drug Deliv. Rev.* **62**, 272–282 (2010).
29. Duncan, R. Development of HPMa copolymer-anticancer conjugates: clinical experience and lessons learnt. *Adv. Drug Deliv. Rev.* **61**, 1131–48 (2009).
30. Etrych, T. *et al.* Biodegradable star HPMa polymer–drug conjugates: Biodegradability, distribution and anti-tumor efficacy. *J. Control. Release* **154**, 241–248 (2011).
31. Immordino, M. L., Dosio, F. & Cattell, L. Stealth liposomes: review of the basic science, rationale, and clinical applications, existing and potential. *Int. J. Nanomedicine* **1**, 297–315 (2006).
32. Zelikin, A. N., Such, G. K., Postma, A. & Caruso, F. Poly(vinylpyrrolidone) for bioconjugation and surface ligand immobilization. *Biomacromolecules* **8**, 2950–3 (2007).
33. Gaertner, F. C., Luxenhofer, R., Blechert, B., Jordan, R. & Essler, M. Synthesis, biodistribution and excretion of radiolabeled poly(2-alkyl-2-oxazoline)s. *J. Control. Release* **119**, 291–300 (2007).
34. Zalipsky, S., Hansen, C. B., Oaks, J. M. & Allen, T. M. Evaluation of blood clearance rates and biodistribution of poly(2-oxazoline)-grafted liposomes. *J. Pharm. Sci.* **85**, 133–7 (1996).
35. Torchilin, V. P. *et al.* New synthetic amphiphilic polymers for steric protection of liposomes in vivo. *J. Pharm. Sci.* **84**, 1049–1053 (1995).
36. Drotleff, S. *et al.* Biomimetic polymers in pharmaceutical and biomedical sciences. *Eur. J. Pharm. Biopharm.* **58**, 385–407 (2004).

37. Kohori, F. *et al.* Control of adriamycin cytotoxic activity using thermally responsive polymeric micelles composed of poly(N-isopropylacrylamide-co-N,N-dimethylacrylamide)-b-poly(d,l-lactide). *Colloids Surfaces B Biointerfaces* **16**, 195–205 (1999).
38. De Souza, R., Zahedi, P., Allen, C. J. & Piquette-Miller, M. Polymeric drug delivery systems for localized cancer chemotherapy. *Drug Deliv.* **17**, 365–75 (2010).
39. Canal, F., Sanchis, J. & Vicent, M. J. Polymer--drug conjugates as nano-sized medicines. *Curr. Opin. Biotechnol.* **22**, 894–900 (2011).
40. Torchilin, V. P. *et al.* New synthetic amphiphilic polymers for steric protection of liposomes in vivo. *J. Pharm. Sci.* **84**, 1049–53 (1995).
41. Torchilin, V. P., Shtilman, M. I., Trubetsky, V. S., Whiteman, K. & Milstein, A. M. Amphiphilic vinyl polymers effectively prolong liposome circulation time in vivo. *Biochim. Biophys. Acta - Biomembr.* **1195**, 181–184 (1994).
42. Woodle, M. C., Engbers, C. M. & Zalipsky, S. New Amphipatic Polymer-Lipid Conjugates Forming Long-Circulating Reticuloendothelial System-Evading Liposomes. *Bioconjug. Chem.* **5**, 493–496 (1994).
43. Whiteman, K. R., Subr, V., Ulbrich, K. & Torchilin, V. P. Poly(HPMA)-coated liposomes demonstrate prolonged circulation in mice. *J. Liposome Res.* **11**, 153–164 (2001).
44. Boyer, C. *et al.* Bioapplications of RAFT polymerization. *Chem. Rev.* **109**, 5402–36 (2009).
45. Woodle, M. C., Engbers, C. M. & Zalipsky, S. New amphipatic polymer-lipid conjugates forming long-circulating reticuloendothelial system-evading liposomes. *Bioconjug. Chem.* **5**, 493–6 (1994).
46. Torchilin, V. P. Recent advances with liposomes as pharmaceutical carriers. *Nat. Rev. Drug Discov.* **4**, 145–60 (2005).
47. Allen, T. M. & Hansen, C. Pharmacokinetics of stealth versus conventional liposomes: effect of dose. *Biochim. Biophys. Acta - Biomembr.* **1068**, 133–141 (1991).
48. Evans, E., Klingenberg, D. J., Rawicz, W. & Szoka, F. Interactions between Polymer-Grafted Membranes in Concentrated Solutions of Free Polymer. *Langmuir* **12**, 3031–3037 (1996).
49. Jeon, S. ., Lee, J. ., Andrade, J. . & De Gennes, P. . Protein—surface interactions in the presence of polyethylene oxide. *J. Colloid Interface Sci.* **142**, 149–158 (1991).
50. Müller, B. W., R. H. Müller, H. C. Particle size, surface hydrophobicity and interaction with serum parenteral fat emulsions and model drug as parameters related to RES uptake. *Clin. Nut* **11**, 289–297 (1992).
51. Moghimi, S. M., Hamad, I., Andresen, T. L., Jørgensen, K. & Szebeni, J. Methylation of the phosphate oxygen moiety of phospholipid-methoxy(polyethylene glycol) conjugate prevents PEGylated liposome-mediated complement activation and anaphylatoxin production. *FASEB J.* **20**, 2591–3 (2006).

52. Torchilin, V. P. & Papisov, M. I. Why do Polyethylene Glycol-Coated Liposomes Circulate So Long?: Molecular Mechanism of Liposome Steric Protection with Polyethylene Glycol: Role of Polymer Chain Flexibility. *J. Liposome Res.* **4**, 725–739 (1994).
53. Needham, D. *et al.* Polymer-Grafted Liposomes: Physical Basis for the “Stealth” Property. *J. Liposome Res.* **2**, 411–430 (1992).
54. Storm, G., Belliot, S. O., Daemen, T. & Lasic, D. D. Surface modification of nanoparticles to oppose uptake by the mononuclear phagocyte system. *Adv. Drug Deliv. Rev.* **17**, 31–48 (1995).
55. Ishihara, T. *et al.* Accelerated blood clearance phenomenon upon repeated injection of PEG-modified PLA-nanoparticles. *Pharm. Res.* **26**, 2270–9 (2009).
56. Ishihara, T. *et al.* Evasion of the accelerated blood clearance phenomenon by coating of nanoparticles with various hydrophilic polymers. *Biomacromolecules* **11**, 2700–6 (2010).
57. Lee, J. & Tripathi, A. Intrinsic viscosity of polymers and biopolymers measured by microchip. *Anal. Chem.* **77**, 7137–47 (2005).
58. Mehrdad, A. & Akbarzadeh, R. Effect of Temperature and Solvent Composition on the Intrinsic Viscosity of Poly(vinyl pyrrolidone) in Water - Ethanol Solutions. 3720–3724 (2010).
59. Rashid, H. U. & Abubakar, S. D. Discontinuity in the variation of intrinsic viscosity of polymers and their mixtures with temperature in dilute solutions. *J. Polym. Sci. Part C Polym. Lett.* **27**, 5–8 (1989).

Chapter 4

Development and Analysis of pH-Sensitive Dendrimers for siRNA Delivery

4.1 INTRODUCTION

The development of new therapeutics is essential for improving public health and is the central aim of countless research efforts. In 2011 alone, pharmaceutical companies spent about \$135 billion on research and development with much of the focus on the discovery of small molecule drugs.¹ Numerous such drugs typically operate by targeting and binding specific proteins and other biomacromolecules. Although this strategy has proven to be successful in the treatment of many ailments, there are still myriad diseases that remain “undruggable”, including for example Ewing’s sarcoma, kidney disease, and myocardial infarction.^{2,3} An alternative treatment option to small molecule drugs was introduced by Fire and Mello in 1998 with the discovery of RNA *interference* (RNAi).⁴ Specifically, short interfering RNA (siRNA) has been shown to be effective at silencing targeted genes responsible for many diseases.

siRNA is a double-stranded RNA molecule composed of 21-25 base pairs that silences genes by inhibiting protein translation.⁵ Briefly, the natural mechanism of action begins in the cytosol of the cell where the siRNA is loaded into an RNA-induced silencing complex (RISC). Next, an enzyme component of the RISC, Ago2, cleaves the siRNA molecule into two single strands. One strand remains on the RISC (guide strand) while the other strand (passenger strand) is discarded. The guide strand on the RISC then has the ability to bind a specific, complementary mRNA molecule through Watson-Crick base pairing. Once bound to the mRNA, the endonuclease portion of the RISC cleaves the mRNA, initiating its degradation and preventing translation of the encoded protein.⁶

Although siRNA has been extensively investigated over the past decade, it has not been translated into clinical application due to difficulties in finding a safe and effective *in vivo* delivery method. Naked siRNA has a very short lifetime in the blood stream and nearly complete enzymatic degradation is observed after 1 h.⁷ Also, the polyanionic character of siRNA stemming from its polyphosphate backbone discourages cellular uptake.⁶ A delivery vehicle is required to overcome these two major obstacles. However, the introduction of a carrier creates many additional parameters that must be considered. Such considerations include proficient attachment of siRNA to the carrier and efficient release once inside the cell – a step that often requires assistance in endosomal escape. Additionally, for clinical use the carrier must also be non-toxic, non-immunogenic, and non-pathogenic. Practical considerations include a facile and inexpensive synthesis and easy administration. These requirements are summarized in Table 1.

Table 1: Criteria for *in vivo* siRNA carriers

• Efficient loading of siRNA
• Protect siRNA from degradation
• Facilitate cellular uptake
• Assist in endosomal escape
• Release siRNA within cytosol
• Non-toxic
• Non-immunogenic
• Non-pathogenic
• Ease of fabrication/large scale production
• Simple administration

For researchers, *in vivo* gene delivery has generally been an exceptionally difficult task to accomplish.⁸ In contrast, viruses are remarkably adept at delivering genetic material to a variety of cells in many chemical environments. By replacing the virus genome with a target gene, efficient delivery can be accomplished.⁹ Unfortunately such delivery methods violate many of the requirements for a carrier including the intrinsic immunogenic effects of viruses, the possibility of pathogenicity, and the inability to fabricate such carriers on a very large scale inexpensively. These issues inherent to viral gene delivery have led to substantial investigation into polymeric carriers as an alternative delivery strategy.

Both linear and branched polycationic polymers have been explored as siRNA delivery vehicles.⁸ Polycationic materials can electrostatically complex polyanionic siRNA to form polyplexes on the nanometer scale. Two early examples of such polycationic materials are polyethylenimine (PEI) and poly(L-lysine) (PLL).^{10,11} At physiological pH, numerous amino groups on these polymers are protonated, accounting for their cationic nature. Though both PEI and PLL complex siRNA efficiently, polycationic materials are generally toxic to cells as they disrupt phospholipid bilayers. Biodegradable alternatives such as poly(β -amino esters) (PBAE) and poly(ketalized serine) have been developed to minimize toxicity while maintaining high rates of transfection.¹²⁻¹⁴ These systems offer improvements, but have not yet achieved simultaneously high transfection rates and low toxicities. Dendritic carriers have also been investigated, including poly(amidoamine) PAMAM and polypropylenimine (PPI).¹⁵ While these systems show promising transfection capabilities, they are prone to cytotoxicity and are not biodegradable.¹⁶ To the best of our knowledge there has been no report of a non-toxic carrier that incorporates all of the requisite properties for an efficient gene delivery vehicle. Herein, we report progress towards such a carrier.

Our laboratory has previously reported the synthesis and application of a biocompatible, PEGylated dendrimer as a delivery vehicle for anti-tumor drugs.¹⁷ This carrier is non-toxic, biodegradable, and can deliver bioactive payloads *in vivo*. We envision that this carrier may also be tailored for gene delivery by installing amines at the core and using peripheral poly(ethylene glycol) (PEG) chains to provide enhanced solubility and protection of the dendrimer-siRNA complex. The high degree of synthetic control inherent in dendrimer fabrication allows for the modular design necessary to fulfill the requirements of a gene delivery vector. First, optimal loading of siRNA can be achieved through a screening of various amine structures that can be attached to the carrier. Second, *in vivo* protection of the payload can be accomplished by appending multiple PEG chains to the periphery of the dendrimer. Third, cellular uptake through passive endocytosis will occur readily as the polyanionic character of siRNA will be negated by the polycationic dendrimers and shielded by the PEG chains. Fourth, endosomal escape, triggered release of the payload, and long term toxicity can be achieved by connecting the amine moieties to the dendrimer via acid-degradable linkages. Once subjected to the acidic environment of the lysosome (pH 4.5-5), the polycationic character of the dendrimer will erode and render the dendrimer non-toxic.¹⁸ In addition, as amine structures begin releasing from the dendrimer, siRNA will start unpacking from the carrier causing an increase in osmotic pressure and endosomal disruption/escape.¹⁹ This siRNA complexation process and biopathway are illustrated in Figure 4.1. The approach outlined above should allow us to address all of the necessary criteria for an siRNA delivery system, and yield a biodegradable, non-toxic carrier

with the ability to effectively transport and deliver siRNA *in vivo*. Herein, the synthesis, complexation capability, and transfection efficiency of dendrimers with both non-degradable amide-linked amine structures and acid-degradable hydrazone-linked amine structures are reported.

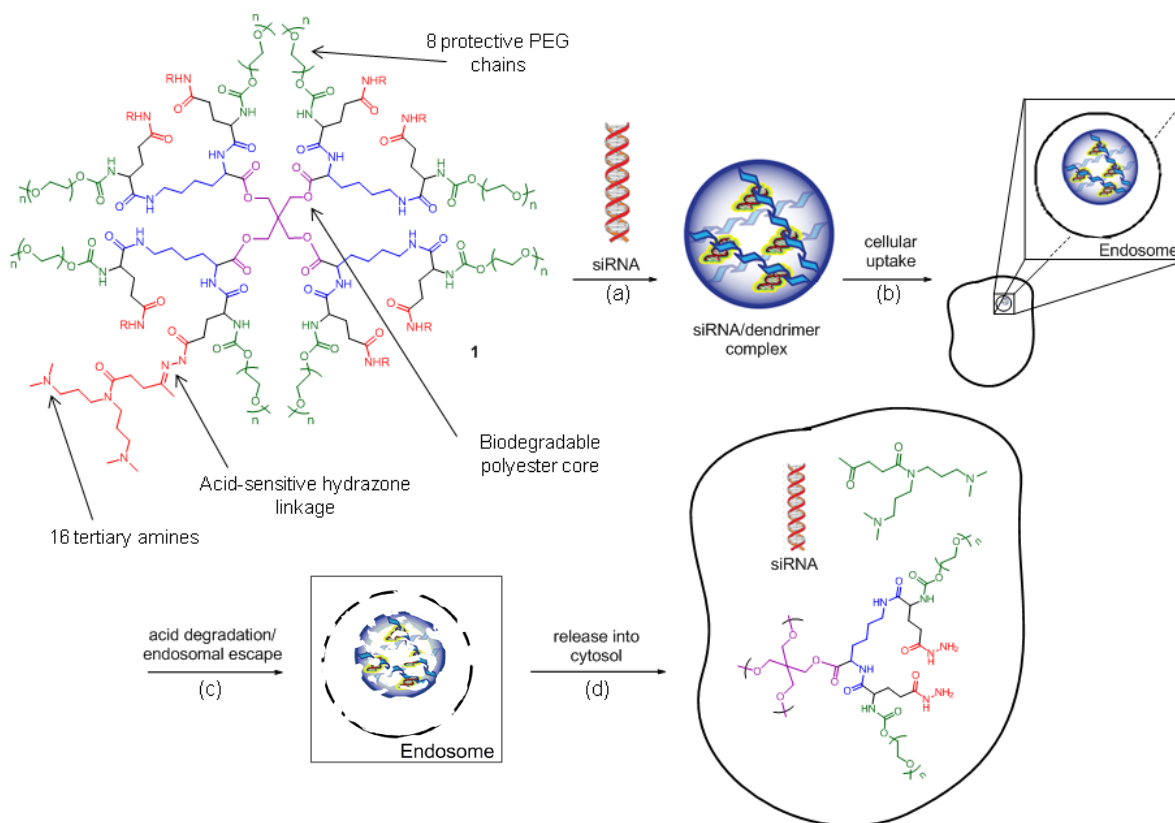


Figure 4.1. Schematic diagram of ester-amide dendrimer as an siRNA carrier. (a) Protonated amines of dendrimer electrostatically complex siRNA. (b) The polyplex is endocytosed into the cell. (c) Endosomal escape occurs assisted by both the proton sponge effect and swelling due to the degradation of hydrazone linkages. (d) After degradation/endosomal escape, naked siRNA is released into cytosol along with non-toxic degradation products.

4.2 EXPERIMENTAL

General: All reagents were purchased from commercial sources and used without further purification unless otherwise noted. Poly(ethylene glycol) derivatives were purchased from Laysan Biosciences Inc. (Arab, AL). Amino acid derivatives were purchased from Bachem (Torrance, CA). The anti-luciferase siRNA (sense strand: 5'-CUU ACG CUG AGU ACU UCG A dTdT-3') was obtained from Dharmacon (Lafayette, CO). Water was purified to a resistance of 18 M Ω using a Barnstead NANOpure® Diamond™ purification system. *N,N*-dimethylformamide (DMF), triethylamine (TEA), and methylene chloride (DCM) were purified

by passing the solvents under nitrogen pressure through two packed columns of neutral alumina within a commercial solvent purification apparatus (Glass Contour). All glassware was flame dried under vacuum or nitrogen purge prior to use and reactions were conducted under a nitrogen atmosphere. Unless otherwise noted, liquid reagents were introduced to the reaction flask via syringe or cannula. Volatile solvents were removed using a rotary evaporator under reduced pressure. All dialyses were performed in MeOH or H₂O using Spectra/POR[®] regenerated cellulose dialysis bags.

Characterization: All NMR spectra were measured in CDCl₃, MeOD (d-4), or D₂O with TMS or solvent signals as the standards. ¹H NMR spectra were recorded with a Bruker AVQ-400, a DRX-500, or an AV-600. All ¹³C NMR spectra were recorded with an AV-600 (at 150 MHz) and were proton-decoupled. MALDI-TOF data was collected on a PerSeptive Biosystems Voyager-DE PRO instrument (Applied Biosystems) in positive ion mode. MALDI samples were prepared using a matrix of a saturated solution of trans-3-indoleacrylic acid in THF unless otherwise specified. For SEC, two PSS columns (7.5 x 300 mm) were used. The particle size was 5 mm. The SEC system consisted of a Waters 510 pump, a Waters U6K injector, a Waters 486 UV-Vis detector, and a Waters 410 differential refractive index detector. The columns were thermostatted at 70 °C. The system was calibrated to linear PEG standards. Dendrimer samples were dissolved in HPLC grade DMF at a concentration of 2 mg/ml and filtered through a 0.2 μm PVDF filter before injection.

Dendrimer synthesis and nomenclature: Compounds **2-5**, **6a**, **7a**, **10**, and **11** were synthesized as previously reported.¹⁷ The synthesis is briefly described below. Dendrimers are named as follows: a pentaerythritol core (PE) with one generation of lysine (G₁) and glutamic acid protected as a benzyl ester for the side chain and with a Boc on the amine (Glu(Bn)Boc) is abbreviated PE-G₁-(Glu(Bn)Boc)₈ because there are eight glutamic acids. The PEGylated versions are abbreviated as PE-G₁-Lys(Glu(Bn)-PEG)₈.

PE-G₁-Lys(Boc)₈ (2): A 20 mL reaction vial was charged with a stir bar, pentaerythritol (353 mg, 2.59 mmol), BocLys(Boc)-ONp (5.50 g, 11.8 mmol), 4-dimethylaminopyridine (DMAP) (125 mg, 1.02 mmol), DMF (5.5 mL) and TEA (1.60 mL, 11.5 mmol). The solution was stirred for 48 h and monitored by MALDI-TOF. Upon completion, *N,N*-dimethylethylene diamine (300 μL, 2.75 mmol) was added to the reaction solution to quench excess BocLys(Boc)-ONp and stirred for 15 min. The reaction solution was then diluted with ether and washed with three 100 mL portions of 1 M NaOH, three 100 mL portions of 1 M, one 100 mL portion DI water, and three 100 mL portions of brine. The organic layer was dried over MgSO₄ and evaporated to dryness under reduced pressure to give **2** as a colorless foam (3.455 g, 93% yield). ¹H NMR (400 MHz, CDCl₃): δ 1.26-1.49 (m, 88H), 1.58-1.83 (m, 8H), 3.09-3.11 (m, 8H), 4.08-4.18 (m, 12H), 4.80 (s, 4H), 5.3-5.6 (br d, 4H). ¹³C NMR (150 MHz, CDCl₃): δ 22.5, 28.3, 28.4, 29.6, 31.5, 39.9, 53.4, 62.2, 79.0, 79.8, 155.7, 156.1. Calc [M]⁺ (C₆₉H₁₂₄N₈O₂₄) m/z = 1448.87. Found MALDI-TOF [M⁺Na]⁺ m/z = 1471.1.

PE-G₁-Lys(NH₃TFA)₈ (3): To a 20 mL reaction vial charged with a stir bar and compound **2** (550 mg, 367 μmol) was added a 1:1 mixture of trifluoroacetic acid (TFA)/DCM (6 mL). The solution was stirred for 1 h and then the solvents were removed under reduced pressure to give **3** as a gummy solid in quantitative yield. ¹H NMR (400 MHz, MeOD): δ 1.40-1.60 (m, 8H), 1.67-1.75 (m, 8H), 1.87-2.10 (m, 8H), 2.99 (t, *J* = 8 Hz, 8H), 4.21 (t, *J* = 6 Hz, 4H), 4.40 (s, 8H). ¹³C

NMR (150 MHz, MeOD): δ 21.8, 26.5, 29.5, 38.7, 42.5, 52.3, 62.9, 161.4, 161.7, 168.6. Calc $[M]^+$ ($C_{29}H_{60}N_8O_8$) $m/z = 648.45$. Found MALDI-TOF $[M^+H]^+$ $m/z = 649.9$.

PE-G₁-Lys(Glu(Bn)Boc)₈ (4): To a 20 mL reaction vial charged with a stir bar, compound **3** (540 mg, 377 μ mol) and BocGlu(OBz)-ONp (1.73 g, 3.77 mmol) was added DMF (6 mL) and TEA (838 μ L, 6.01 mmol). The reaction solution was stirred for 4 h and then quenched with *N,N*-dimethylethylene diamine (50.0 μ L, 690 μ mol). The reaction mixture was diluted with ethyl acetate (100 mL) and washed with three 50 mL portions of 1 M NaHSO₄, three 50 mL portions of saturated K₂CO₃, one 50 mL portion of DI water, and one 50 mL portion of brine. The organic layer was dried over MgSO₄ and evaporated to dryness under reduced pressure to give **4** as a colorless foam (171 mg, 87% yield). ¹H NMR (400 MHz, MeOD): δ 1.22-1.60 (bm, 92H), 1.65-1.74 (m, 4H), 1.76-1.91 (m, 12H), 1.92-2.16 (m, 8H), 2.44-2.58 (m, 16H), 3.10-3.20 (m, 8H), 4.10-4.25 (m, 12H), 4.35-4.40 (m, 4H) 5.05-5.11 (2s, 16H), 7.25-7.38 (m, 40H). ¹³C NMR (150 MHz, MeOD): δ 24.0, 29.0, 31.7, 40.8, 44.6, 54.5, 65.0, 129.4, 129.8, 137.3, 163.4, 163.8, 170.7. Calc $[M]^+$ ($C_{165}H_{228}N_{16}O_{48}$) $m/z = 3201.59$. Found MALDI-TOF $[M^+Na]^+$ $m/z = 3219.2$.

PE-G₁-Lys(Glu(Bn)NH₃TFA)₈ (5): To a 20 mL reaction vial charged with a stir bar and compound **4** (700 mg, 219 μ mol) was added a 1:1 mixture of TFA/DCM (10 mL). The solution was stirred for 1 h and then the solvents were removed under reduced pressure to give **5** as a gummy solid in quantitative yield. ¹H NMR (400 MHz, D₂O): δ 1.09-1.35 (m, 16H), 1.42-1.65 (m, 8H), 1.90-2.20 (m, 16H), 2.34-2.41 (m, 8H), 2.48-2.60 (m, 8H), 2.79-2.90 (m, 4H), 3.00-3.12 (m, 8H), 3.82-3.96 (m, 12H), 4.04 (t, *J* = 4.4 Hz, 4H), 4.25-4.33 (m, 4H), 4.85-5.00 (m, 16H), 7.14-7.26 (m, 40H). ¹³C NMR (150 MHz, MeOD): δ 24.2, 27.8, 29.8, 30.4, 30.6, 31.7, 40.3, 53.6, 53.9, 54.1, 64.0, 67.9, 116.4, 118.3, 129.3, 129.5, 129.7, 137.4, 161.1, 161.4, 169.7, 170.2, 172.7, 173.6, 173.8. Calc $[M]^+$ ($C_{125}H_{164}N_{16}O_{32}$) $m/z = 2402.73$. Found MALDI-TOF $[M^+Na]^+$ $m/z = 2421.3$.

PE-G₁-Lys(Glu(Bn)PEG5k)₈ (6a): To a 20 mL reaction vial charged with a stir bar and compound **5** (100 mg, 30.9 μ mol), PNP-PEG carbonate (1.272 g, 247 μ mol), DMF (4 mL), and TEA (150 μ L, 1.076 mmol) were added. The reaction mixture was stirred vigorously for 48 h and then quenched with *N,N*-dimethylethylene diamine (50.0 μ L, 458 μ mol) and stirred for 1 h. To acylate any remaining primary amines that had not reacted with the PNP-PEG carbonate, acetic anhydride (400 μ L, 4.24 mmol) was added and the reaction mixture was stirred for an additional hour. The reaction mixture was precipitated into ether (300 mL) and **6a** was collected by filtration as a colorless solid (1.209 g, 95%). Residual free PEG was removed by dialysis using 100,000 Da MWCO tubing against MeOH for 24 h. ¹H NMR (500 MHz, D₂O): δ 1.23-1.80 (br m, 24H), 1.80-2.10 (br d, 16H), 2.38-2.55 (br s, 16H), 3.10-3.20 (br s, 8H), 3.35 (s, 24H), 3.40-4.00 (br m, ~3900H), 4.00-4.40 (br m, 36H), 5.03-5.12 (br s, 16H), 7.26-7.41 (br m, 40H). DMF SEC: M_n : 36,000 Da, M_w : 38,000 Da, PDI: 1.05.

PE-G₁-Lys(Glu(Bn)PEG2k)₈ (6b): See **6a** for procedure. Compound **5** (109 mg, 34.2 μ mol), PNP-PEG carbonate (576 mg, 268 μ mol), DMF (4 mL), TEA (150 μ L, 1.076 mmol), *N,N*-dimethylethylene diamine (50.0 μ L, 458 μ mol), acetic anhydride (400 μ L, 4.24 mmol), yield: 617 mg (95%). ¹H NMR (500 MHz, D₂O): δ 1.23-1.80 (br m, 24H), 1.80-2.10 (br d, 16H), 2.38-2.55 (br s, 16H), 3.10-3.20 (br s, 8H), 3.35 (s, 24H), 3.40-4.00 (br m, ~1450H), 4.00-4.40 (br m, 36H), 5.03-5.12 (br s, 16H), 7.26-7.41 (br m, 40H). DMF SEC: M_n : 13,000 Da, M_w : 13,000 Da, PDI: 1.02.

PE-G₁-Lys(Glu(Bn)PEG200Da)₈ (6c): PEG-PNP carbonate was formed *in situ* by adding tetraethylene glycol (215 mg, 1.03 mmol) to a stirring solution of PNP-chloroformate (189 mg, 939 μmol) in DMF (6 mL) in a 20 mL reaction vial. After stirring overnight, compound **5** (312 mg, 98.0 μmol) and TEA (150 μL, 1.076 mmol) were added. The reaction mixture was stirred vigorously for 48 h and then quenched with *N,N*-dimethylethylene diamine (50.0 μL, 458 μmol) and stirred for 1 h. To acylate any remaining primary amines that had not reacted with the PNP-PEG carbonate, acetic anhydride (400 μL, 4.24 mmol) was added and stirred for an additional hour. Residual free PEG was removed by dialysis using 3,500 Da MWCO tubing against MeOH for 24 h to yield a colorless solid (398 mg, 95%). ¹H NMR (500 MHz, CDCl₃): δ 1.18-1.58 (br m, 16H), 1.59-1.79 (br m, 8H), 1.90-2.10 (br d, 16H), 2.35-2.58 (br s, 16H), 3.02-3.15 (br s, 4H), 3.31-3.4 (s, 24H), 3.40-3.80 (br m, ~128H), 4.00-4.70 (br m, 36H), 5.01-5.17 (br s, 16H), 7.25-7.41 (br m, 40H). DMF SEC: M_n: 3,000 Da, M_w: 3,000 Da, PDI: 1.01. Calc [M]⁺ (C₂₀₅H₃₀₈N₁₆O₈₀) m/z = 4276.70. Found MALDI-TOF [M⁺H]⁺ m/z = 4275.7.

PE-G₁-Lys(Glu(Bn)Ac)₈ (6d): To a 20 mL reaction vial charged with a stir bar and compound **5** (372 mg, 115 μmol), acetic anhydride (0.500 mL, 5.30 mmol), DMF (10 mL), and TEA (1.00 mL, 7.17 mmol) were added. The reaction mixture was stirred vigorously overnight. The acylated dendrimer **6d** was isolated by dialysis in a 3,500 MWCO bag yielding a gummy solid (304 mg, 97%). ¹H NMR (400 MHz, MeOD): δ 1.35-1.45 (m, 8H), 1.49-1.55 (m, 8H), 1.68-1.77 (m, 4H), 1.86-1.95 (br m, 12H), 1.95 (s, 24H), 2.03-2.13 (br m, 8H), 2.33-2.48 (br m, 8H), 2.39-2.45 (br m, 8H), 3.14-3.25 (br m, 8H), 4.18-4.25 (br m, 8H), 4.28-4.35 (br m, 4H), 4.39-4.46 (m, 8H), 5.05-5.12 (br m, 16H), 7.21-7.39 (br m, 40H). ¹³C NMR (150 MHz, MeOD): δ 22.7, 22.8, 23.8, 24.1, 28.6, 28.7, 29.8, 31.58, 31.63, 31.9, 40.1, 53.9, 54.3, 63.9, 67.6, 129.3, 129.4, 129.72, 129.73, 137.71, 137.74, 173.0, 173.4, 173.7, 173.9, 174.3, 174.4. DMF SEC: M_n: 2,000 Da, M_w: 2,000 Da, PDI: 1.01. Calc [M]⁺ (C₁₄₁H₁₈₀N₁₆O₄₀) m/z = 2737.25. Found MALDI-TOF [M⁺Na]⁺ m/z = 2753.8.

PE-G₁-Lys(GluPEG5k)₈ (7a): To a 20 mL reaction vial charged with a stir bar, compound **6a** (100 mg, 2.32 μmol), and MeOH (3 mL) was added activated Pd/C (10 wt %, 10 mg). The reaction mixture was stirred overnight under a hydrogen atmosphere, then filtered and solvent evaporated under reduced pressure to give **7** as a colorless solid (99.0 mg, 100%). ¹H NMR (500 MHz, D₂O): δ 1.23-1.80 (br m, 24H), 1.80-2.10 (br d, 16H), 2.38-2.55 (br s, 16H), 3.10-3.20 (br s, 8H), 3.35 (s, 24H), 3.40-4.00 (br m, ~3900H), 4.00-4.40 (br m, 36H).

PE-G₁-Lys(GluPEG2k)₈ (7b): See **7a** for procedure. Compound **6b** (100 mg, 5.26 μmol), Pd/C (10 wt %, 10 mg), MeOH (3 mL), yield: 97 mg (100%). ¹H NMR (600 MHz, D₂O): δ 1.21-1.60 (br m, 16H), 1.72-1.79 (br m, 4H), 1.78-1.99 (br m, 12H), 2.02-2.19 (br m, 8H), 2.38-2.55 (br s, 16H), 3.10-3.20 (br s, 8H), 3.36 (s, 24H), 3.40-4.00 (br m, ~1,450H), 4.00-4.60 (br m, 36H).

PE-G₁-Lys(GluPEG200Da)₈ (7c): See **7a** for procedure. Compound **6c** (100 mg, 28.1 μmol), Pd/C (10 wt %, 10 mg), MeOH (3 mL), yield: 83.5 mg (100%). ¹H NMR (500 MHz, MeOD): δ 1.23-1.80 (br m, 24H), 1.80-2.10 (br d, 16H), 2.38-2.55 (br s, 16H), 3.10-3.20 (br s, 8H), 3.36 (s, 24H), 3.40-4.00 (br m, ~128H), 4.00-4.60 (br m, 36H). Calc [M]⁺ (C₁₄₉H₂₆₀N₁₆O₈₀) m/z = 3553.68. Found MALDI-TOF [M⁺Na]⁺ m/z = 3571.4.

PE-G₁-Lys(GluAc)₈ (7d): See **7a** for procedure. Compound **6d** (100 mg, 36.5 μmol), Pd/C (10 wt %, 10 mg), MeOH (3 mL), yield: 74.0 mg (100%). ¹H NMR (600 MHz, MeOD): δ 1.35-1.45 (br m, 8H), 1.49-1.55 (br m, 8H), 1.68-1.77 (br m, 4H), 1.86-1.95 (br m, 12H), 2.00 (s, 24H),

2.03-2.13 (br m, 8H), 2.33-2.48 (br m, 8H), 2.39-2.45 (br m, 8H), 3.14-3.25 (m, 8H), 4.18-4.25 (br m, 8H), 4.28-4.35 (br m, 4H), 4.39-4.46 (br m, 8H). ¹³C NMR (150 MHz, MeOD): δ 21.0, 22.48, 22.52, 23.9, 28.6, 28.7, 29.6, 31.7, 31.8, 39.9, 53.7, 54.0, 54.4, 172.7, 173.2, 173.3, 173.8, 174.0, 177.06, 177.10. Calc [M]⁺ (C₈₅H₁₃₂N₁₆O₄₀) m/z = 2016.88. Found MALDI-TOF [M⁺Na]⁺ m/z = 2037.8.

PE-G₁-Lys(Glu(N)PEG5k)₈ (9a): To a 20 mL reaction vial charged with a stir bar, compound **7** (70.0 mg, 1.06 μmol), and DMF (2 mL) was added *O*-(Benzotriazol-1-yl)-*N,N,N',N'*-tetramethyluronium hexafluorophosphate (HBTU) (33.2 mg, 87.5 μmol). Next, 3,3'-iminobis(*N,N*-dimethylpropylamine) (16.38 mg, 875 μmol) was added. The reaction mixture was stirred overnight and then diluted with MeOH (3 mL) and dialyzed in a 100,000 Da MWCO bag. Next, the solvent was removed under reduced pressure yielding **8** as a colorless solid (47 mg, 97%). ¹H NMR (500 MHz, D₂O): δ 1.25-1.29 (br m, 8H), 1.31-1.44 (br m, 8H), 1.46-1.53 (br m, 8H), 1.54-1.93 (br m, 48H), 1.95-2.58 (br m, 144H), 3.15-3.47 (br s, 64H), 3.48-3.77 (br m, ~3900H), 3.78-4.40 (br m, ~36H).

PE-G₁-Lys(Glu(N)PEG2k)₈ (9b): See **9a** for procedure; EDC and DMAP were used in place of HBTU. Compound **7b** (62.0 mg, 3.26 μmol), DMF (2 mL), EDC (163.9 mg, 855 μmol), 3,3'-iminobis(*N,N*-dimethylpropylamine) (160 mg, 855 μmol), DMAP (4.00 mg, 32.8 μmol), yield: 62.0 mg (95%). ¹H NMR (500 MHz, D₂O): δ 1.12-1.53 (br m, 24H), 1.54-1.94 (br m, 48H), 1.96-2.58 (br m, 144H), 3.15-3.47 (br s, 64H), 3.47-3.77 (br m, ~1,450H), 3.78-4.40 (br m, ~36H).

PE-G₁-Lys(Glu(N)PEG200Da)₈ (9c): See **9a** for procedure. Compound **7c** (62 mg, 17.4 μmol), DMF (2 mL), HBTU (99.0 mg, 261 μmol), 3,3'-iminobis(*N,N*-dimethyl-propylamine) (48.9 mg, 261 μmol), yield: 75.3 mg (95%). ¹H NMR (500 MHz, D₂O): δ 1.13-1.61 (br m, 24H), 1.62-2.00 (br d, 48H), 2.00-2.86 (br m, 144H), 3.05-3.45 (br m, 64H), 3.46-3.91 (br m, ~128H), 3.95-4.45 (br m, 36H).

PE-G₁-Lys(Glu(N)Ac)₈ (9d): See **9a** for procedure; EDC and DMAP were used in place of HBTU. Compound **7d** (71.0 mg, 34.8 μmol), DMF (2 mL), EDC (271 mg, 1.41 mmol), 3,3'-iminobis(*N,N*-dimethylpropylamine) (265 mg, 1.41 mmol), DMAP (2.00 mg, 167 μmol), yield: 99.0 mg (96%). ¹H NMR (600 MHz, MeOD): δ 1.12-1.23 (br m, 8H), 1.31-1.45 (br m, 8H), 1.49-1.55 (br m, 8H), 1.65-1.95 (br m, 48H), 1.96-2.02 (s, 24H), 2.03-2.13 (br m, 8H), 2.23-2.60 (br m, 152H), 3.10-3.25 (br m, 48H), 4.11-4.50 (br m, 20H). ¹³C NMR (150 MHz, MeOD): δ 22.8, 23.4, 26.0, 27.7, 28.7, 28.9, 29.2, 30.5, 32.0, 35.9, 39.1, 41.1, 44.4, 45.4, 47.3, 48.7, 54.4, 57.6, 58.0, 58.5, 63.4, 161.3, 161.8, 173.3, 174.2.

PE-G₁-Lys(Glu(NNBoc)PEG5k)₈ (10): To a 20 mL reaction vial charged with a stir bar, compound **7a** (467 mg, 10.9 μmol), and DCM (5 mL) was added EDC (143 mg, 746 μmol) at 0 °C. Next, *t*-butyl carbazate (61.6 mg, 467 μmol) was added at 0 °C followed by DMAP (10.0 mg, 82.0 μmol). The reaction solution was allowed to warm to room temperature over 3 h and stirred overnight. The reaction solution was then diluted with MeOH (3 mL) and dialyzed in a 100,000 Da MWCO bag. Next, the solvent was removed under reduced pressure yielding **10** as a colorless solid (445 mg, 95%). ¹H NMR (500 MHz, D₂O): δ 1.30-1.60 (br m, 100H), 1.64-2.23 (br m, 20H), 2.32-2.54 (br s, 16H), 3.09-3.25 (br s, 8H), 3.38 (s, 24H), 3.50-3.92 (br m, ~3900H), 4.00-4.51 (br m, 36H).

PE-G₁-Lys(Glu(NNH₃TFA)PEG5k)₈ (11): To a 20 mL reaction vial charged with a stir bar and compound **10** (100 mg, 2.33 μmol) was added a 1:1 mixture of TFA/DCM (3 mL). The solution was stirred for 1 h and then the solvents were removed under reduced pressure to give **11** in quantitative yield as a gummy solid. ¹H NMR (500 MHz, D₂O): δ 1.13-1.60 (br m, 24H), 1.67-2.20 (br m, 16H), 2.30-2.61 (br s, 16H), 3.0-3.15 (br s, 8H), 3.36 (s, 24H), 3.40-4.00 (br m, ~3900H), 4.00-4.60 (br m, 36H).

PE-G₁-Lys(Glu(Hydrazone)PEG200Da)₈ (1a): To a 20 mL reaction vial charged with a stir bar and compound **11** (60 mg, 19 μmol) was added MeOH (3 ml), pyridine (100 μl) and acetic acid (100 μl). Under Ar, amino ketone **12** (51.5 mg, 190 μmol) was added. The solution was stirred at 60 °C for 12 h. Dialysis in MeOH yielded **1b** as a colorless solid (94%). ¹H NMR (500 MHz, D₂O): δ 1.13-1.61 (br m, 24H), 1.62-2.86 (br m, 224H), 3.05-3.45 (br m, 64H), 3.46-3.91 (br m, ~128H), 3.95-4.45 (br m, 36H).

PE-G₁-Lys(Glu(Hydrazone)PEG5k)₈ (1b): To a 20 mL reaction vial charged with a stir bar and compound **11** (60 mg, 1.5 μmol) was added MeOH (3 ml), pyridine (100 μl) and acetic acid (100 μl). Under Ar, amino ketone **12** (4.1 mg, 15 μmol) was added. The solution was stirred at 60 °C for 12 h. Dialysis in MeOH yielded **1b** as a colorless solid (96%). ¹H NMR (500 MHz, D₂O): δ 1.25-1.29 (br m, 8H), 1.31-1.44 (br m, 8H), 1.46-1.53 (br m, 8H), 1.54-1.93 (br m, 48H), 1.95-2.66 (br m, 184H), 3.15-3.47 (br s, 64H), 3.48-3.77 (br m, ~3900H), 3.78-4.40 (br m, ~36H).

N,N-bis(3-(dimethylamino)propyl)-acetoacetamide (12): To a round bottom flask charged with a stir bar and amine **8** (2 g, 10.6 mmol) was added m-xylene (5 ml). The flask was sparged with Ar for 10 minutes and then t-butyl acetoacetate was added (1.86 g, 11.7 mmol). The solution was heated at 140 °C for 15 minutes and immediately purified through fractional distillation (yield = 95%). ¹H NMR (500 MHz, CDCl₃): δ 1.62-1.77 (sep, *J* = 7 Hz, 4H), 2.13-2.33 (m, 19H), 3.23-3.30 (t, *J* = 7 Hz, 2H), 3.30-3.39 (t, *J* = 7 Hz, 2H), 3.59-3.64 (s, 1.5H), 5.10-5.14 (s, 0.25H), 14.84-14.88 (s, 0.25H). Calc [M⁺H]⁺ (C₁₄H₂₉N₃O₂) m/z = 272.2338. Found HRMS [M⁺H]⁺ m/z = 272.2330.

Dendrimer/siRNA complexation: All solutions were prepared with 1x PBS buffer (pH 7.4). Dendrimer solutions were prepared at various concentrations according to the desired final nitrogen to phosphate (N:P) ratio (10:1 and 100:1). Next, a 0.6 μM siRNA solution was prepared. Equal volumes of dendrimer solution were added to siRNA solution. The mixtures were gently vortexed for 20 min at room temperature. For release studies, after vortexing, the solution was adjusted to the desired pH with acetate buffer and incubated for either 24 h or 48 h before each gel was run.

Agarose gel electrophoresis retardation assay: Gel electrophoresis was performed with agarose gel (1.0% w/v) in tris-acetate-EDTA buffer (40 mM) with one drop of ethidium bromide. Due to cost considerations, complementary DNA was used to study complexation. The DNA/dendrimer complexes were formed as described above for siRNA. The solution containing the complexes was added to the gel (20 μL) and electrophoresed at 100 V for 30 min. The DNA bands were visualized under a UV transilluminator at 365 nm.

Cell lines and culture: HeLa cell line stably expressing firefly luciferase (HeLa-*luc*) were maintained in Dulbecco's Modified Eagle's Medium (DMEM) supplemented with 10% (v/v)

fetal bovine serum (FBS), 1% GlutaMAX, and 500 $\mu\text{g}/\text{mL}$ Zeocin (all purchased from Invitrogen except the serum, which was purchased from Hyclone (Logan, UT)). Cell incubations were performed in a water-jacketed 37 $^{\circ}\text{C}/5\%$ CO_2 incubator.

***In vitro* siRNA/plasmid DNA transfection assay:** HeLa-*luc* cells were seeded (15,000 cells/well) into each well of a 96-well clear tissue culture plate and allowed to attach overnight in growth medium. Growth medium was composed of DMEM (with phenol red), 10% FBS, and 1% GlutaMAX. Polyplexes were prepared as previously mentioned. The polyplex samples were then serially diluted in growth medium to give 1 μg siRNA well⁻¹. Existing medium was replaced with 100 μl of each polyplex solution in triplicate wells. The cells were allowed to grow for an additional 48 h before being analyzed for gene silencing. Hyperbranched 25,000 kDa PEI purchased from BASF (Ludwigshafen, Germany) was used as a positive control for siRNA delivery. As a negative control, an equivalent dose of free siRNA in medium and medium alone was used.

After 48 h, the cells were washed with PBS (containing Mg^{2+} and Ca^{2+} , 3 x 100 μl). Glo Lysis Buffer (120 μl , Promega, Madison, WI) was added to each well, and the plate was mixed at rt using a vortexer (Fisher Scientific). After 20 min, samples from each well (100 μL) were transferred to the wells of a white 96-well tissue culture plate (Corning, Lowell, MA). Steady-Glo luciferase assay reagent (Promega) was reconstituted according to the manufacturer's instructions and injected into each well in series (100 μL well⁻¹) using a GloMax 96 microplate luminometer (Promega). After a 10 s post-injection delay, each well was read with a 2 s integration time. QuantiLum Recombinant Luciferase (Promega) in Glo Lysis Buffer was used as a standard.

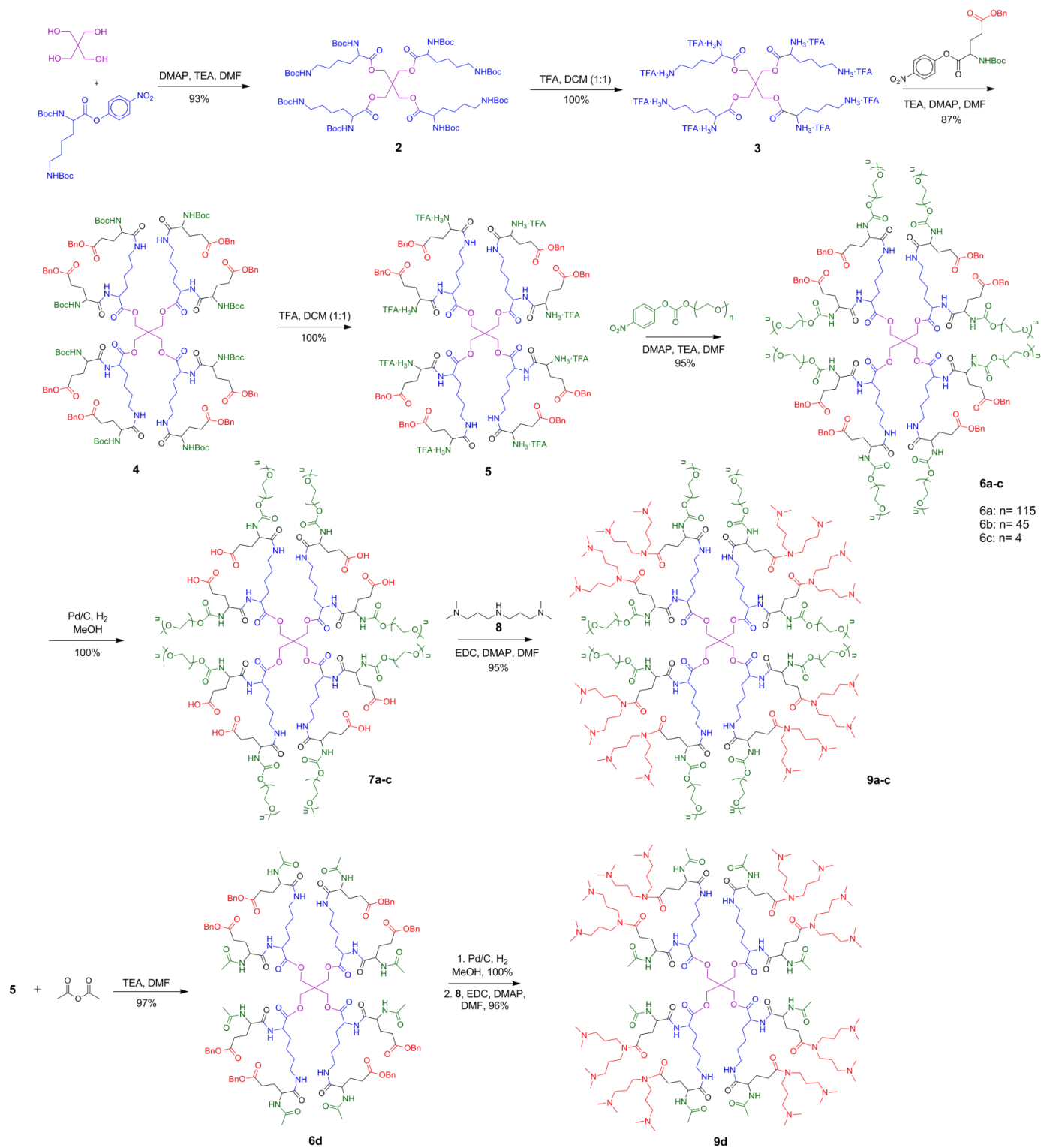
Total protein assay: Cells treated identically and in parallel with transfection assays were tested on a second 96-well plate. After washing, the cells were lysed with M-PER Mammalian Protein Extraction Reagent (50 μL well⁻¹, Pierce, Rockford, IL) by incubating for 10 min at rt. PBS (50 μL well⁻¹) was then added and the plate was briefly vortexed to mix. Samples from each well (50 μL) were transferred to a black 96-well plate (Corning) already containing PBS (100 μL well⁻¹). A solution of 3 mg mL^{-1} fluorescamine in acetone (50 μL) was added to each well, and the plate was briefly vortexed to mix. After 5 min, fluorescence was measured using a SpectraMax Gemini XS reader (ex. = 400 nm, em. = 460 nm). Protein concentrations were determined using bovine serum albumin as a standard.

Cell viability assay: Cells treated identically and in parallel with transfection assays were tested on a third 96-well plate. A 2.92 mg mL^{-1} solution of MTT (3-(4,5-dimethyl-2-thiazolyl)-2,5-diphenyl-2H-tetrazolium bromide) in medium (40 μL) was added directly to each well, and the plate was returned to the incubator. After 30 min, the medium was replaced with 200 μL well⁻¹ of DMSO. After the crystals had dissolved, 25 μL well⁻¹ of glycine buffer (0.1 M glycine, 0.1 M NaCl, pH 10.5) was added, and the samples were diluted by adding 50 μL of sample to 133 μL of DMSO and 17 μL of glycine buffer. The absorbance at 570 nm was measured using a SpectraMax 190 reader (Molecular Devices). Cell viability was normalized to absorbance measured from untreated cells. Data are represented as a mean of three measurements.

4.3 RESULTS AND DISCUSSION

Dendrimer design and synthesis: Dendrimer **1** in Figure 4.1 has many characteristics that make it ideal for gene delivery. First, the polyester core makes the dendrimer biodegradable. Second, the bifunctional periphery of the dendrimer allows for strict control over the attachment of both amine structures and PEG chains. By linking the amine structure to the dendrimer through a hydrazone, any toxic polycationic character will be quickly eliminated once in the acidic environment of the lysosome. Furthermore, the modular synthesis allows for the evaluation of many amine derivatives in order to achieve the best possible gene complexation. The same synthetic control and versatility can also be advantageous in the attachment of PEG groups to protect the payload.

The ability of PEG to protect foreign compounds is well documented and could play a vital role in protecting the siRNA payload during *in vivo* gene delivery.²⁰ Longer PEG chains could provide greater protection of the dendrimer/payload but could also potentially interfere with siRNA complexation through steric hindrance. In dendrimer **1**, eight large PEG chains surrounding the dendrimer would potentially shield the 16 amines at the core and inhibit the electrostatic interaction necessary for complexation. Moreover, as siRNA behaves as a rigid rod about 6 nm in length, sterics may become a serious concern.⁶ In order to identify the optimized PEG length, four dendrimers were synthesized that each displayed PEG chains of varying molecular weight (5 kDa, 2 kDa, 200 Da, 0 Da [acylated]). We chose first to study a model dendrimer carrier with our amine structures linked through a non-degradable amide bond rather than a degradable hydrazone linkage. This approach allows for a more rapid screening of variations of the dendrimer (e.g., PEG length or amine structure). The general synthetic route is shown in Scheme 4.1.



Scheme 4.1. Synthesis of amide-linked polyamine dendrimers.

Biodegradable polyester core **2** was formed by treating pentaerythritol with the *p*-nitrophenyl (PNP) ester of Boc-protected lysine. Boc cleavage by TFA and subsequent coupling of orthogonally protected PNP-glutamic acid gave **4**, a bifunctional dendrimer with eight protected amines and eight protected carboxylic acids. A second Boc cleavage followed by a coupling of PEG-PNP activated carbonate afforded the PEGylated dendrimer **6a-c**. PEG chains of 200 Da, 2 kDa, 5 kDa, or acetyl groups were attached to give a small library of dendrimers with increasing hydrodynamic volume, as confirmed by size exclusion chromatography (SEC) (Figure 4.2) measurements. Excess PNP-PEG was quenched with *N,N*-dimethylethylene diamine and followed by treatment with acetic anhydride to ensure the capping of any remaining primary amines. The non-PEGylated derivative **6d** was acylated with acetic anhydride and all four derivatives were purified by dialysis. Each dendrimer derivative had a polydispersity index below 1.1, which is beneficial in providing reproducible dendrimer-siRNA formulations. Next, the benzyl esters were removed by Pd/C catalyzed hydrogenolysis to afford eight carboxylic acid functional groups at the periphery of **7a-d**. To install the amine moieties, amidation was performed with 3,3'-iminobis(*N,N*-dimethylpropylamine) (**8**) and either 1-ethyl-3-(3-dimethylaminopropyl)carbodiimide (EDC) or *O*-(benzotriazol-1-yl)-*N,N,N',N'*-tetramethyluronium hexafluorophosphate (HBTU). After purification by dialysis, the amide-linked dendrimers **9a-d** were isolated in excellent overall yields without requiring chromatographic purification.

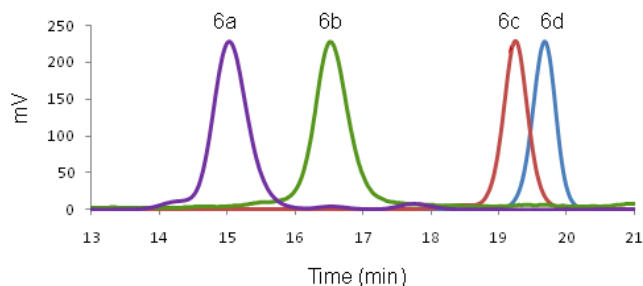
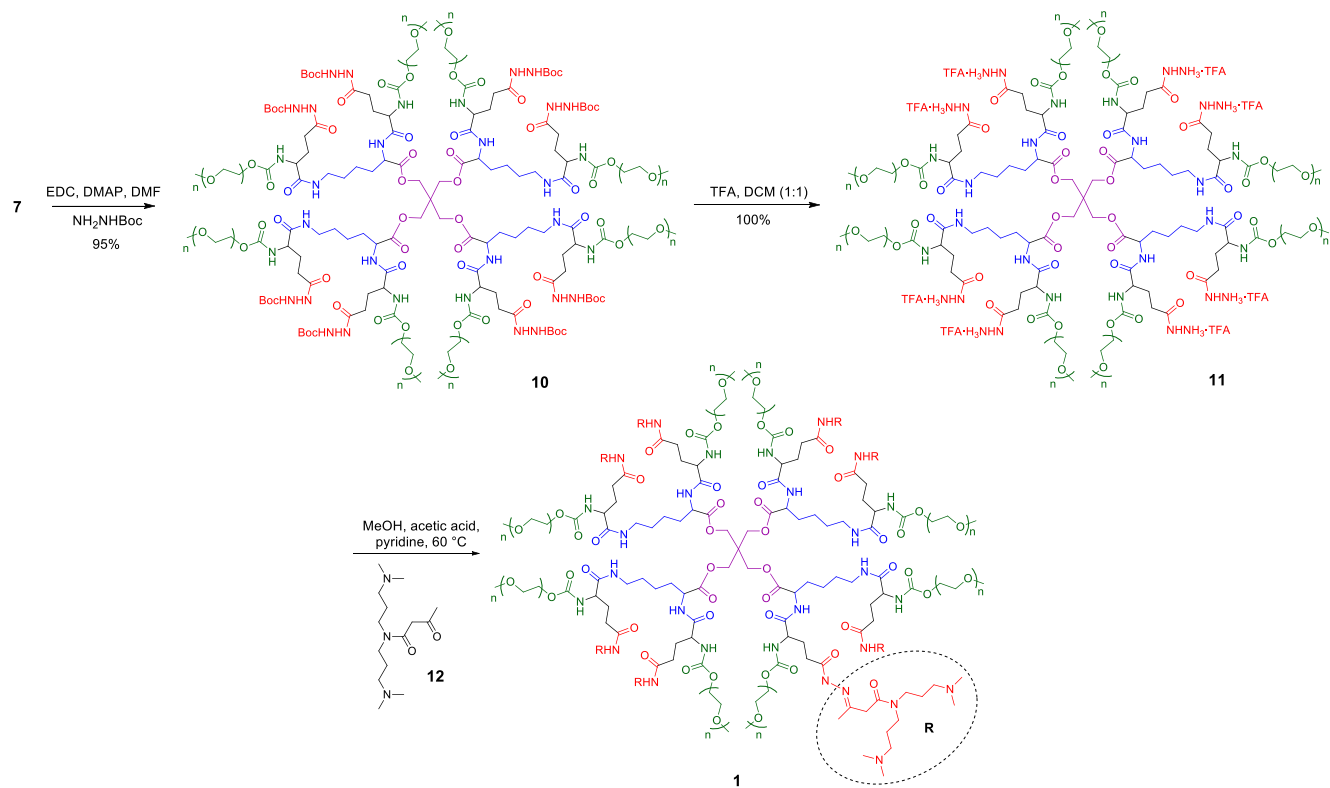
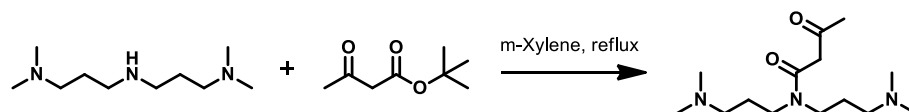


Figure 4.2. Normalized SEC trace of PEGylated dendrimers; **6a** $M_w = 38$ kDa, **6b** $M_w = 13$ kDa, **6c** $M_w = 3$ kDa, **6d** $M_w = 2$ kDa as calibrated with linear PEG standards.

As a parallel strategy, progress was made toward dendrimers with a hydrazone linkage of the amine (Scheme 4.2). To form the acid-degradable hydrazone derivative, *t*-butyl carbazate was used in the EDC coupling to **7** rather than amine **8** to yield **10**. The Boc group was quantitatively removed by TFA, yielding hydrazide dendrimer **11**. Hydrazone formation was accomplished by stirring **11** with amino ketone **12** in 95% methanol (MeOH) with 2.5% acetic acid and 2.5% pyridine (v/v %) at 60 °C to yield acid degradable, polycationic dendrimer **1**.¹⁷ Dendrimer **1** was synthesized with both 0.2 kDa PEG chains (**1a**) and 5 kDa PEG chains (**1b**). Amino ketone **12** was synthesized by refluxing amine **8** and *t*-butyl acetoacetate in *m*-xylene followed by purification by fractional distillation (Scheme 4.3).

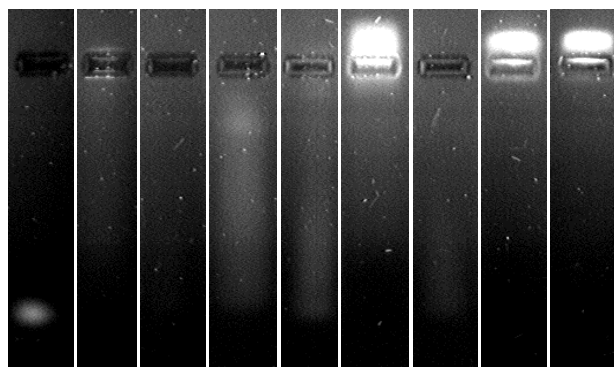


Scheme 4.2. Synthesis of dendrimer with hydrazone linked amine (**1**).



Scheme 4.2. Synthesis of amino ketone **12**

DNA complexation with amide-linked dendrimer: The first step in the evaluation of a new carrier is the assessment of its ability to complex siRNA. Gel electrophoresis was used to assess the ability of the amine functionalized dendrimers with various PEG lengths to complex siRNA. Due to cost considerations, DNA of complementary size and sequence was used rather than siRNA to study complexation. Dendrimers were incubated with DNA before being loaded onto a 1.0% agarose gel containing ethidium bromide (EtBr). Equal concentrations and volumes of DNA were complexed with the dendrimers, however, the intensity of the bands varied greatly. This could possibly be due to streaking of polyplexes which would dilute the fluorescence across the gel or the PEGylated dendrimers providing a hydrophobic core where EtBr is not quenched as readily by water. The complexation results of the amide-linked dendrimers are presented in Figure 4.3.



Lane:	1	2	3	4	5	6	7	8	9
Compound:	DNA	9d	9d	9c	9c	9b	9b	9a	9a
N:P ratio:	-	100:1	10:1	100:1	10:1	100:1	10:1	100:1	10:1

Figure 4.3. Gel electrophoresis of dendrimer/DNA complexes. Qualitatively, free DNA travels down the gel while complexed DNA remains baseline. Lanes 2-9 vary by nitrogen:phosphorous (N:P) ratio and length of PEG chains; lane 1 is bare DNA as a control.

Interestingly, an improvement in binding was observed with increasing PEG length. The 5 kDa PEG derivative (**9a**) demonstrated the strongest complexation and was the only derivative to show complete complexation at N:P ratios as low as 10:1 (N:P ratio is the nitrogen to phosphorous ratio where *N* is the number of basic amines and *P* is the number of phosphorous atoms). The 2 kDa PEG derivative (**9b**) also exhibited excellent complexation at N:P = 100:1, though incomplete complexation at N:P = 10:1. In contrast, the 200 Da derivative (**9c**) only afforded minimal complexation at N:P=100:1 and even less at N:P = 10:1. The acylated dendrimer (**9d**) achieved slightly better binding than the 200 Da derivative (**9c**), however it did not complex as well as either of the higher molecular weight PEG derivatives.

These results caused us to reevaluate our original hypothesis, and consider the possible positive effects of PEG on siRNA binding. Previous work has shown both positive and negative correlations of PEG length on oligonucleotide complexation.²¹ Different molecular weights and loadings of PEG chains attached to carriers have been shown to affect complex morphology and stability considerably, with higher molecular weight PEG chains often leading to more compact and stronger polyplexes. Additionally, the ability of PEG to aid in DNA condensation has previously been reported.²² These results suggest that longer PEG arms may influence not only siRNA loading but also complex stability. Future experiments are needed to explore how the length of the PEG chains affects the size of the siRNA/dendrimer conjugates.

***In vitro* transfection and cytotoxicity with amide-linked dendrimer:** Once the complexation abilities of the dendrimers were determined, the transfection potential of **9a-c** was investigated. HeLa cells stably expressing firefly luciferase (HeLa-*luc*) were treated with anti-luciferase siRNA/dendrimer complexes (1 μ g siRNA in 100 μ l of medium well⁻¹) and incubated for 48 h. In this experiment, cells successfully transfected with siRNA will display a decrease in bioluminescence. Three dendrimers were tested in this preliminary study. The 5 kDa PEG arm

dendrimer **9a**, the 200 Da PEG arm dendrimer **9c**, and the non-PEGylated dendrimer **9d** were chosen to give a distribution of dendrimers with long PEG arms, short PEG arms, and no PEG arms. All dendrimers were tested at an N:P ratio of 100:1 as this was the ratio in which the best complexation was observed. The cell viability was also measured with an MTT assay during the transfection experiments. Figure 4.4 illustrates the transfection capabilities of the dendrimers and the corresponding cytotoxicities.

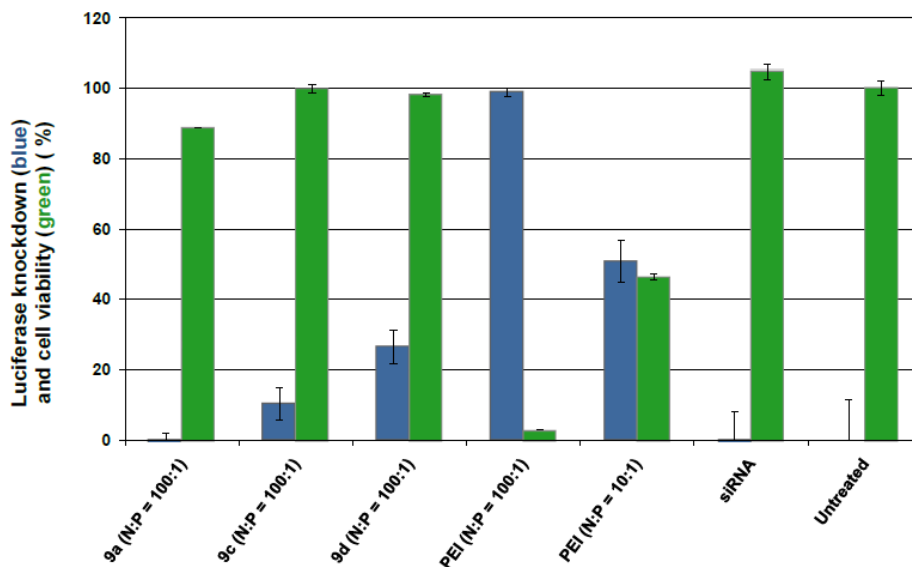


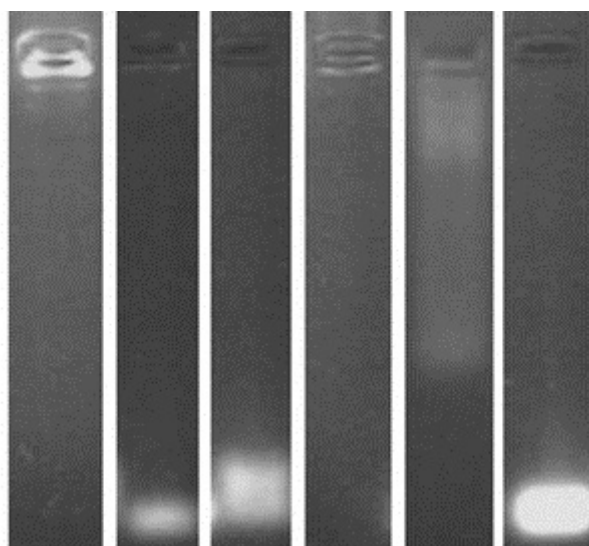
Figure 4.4. *In vitro* transfection and cytotoxicity of dendrimers (1 μg siRNA in 100 μl of medium well⁻¹). Transfection (blue) reported as percent knockdown of luciferase. Cytotoxicity (green) reported as cell viability in comparison to untreated cells.

In vitro transfection was observed, and luciferase silencing was most predominant for the non-PEGylated dendrimer (**9d**) at just over 25%. Dendrimer **9c** showed lower transfection capabilities with only about 10% silencing, and dendrimer **9a** did not demonstrate any significant transfection. Encouragingly, none of the dendrimers exhibited significant cytotoxicity. As a positive control, PEI was used and demonstrated high transfection but also high cytotoxicity. As a negative control, cells were also treated with an equivalent dose of siRNA without a delivery vector. These cells showed no transfection and no decrease in viability.

The dendrimers that complexed well in the gel electrophoresis studies performed poorly in the transfection experiments. Dendrimers with longer PEG chains complexed efficiently, but showed reduced *in vitro* transfection capabilities. These results suggest that the low transfection seen with the dendrimers may be due to an inability to release the siRNA once in the cell, a key step in the transfection pathway. Dendrimer **9d**, which displayed poor complexation capabilities, was the most successful in transfection, possibly due to its weaker interactions with siRNA. However, we envisioned that by installing amine moieties through a pH-sensitive linkage to the dendrimer, efficient release of siRNA within the cell may be achievable. These results suggest

that after appropriate tuning to achieve high transfection, the reported dendrimers may offer a less toxic method for *in vivo* siRNA delivery.

DNA complexation and release with hydrazone-linked dendrimer: Dendrimers with non-degradable amide linkages to amine moieties demonstrated the ability to complex DNA, however, the siRNA transfection efficiencies were low. This might be due to the inability to release the siRNA from the carrier and could potentially be improved through a triggered release mechanism. Dendrimers **1a** and **1b** were synthesized with a pH-sensitive hydrazone linkage in order to trigger release upon exposure to the acidic environment of the lysosome. By gel electrophoresis, both of these dendrimers complexed DNA at pH 7.4, and released the DNA after incubation at pH 5.0 (Figure 4.5).



Lane:	1	2	3	4	5	6
Compound:	1a	1a	1a	1b	1b	1b
pH	7.4	5.0	5.0	7.4	5.0	5.0
Time (h)	48	24	48	48	24	48

Figure 4.5. Gel electrophoresis of pH-sensitive dendrimer/DNA complexes. All complexes were formed at N:P = 100:1 at pH 7.4. pH was then adjusted accordingly and complexes were incubated for either 24 or 48 h as labeled.

***In vitro* transfection and cytotoxicity with hydrazone-linked dendrimer:** After demonstrating the ability of the pH-sensitive dendrimers to complex DNA at pH 7.4 and release DNA at pH 5.0, the transfection capabilities of these dendrimers was investigated. Similar to the transfection experiments with the amide linked dendrimers, HeLa cells stably expressing firefly luciferase (HeLa-*luc*) were treated with anti-luciferase siRNA/dendrimer complexes (1 μ g siRNA in 100 μ l of medium well⁻¹) and incubated for 48 h. As expected, the pH-sensitive dendrimers **1a** and **1b**

offer improved transfection abilities over the dendrimers with non-degradable amide linkages (Figure 4.6). Both dendrimers **1a** and **1b** were tested at N:P = 100:1 and yield ~40% knockdown in the luciferase assay. Dendrimer **1b**, with 5 kDa PEG arms, was less toxic than dendrimer **1a**, which may be due to the ability of PEG to shield surface charges of the complex. Overall, these results suggest that the ability of the dendrimer to release the siRNA at the proper time plays an important role in transfection efficiency, and by adding degradable linkages to amine moieties, transfection efficiency can be greatly improved.

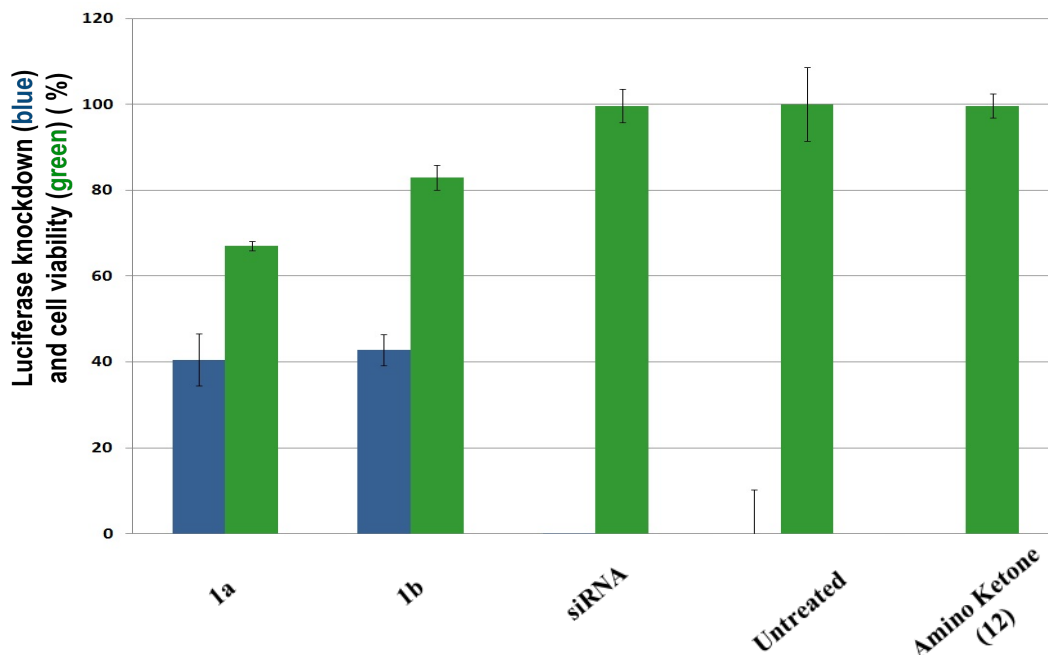


Figure 4.6. *In vitro* transfection and cytotoxicity of pH-sensitive dendrimers **1a** and **1b** at N:P = 100 (1 μ g siRNA in 100 μ l of medium well⁻¹). Transfection (blue) reported as percent knockdown of luciferase. Cytotoxicity (green) reported as cell viability in comparison to untreated cells. Degradation byproduct amino ketone **12** was also evaluated.

4.4 CONCLUSIONS AND OUTLOOK

In this work we have made progress towards the development of a non-toxic siRNA delivery vector. The ability to manipulate the two peripheral functional groups of our biodegradable dendrimer individually allows us to construct a more efficient siRNA carrier. We have bound 16 tertiary amines to the core of the dendrimer and demonstrated the ability of these dendrimers to electrostatically bind siRNA. Varying lengths of PEG have also been attached to the dendrimer, and more efficient binding with longer PEG chains has been observed. Although this result was initially unexpected, it may suggest that dendrimers with longer PEG chains will not only offer better *in vivo* protection, but also be more effective at siRNA loading. However, preliminary *in vitro* transfection experiments with amide-linked dendrimers demonstrated that the high complexation efficiency may inhibit siRNA release once within the cell, and thus

require a triggered release. This was not seen with the pH-sensitive dendrimers where the length of the PEG arms did not affect transfection efficiency, but longer PEG arms did lead to decreased toxicity. These hydrazone-linked dendrimers were shown to both complex siRNA at pH 7.4 and release siRNA at pH 5.0. Additionally, in the luciferase knockdown assay, the hydrazone-linked dendrimer with 5 kDa arms achieved over 40% knockdown with minimal toxicity.

In the future, further transfection efficiency may be achieved by exploring amine moieties other than **8** and **12**. As an example, spermine – one of many polyamine compounds which have commonly found application in gene delivery – will be investigated in our system.²³ Additionally, end-group functionalization of PEG chains, attachment of targeting groups, and increasing dendrimer generation are possibilities for further improving the transfection ability of these carriers. Further improvement in the hydrazone dendrimers as siRNA delivery systems would be followed by an assessment of their knockdown abilities in an *in vivo* model.

4.5 ACKNOWLEDGEMENTS

I gratefully acknowledge Dr. Derek van der Poll and Dr. Kyle Broaders for their scientific input regarding this project. I also thank Dr. Jessica Cohen and Dr. Peter Wich for help with cell experiments, and Dr. William Floyd for scaling up **5**.

4.6 REFERENCES

1. EvaluatePharma (2012) World preview 2018: Embracing the patent cliff. London: EvaluatePharma, p 15 <https://www.evaluatepharma.com/secure/FileResourceDownload.aspx?id=98a75eab-95f6-41d8-903f-4732848fdf78>. (accessed October 20, 2013).
2. Whitehead, K. A.; Langer, R.; Anderson, D. G. *Nat. Rev. Drug Disc.* **2009**, *8*, 129-38.
3. Ku, G.; McManus, M. T. *Hum. Gene Ther.* **2008**, *19*, 17-26.
4. Fire, A.; Xu, S.; Montgomery, M. K.; Kostas, S. A.; Driver, S. E.; Mello, C. C. *Nature* **1998**, *391*, 806-811.
5. Elbashir, S. M. *Nature* **2001**, *411*, 494-498.
6. Gary, D. J.; Puri, N.; Won, Y. *J. Controll. Release* **2007**, *121*, 64-73.
7. Chiu, Y.; Rana, T.M. *RNA* **2003**, *9*, 1034-1048.
8. Nguyen, D. N.; Green, J. J.; Chan, J. M.; Langer, R.; Anderson, D. G. *Adv. Mater.* **2009**, *21*, 847-867
9. Barquintero, J.; Eixarch, H.; Pérez-Melgosa, M. *Gene Ther.* **2004**, *11 Suppl 1*, S3-9.

10. Boussif, O.; Lezoualch, F.; Zanta, M. A.; Mergny, M. D.; Scherman, D.; Demeneix, B.; Behr, J. P. *Proc. Natl. Acad. Sci. U. S. A.* **1995**, *92*, 7297-7301.
11. Wagner, E.; Ogris, M.; Zauner, W. *Adv. Drug Delivery Rev.* **1998**, *30*, 97-113.
12. Lynn, D. M.; Langer, R. *Gene.* **2000**, 10761-10768. Green, J. J.; Shi, J.; Chiu, E.; Leshchiner, E. S.; Langer, R.; Anderson, D. G. *Bioconjugate Chem.* **2006**, *17*, 1162-9.
13. Anderson, D. G.; Akinc, A.; Hossain, N.; Langer, R. *Mol. Ther.* **2005**, *11*, 426-34.
14. Shim, M. S.; Kwon, Y. J. *Biomaterials* **2010**, *31*, 3404-13.
15. Dufès, C.; Uchegbu, I. F.; Schätzlein, A. G. *Adv. Drug Delivery Rev.* **2005**, *57*, 2177-202.
16. Luo, D.; Haverstick, K.; Belcheva, N.; Han, E.; Saltzman, W. M. *Cell* **2002**, 3456-3462.
17. van der Poll, D. G.; Kieler-Ferguson, H. M.; Floyd, W. C.; Guillaudeu, S. J.; Jerger, K.; Szoka, F. C.; Fréchet, J. M. *Bioconjugate Chem.* **2010**, *21*, 764-73.
18. Mellman, I., Fuchs, R., and Helenius, A. *Annu. Rev. Biochem.* **1986** *55*, 773-700.
19. Shim, M. S.; Kwon, Y. J. *Biomacromolecules* **2008**, *9*, 444-55.
20. van Vlerken, L. E.; Vyas, T. K.; Amiji, M. M. *Pharm Res.* **2007**, *24*, 1405-14.
21. Petersen, H.; Fechner, P. M.; Martin, A. L.; Kunath, K.; Stolnik, S.; Roberts, C. J.; Fischer, D.; Davies, M. C.; Kissel, T. *Bioconjugate Chem.* **2002**, *13*, 845-54.
22. Kleideiter, G., Nordmeier, E. *Polymer* **1999**, *40*, 4025-4033.
23. Hardy, J. G.; Kostianen, M. a.; Smith, D. K.; Gabrielson, N. P.; Pack, D. W. *Bioconjugate Chem.* **2006**, *17*, 172-8.

Chapter 5

Conclusions and Future Perspectives

5.1 OVERVIEW

In the field of drug delivery, polymers have proven to be a valuable tool. The diversity of polymer architectures, physical properties, and *in vivo* activity make them suitable for many drug delivery applications. With the development of new polymerization and post-polymerization techniques over the last few decades, it has become possible to tailor polymer attributes for specific systems.¹ For example, features such as improved pharmacokinetics and biodistribution, active or passive targeting, and responsive drug release through internal or external triggers can be installed in many polymeric delivery platforms.

Much of the earliest research on polymer drug delivery focused on polymers for altered pharmacokinetics and biodistribution.^{2,3,4,5} Today, polymers for extended circulation are still the most prominent class of polymers for drug delivery in the clinic.⁶ Specifically, PEGylated materials including proteins and liposomes have experienced success in clinical settings.⁷ However, other types of polymers have also shown promise in preclinical research and early stage clinical trials.^{6,8,9} In this thesis, I have explored both the old and the new. I have synthesized and evaluated new PEG derivatives for incorporation into liposomes, investigated a library of polymers for extended circulation, and developed a bio-responsive dendrimer for siRNA delivery.

5.2 SUMMARY OF FINDINGS

In chapter 2, I describe the synthesis of two disterol PEG molecules and the subsequent incorporation of those molecules into liposomes. PEG-DiCHEMS and PEG-DiChol are attractive candidates as alternatives to PEG-DSPE which can phase separate in lipid membranes, leading to broader phase transition temperature ranges and possible loss of the PEG from the membrane. The disterol PEGs were evaluated by DSC in formulation with DPPC. DPPC/disterol PEG liposomes encapsulating CF were formulated, and the temperature dependent leakage of CF was measured by fluorimetry. Initial results suggest that PEG-DiCHEMS at 20 mole percent in DPPC liposomes may have a favorable leakage profile, though further analysis will need to be performed.

In chapter 3, I describe the evaluation of a panel of synthetic polymers for extended circulation. These polymers were synthesized with controlled polymerization techniques to allow for well-defined polymer structures with low polydispersity. After characterizing the physical properties of these polymers under consistent experimental conditions, it was determined that each had a lower intrinsic viscosity than PEG, the current gold standard for extended circulation. Next, lipid anchors were conjugated to the terminus of each polymer for incorporation into fluorescently labeled liposomes. The ability of each polymer to extend the circulation half-life of the liposomes was then evaluated in mice and rats. Both PEG and PMOX coated liposomes had the longest circulation half lives in mice (16.3 h and 14.8 h, respectively) and rats (33.6 h and 30.5 h, respectively), though PVP also significantly increased circulation half life in both species (mice: 9.8 h, rats: 20.7 h). Importantly, I found that similarly to PEG, PMOX has an accelerated

blood clearance (ABC) effect upon repeated administration. Furthermore, none of the other polymers investigated, including PVP, displayed such an effect.

In Chapter 4, I describe the synthesis, characterization, and evaluation of biodegradable, pH-responsive dendrimers for siRNA delivery. These dendrimers with complex structures were achieved through a straight-forward synthetic route with minimal reaction and purification steps. Chemical features included a biodegradable polyester core and two orthogonal sets of 8 functional groups each for the attachment of a variety of chemical moieties, including amines, PEG, cell penetrating peptides, and endosomal escape aids. Additionally, the synthesis allowed for the attachment of these groups at the end of the synthetic route, facilitating a screen of various chemical moieties. By attaching amine structures to the dendrimer periphery through pH-sensitive, acyl hydrazone linkages, the polycationic character of the dendrimer is diminished once exposed to the acidic environment of the lysosome. Through gel electrophoresis, we demonstrated the ability of these materials to efficiently bind genetic material at pH 7.4, and release it at pH 5. We also evaluated these materials in an *in vitro* knockdown assay using HeLa cells stably expressing firefly luciferase. Dendrimers complexed with anti-luciferase siRNA were able to decrease the firefly luciferase with minimal associated cytotoxicity. The dendrimers with 16 tertiary amines attached through acyl hydrazones and eight 5 kDa PEG chains achieved ~40% knockdown with cell viability above 80% (N:P = 100).

5.3 FUTURE DIRECTIONS

Of all polymers investigated for drug delivery systems, PEG has been one of the most successful, and there is little evidence to suggest that this trend will not continue. In the last decade, the PEGylate therapeutics Somavert and Macugen from Pfizer (2003 and 2004, respectively) and Cimzia from UCB S.A. (2008) have earned FDA approval, and many more PEGylated materials have recently entered clinical trials.⁷ One of the core benefits of PEGylation is extended circulation through increased mass (and thus decreased renal clearance) and steric shielding.¹⁰ PEG is excellent at increasing the circulation half-life of therapeutics, and probably will continue to be used for this purpose for years to come, though alternative methods for increased circulation times of therapeutics are being developed. Many other polymers are also to extend circulation half-lives, including: HPMA (poly[N-(2-hydroxypropyl) methacrylamide])¹¹, PVP (poly(vinylpyrrolidone)),⁷ PMOX (poly(2-methyl-2-oxazoline)),^{12,13,14} PAcM (poly(N-acryloyl morpholine)),¹⁵ PG (polyglycerol),¹⁶ poly(amino acids)^{17,18} and polysaccharides.¹⁹ Though these alternatives may not extend circulation to the same extent as PEG, they can offer other advantages such as improved physical properties, biodegradability, decreased immune response, and increased drug loading. Additionally, non-polymer based methods for extended circulation are being developed, such as peptide-conjugation designed to interact with neonatal Fc receptor (FcRn) for protein recycling.²⁰

It is interesting to note that PEGylated small molecule drugs have not found the same success as PEGylated proteins, though a variety of PEG-small molecule conjugates have recently entered clinical trials.²¹ One of the central challenges to effective small molecule delivery with PEG is the lack of available functional sites on the PEG backbone for conjugation, typically leading to low weight percent drug loading. Because of this drawback, other polymers that can achieve high weight percent drug loading and maintain many of the same advantages of

PEGylation (increased solubility, extended circulation, *etc.*) may prove to be valuable alternatives. For example, HPMA is a polymer that has an abundance of backbone hydroxyl groups available for drug conjugation and has recently entered clinical trials as a conjugate to a variety of therapeutics.^{22,23,11} Additionally, poly(oxazolines) have shown potential as polymer conjugates to small molecule drugs due to the ability to incorporate functionalized monomers into the backbone of the polymer.^{24,25} Furthermore, block copolymers of oxazolines are able to form polymer micelles with impressive drug loading efficiencies within a hydrophobic core.²⁶ Recently, these and other colloidal carrier systems have received much interest due to their high, non-covalent loading capacity.

Many self-assembling polymeric nanoparticles based on amphiphilic block copolymers for drug delivery are currently being investigated.²⁷ These materials have a core-shell architecture where the drug is loaded into the hydrophobic core of the micelle and protected from opsonization by a hydrophilic polymer shell. Common examples of block copolymers used for this application include PEG,^{28,29} HPMA,²³ and oxazoline²⁴ block copolymers. Many such materials show great promise due to their many favorable properties (such as extended circulation, tailorable size and functional groups, and high drug loading) and are currently in ongoing clinical trials.^{30,31}

To date, the most successful polymeric drug delivery systems have been some of the simplest. Overly-complicated structures, stimuli-responsive release mechanisms, and other extravagant polymeric designs are often of interest in academic research, but translate poorly to the clinic. This is likely due to many factors, including: over-simplified laboratory assays and models that are not representative of the vast *in vivo* variables encountered during parenteral drug delivery; the incomplete understanding of the exact *in vivo* interactions of many materials; and difficulties in determining and analyzing the *in vivo* fate of such materials. A striking example of this is the recent discovery of an ABC immune response to PEG upon repeated administration. Though the first clinical PEGylated therapeutic was approved in 1990,³² it was more than 10 years later that the ABC phenomenon was discovered and investigated in depth.³³ Although the mechanism of the ABC phenomenon is now understood in much greater detail, some parts remain unclear. For instance, why do some polymers illicit this immune response while others avoid it completely?

Currently, the chemical techniques to produce materials with many different desirable features are available, however predicting, designing, and analyzing an effective product remains a major challenge in many cases. Advanced chemical structures and features will likely become increasingly prominent in the clinic; however, it is important to first thoroughly understand the biology behind these materials in order to properly apply them. It is well established that polymers can improve the biological activity of many therapeutics, and with improved chemical and biological understanding, polymers are likely to become even more valuable in the field of drug delivery.

5.4 REFERENCES

1. *Polymeric Drugs and Drug Delivery Systems (Google eBook)*. **34**, 328 (CRC Press, 2000).
2. Roseman, T. J. & Higuchi, W. I. Release of medroxyprogesterone acetate from a silicone polymer. *J. Pharm. Sci.* **59**, 353–357 (1970).
3. Wise, D. L. *et al.* No Title. **19**, 4–10 (1976).
4. Schwope, A. D., Wise, D. L. & Howes, J. F. Lactic/glycolic acid polymers as narcotic antagonist delivery systems. *Life Sci.* **17**, 1877–1885 (1975).
5. Abuchowski, A., van Es, T., Palczuk, N. C. & Davis, F. F. Alteration of immunological properties of bovine serum albumin by covalent attachment of polyethylene glycol. *J. Biol. Chem.* **252**, 3578–3581 (1977).
6. Duncan, R. The dawning era of polymer therapeutics. *Nat. Rev. Drug Discov.* **2**, 347–60 (2003).
7. Knop, K., Hoogenboom, R., Fischer, D. & Schubert, U. S. Poly(ethylene glycol) in drug delivery: pros and cons as well as potential alternatives. *Angew. Chem. Int. Ed. Engl.* **49**, 6288–308 (2010).
8. Nguyen, D. N., Green, J. J., Chan, J. M., Langer, R. & Anderson, D. G. Polymeric Materials for Gene Delivery and DNA Vaccination. *Adv. Mater.* **21**, 847–867 (2009).
9. Matsumura, Y. & Kataoka, K. Preclinical and clinical studies of anticancer agent-incorporating polymer micelles. *Cancer Sci.* **100**, 572–579 (2009).
10. Owens, D. E. & Peppas, N. A. Opsonization, biodistribution, and pharmacokinetics of polymeric nanoparticles. *Int. J. Pharm.* **307**, 93–102 (2006).
11. Lammers, T., Ulbrich, K., Duncan, R. & Vicent, M. J. Do HPMA copolymer conjugates have a future as clinically useful nanomedicines? A critical overview of current status and future opportunities. *Adv. Drug Deliv. Rev.* **62**, 272–282 (2010).
12. Woodle, M. C., Engbers, C. M. & Zalipsky, S. New amphipatic polymer-lipid conjugates forming long-circulating reticuloendothelial system-evading liposomes. *Bioconjug. Chem.* **5**, 493–6 (1994).
13. Zalipsky, S., Hansen, C. B., Oaks, J. M. & Allen, T. M. Evaluation of blood clearance rates and biodistribution of poly(2-oxazoline)-grafted liposomes. *J. Pharm. Sci.* **85**, 133–7 (1996).

14. Gaertner, F. C., Luxenhofer, R., Blechert, B., Jordan, R. & Essler, M. Synthesis, biodistribution and excretion of radiolabeled poly(2-alkyl-2-oxazoline)s. *J. Control. Release* **119**, 291–300 (2007).
15. Ranucci, E. *et al.* Synthesis and molecular weight characterization of low molecular weight end-functionalized poly(4-acryloylmorpholine). *Macromol. Chem. Phys.* **195**, 3469–3479 (1994).
16. Abu Lila, A. S., Nawata, K., Shimizu, T., Ishida, T. & Kiwada, H. Use of polyglycerol (PG), instead of polyethylene glycol (PEG), prevents induction of the accelerated blood clearance phenomenon against long-circulating liposomes upon repeated administration. *Int. J. Pharm.* **456**, 235–242 (2013).
17. Metselaar, J. M. *et al.* A novel family of L-amino acid-based biodegradable polymer-lipid conjugates for the development of long-circulating liposomes with effective drug-targeting capacity. *Bioconjug. Chem.* **14**, 1156–64
18. Li, C. Poly(l-glutamic acid)–anticancer drug conjugates. *Adv. Drug Deliv. Rev.* **54**, 695–713 (2002).
19. Doh, K.-O. & Yeo, Y. Application of polysaccharides for surface modification of nanomedicines. *Ther. Deliv.* **3**, 1447–56 (2012).
20. Sockolosky, J. T., Tiffany, M. R. & Szoka, F. C. Engineering neonatal Fc receptor-mediated recycling and transcytosis in recombinant proteins by short terminal peptide extensions. *Proc. Natl. Acad. Sci. U. S. A.* **109**, 16095–100 (2012).
21. Li, W., Zhan, P., De Clercq, E., Lou, H. & Liu, X. Current drug research on PEGylation with small molecular agents. *Prog. Polym. Sci.* **38**, 421–444 (2013).
22. Lammers, T., Kiessling, F., Hennink, W. E. & Storm, G. Drug targeting to tumors: Principles, pitfalls and (pre-) clinical progress. *J. Control. Release* **161**, 175–187 (2012).
23. Duncan, R. Development of HPMA copolymer-anticancer conjugates: clinical experience and lessons learnt. *Adv. Drug Deliv. Rev.* **61**, 1131–48 (2009).
24. Gumbleton, M., Adams, N. & Schubert, U. S. Poly(2-oxazolines) in biological and biomedical application contexts. *Adv. Drug Deliv. Rev.* **59**, 1504–1520 (2007).
25. Hoogenboom, R. Poly(2-oxazoline)s: a polymer class with numerous potential applications. *Angew. Chem. Int. Ed. Engl.* **48**, 7978–94 (2009).
26. Luxenhofer, R. *et al.* Doubly amphiphilic poly(2-oxazoline)s as high-capacity delivery systems for hydrophobic drugs. *Biomaterials* **31**, 4972–9 (2010).

27. Peppas, N. A., Kataoka, K., Harada, A. & Nagasaki, Y. Block copolymer micelles for drug delivery: Design, characterization and biological significance. *Adv. Drug Deliv. Rev.* **64**, 37–48 (2012).
28. He, G., Ma, L. L., Pan, J. & Venkatraman, S. ABA and BAB type triblock copolymers of PEG and PLA: a comparative study of drug release properties and “stealth” particle characteristics. *Int. J. Pharm.* **334**, 48–55 (2007).
29. Shim, M. S. & Kwon, Y. J. Acid-transforming polypeptide micelles for targeted nonviral gene delivery. *Biomaterials* **31**, 3404–13 (2010).
30. Wang, A. Z., Langer, R. & Farokhzad, O. C. Nanoparticle delivery of cancer drugs. *Annu. Rev. Med.* **63**, 185–98 (2012).
31. Gong, J., Chen, M., Zheng, Y., Wang, S. & Wang, Y. Polymeric micelles drug delivery system in oncology. *J. Control. Release* **159**, 312–323 (2012).
32. Levy, Y. *et al.* Adenosine deaminase deficiency with late onset of recurrent infections: Response to treatment with polyethylene glycol-modified adenosine deaminase. *J. Pediatr.* **113**, 312–317 (1988).
33. Dams, E. T. *et al.* Accelerated blood clearance and altered biodistribution of repeated injections of sterically stabilized liposomes. *J. Pharmacol. Exp. Ther.* **292**, 1071–9 (2000).